Numerical test of AdS/CFT correspondence for M2-branes

Masazumi Honda

A dissertation submitted for the degree of

Doctor of Philosophy

Department of Particle and Nuclear Physics
School of High Energy Accelerator Science
The Graduate University for Advanced Studies

Acknowledgements

First of all, I would like to express my gratitude to Professor Jun Nishimura for his guidance and advise. I would also like to thank M. Fujitsuka, M. Hanada, Y. Honma, Y. Imamura, G. Ishiki, S-W. Kim, S. Shiba, A. Tsuchiya, D. Yokoyama and Y. Yoshida for collaborations. I am also grateful to Harish-Chandra Research Institute, Niels Bohr Institute, Albert Einstein Institute, Kavli Institute for theoretical physics and International Centre for Theoretical Physics-South American Institute for Fundamental Research for hospitality during writing this thesis. I am supported by Grant-in-Aid for JSPS fellows (No. 22-2764). Numerical simulations have been carried out on PC clusters at KEK Theory Center and B-factory Computer System. Finally, I would like to thank very much for my friends, family, girlfriend and cats for useful conversations, support and encouragement.

Abstract

We show that the ABJM theory, which is an $\mathcal{N} = 6$ superconformal $\mathrm{U}(N) \times \mathrm{U}(N)$ Chern-Simons gauge theory, can be studied for arbitrary N at arbitrary coupling constant by applying a simple Monte Carlo method to the matrix model that can be derived from the theory by using the localization technique. This opens up the possibility of probing the quantum aspects of M-theory and testing the AdS_4/CFT_3 duality at the quantum level. Here we calculate the free energy, and confirm the $N^{3/2}$ scaling in the M-theory limit predicted from the gravity side. We also find that our results nicely interpolate the analytical formulae proposed previously in the M-theory and type IIA regimes. Furthermore, we show that some results obtained by the Fermi gas approach can be clearly understood from the constant map contribution obtained by the genus expansion. The method can be easily generalized to the calculations of BPS operators and to other theories that reduce to matrix models. We also study the supersymmetric Wilson loops in the ABJM theory. Our result nicely interpolates the expressions at weak and strong coupling regions.

Contents

Forward

M-theory is an eleven-dimensional theory, which has been proposed as a strong coupling limit of the type IIA superstring theory. It has been also expected that the M-theory includes the eleven-dimensional supergravity (11d SUGRA) as a low-energy limit. The 11d SUGRA consists of the graviton, gravitino and three-form gauge field. The three-form field in eleven dimensions electrically (magnetically) couples to two(five)-dimensional object. Such objects naturally appear as black brane solutions conserving a part of supersymmetries in the 11d SUGRA. On the analogy of the relation between such solutions in the ten-dimensional supergravities and objects in the superstring theories as string, NS5-brane and D-branes, we can expect that the M-theory has fundamental two- and five-dimensional objects. These objects are called as "M2-brane" and "M5-brane", respectively. In this thesis, we focus on Physics of the multiple M2-branes.

As well known, a low-energy limit of parallel N Dp-branes is described by the $(p+1)$-dimensional $U(N)$ maximally supersymmetric Yang-Mills theory. This $U(N)$ gauge symmetry can be intuitively understood by the facts that open string includes spin-1 massless boson in its spectrum and have an $U(1)$ charge called as a Chan-Paton factor. What is a low-energy effective theory of the parallel N M2-branes? Unfortunately, we have not an established answer to this question yet as we will argue below.

From the single M2-brane analysis and implication of the AdS/CFT correspondence, we expect that the low energy effective theory for N M2-branes has the following properties:

- Three dimensional conformal symmetry
- $\mathcal{N}=8$ supersymmetry
- $SO(8)$ R-symmetry
- Moduli space: $\mathcal{M}=(\mathbb{R}^8)^N/S_N$
- Identical to the three dimensional $U(N)$ $\mathcal{N}=8$ super Yang-Mills theory in a strong Yang-Mills gauge coupling limit
- Dual to the classical 11d SUGRA on $AdS_4\times S^7$ for $N\gg 1$.

Such a theory had not been found for long years. There are many reasons for this. One of most serious obstacle is difficulty of quantization of supermembrane [1] while there is a M(atrix) conjecture [2]. This prevents us from finding spectrum and something like a Chan-Paton factor for M2-branes. Another difficulty is that it is not easy to construct gauge theory with conformal and high supersymmetry except for four dimensions. Since Yang-Mills action is scale invariant only for four dimensions, we can use only Chern-Simons term of vector multiplet and marginal term of chiral multiplet for the construction. Indeed in 1990's, a maximal supersymmetric extension of Chern-Simons theory had been $\mathcal{N}=3$ [3, 4] (see also [5]).

Meanwhile the Bagger-Lambert-Gustavsson (BLG) theory [6, 7] based on the Lie 3-algebra $[X^a,X^b,X^c]=f^{abc}{}_dX^d$ appeared. If we take the structure constant f^{abcd} to be totally anti-symmetric, then the BLG theory generically has manifest $\mathcal{N}=8$ supersymmetry, $SO(8)$

R-symmetry and conformal symmetry. In spite of such successful structures, it is known that the only nontrivial solution for a generalized Jacobi identity is the A_4 algebra defined by $f^{abcd} = \epsilon^{abcd}$ [8, 9]. Then the resulting A_4 BLG theory can be rewritten as the $SU(2) \times SU(2)$ Chern-Simons matter theory with a Chern-Simons level k [10]. Actually moduli space analysis of this theory [11, 12] implies that the interpretation as two indistinguishable M2-branes on $\mathbb{R}^8/\mathbf{Z}_k$ can be possible only for $k = 1$ and $k = 2$. After proposed the BLG theory, it has been found that $\mathcal{N} = 4$ superconfomal Chern-Simons theory can be constructed by a type of quiver gauge theory [13, 14].

In 2008, Aharony, Bergman, Jafferis and Maldacena (ABJM) [15] has proposed a $U(N) \times U(N)$ theory with Chern-Simons levels k and $-k$ coupled to bi-fundamental matters. The on-shell supersymmetric Lagrangian of the theory is given by

$$
\begin{aligned}
&\mathcal{L}_{U(N)\times U(N)} \\
&= k\,\mathrm{Tr}\Bigg[\frac{1}{2}\epsilon^{\mu\nu\rho}\left(-A_\mu\partial_\nu A_\rho - \frac{2}{3}A_\mu A_\nu A_\rho + \tilde{A}_\mu\partial_\nu\tilde{A}_\rho + \frac{2}{3}\tilde{A}_\mu\tilde{A}_\nu\tilde{A}_\rho\right) \\
&\qquad + \left(-D_\mu\bar{\Phi}^\alpha D^\mu\Phi_\alpha + i\bar{\Psi}^\alpha \not{D}\Psi_\alpha\right) - i\epsilon^{\alpha\beta\gamma\delta}\Phi_\alpha\bar{\Psi}_\beta\Phi_\gamma\bar{\Psi}_\delta + i\epsilon_{\alpha\beta\gamma\delta}\bar{\Phi}^\alpha\Psi^\beta\bar{\Phi}^\gamma\Psi^\delta \\
&\qquad + i\left(-\bar{\Psi}_\beta\Phi_\alpha\bar{\Phi}^\alpha\Psi^\beta + \Psi_\beta\bar{\Phi}_\alpha\Phi^\alpha\bar{\Psi}^\beta + 2\bar{\Psi}_\alpha\Phi_\beta\bar{\Phi}^\alpha\Psi^\beta - 2\Psi^\beta\bar{\Phi}^\alpha\Phi_\beta\bar{\Psi}_\alpha\right) \\
&\qquad + \frac{1}{3}\left(\Phi_\alpha\bar{\Phi}^\beta\Phi_\beta\bar{\Phi}^\gamma\Phi_\gamma\bar{\Phi}^\alpha + \Phi_\alpha\bar{\Phi}^\alpha\Phi_\beta\bar{\Phi}^\beta\Phi_\gamma\bar{\Phi}^\gamma\right. \\
&\qquad\qquad \left. + 4\Phi_\beta\bar{\Phi}^\alpha\Phi_\gamma\bar{\Phi}^\beta\Phi_\alpha\bar{\Phi}^\gamma - 6\Phi_\gamma\bar{\Phi}^\gamma\Phi_\beta\bar{\Phi}^\alpha\Phi_\alpha\bar{\Phi}^\beta\right)\Bigg],
\end{aligned}
$$

where A_μ and $\tilde{A}_\mu$ are $U(N)$ gauge fields, and Φ_α and Ψ_α ($\alpha = 1, 2, 3, 4$) are bosonic and fermionic complex bi-fundamental fields, respectively. This theory has $\mathcal{N} = 8$ supersymmetry for $k = 1, 2$ and $\mathcal{N} = 6$ supersymmetry for $k \geq 3$. It has been conjectured to be dual to M-theory on $AdS_4 \times S^7/\mathbb{Z}_k$ for $k \ll N^{1/5}$, and to type IIA superstring on $AdS_4 \times \mathbb{C}P^3$ in the planar large-N limit with the 't Hooft coupling constant $\lambda = N/k$ kept fixed.

From the viewpoint of quantum gravity, the ABJM theory is important since it may provide us with a nonperturbative definition of type IIA superstring theory or M-theory on AdS_4 backgrounds since the theory is well-defined for finite N. One may draw a precise analogy with the way maximally supersymmetric Yang-Mills theories may provide us with nonperturbative formulations of type IIA/IIB superstring theories on D-brane backgrounds through the gauge/gravity duality [16, 17, 18, 19]. In particular, the M-theory limit is important given that M-theory is not defined even perturbatively, although there is a well-known conjecture on its nonperturbative formulation in the infinite momentum frame in terms of matrix quantum mechanics [2]. The planar limit, which corresponds to type IIA superstring theory, has interest on its own since it may allow us to perform more detailed tests of the gauge/gravity duality than in the case of AdS_5/CFT_4. In particular, we may hope to calculate the $1/N$ corrections to the planar limit, which enables us to test the gauge/gravity duality at the quantum string level, little of which is known so far.

In all these prospectives, one needs to study the ABJM theory in the strong coupling regime. As in the case of QCD, it would be nice if one could study the ABJM theory on a lattice by Monte Carlo methods. This seems quite difficult, though, for the following three reasons. Firstly, the construction of the Chern-Simons term on the lattice is not straightforward, although there is a proposal [20, 21] based on its connection to the parity anomaly. Secondly, the Chern-Simons term is purely imaginary in the Euclidean formulation, which causes a technical problem known as the sign problem when one tries to apply the idea of importance sampling. Thirdly, the lattice discretization necessarily breaks supersymmetry, and one needs to restore it in the continuum limit by fine-tuning the coupling constants of the supersymmetry breaking relevant operators. (See, for instance, ref. [22].) This might, however, be overcome by the use of a non-lattice regularization of the ABJM theory [23] based on the large-N reduction on S^3 [24, 25], which is shown to be useful in studying the planar limit of the 4d $\mathcal{N} = 4$ super Yang-Mills theory [26, 27, 28].

What we do here instead is to apply Monte Carlo methods not to the original theory but to a matrix model obtained after a huge reduction of the degrees of freedom due to supersymmetry. In fact, it has been known for a while in certain supersymmetric theories that one can reduce the path integral to a finite dimensional matrix model by using the so-called localization technique. Such a technique was applied [29] to 4d $\mathcal{N} = 4$ super Yang-Mills theory, and some conjecture on the half-BPS Wilson loops [30, 31] has been confirmed. In ref. [32], the same technique has been applied to the ABJM theory on three-sphere S^3, and its partition function was shown to reduce to a matrix integral

$$\begin{aligned} Z(N,k) &= \frac{1}{(N!)^2} \int \frac{d^N\mu}{(2\pi)^N} \frac{d^N\nu}{(2\pi)^N} \\ &\qquad \frac{\prod_{i<j}\left(2\sinh\frac{\mu_i-\mu_j}{2}\right)^2\left(2\sinh\frac{\nu_i-\nu_j}{2}\right)^2}{\prod_{i,j}\left(2\cosh\frac{\mu_i-\nu_i}{2}\right)^2} \exp\left[\frac{ik}{4\pi}\sum_{i=1}^{N}(\mu_i^2-\nu_i^2)\right] , \end{aligned}$$

which is commonly referred to as the ABJM matrix model. By using this matrix model, the free energy of the ABJM theory has been studied intensively [33, 34, 35, 36, 37, 38, 39, 40]. In ref. [34] the planar limit and the $1/N$ corrections around it have been studied employing a technique from topological string theory, and the on-shell action of the type IIA supergravity on $AdS_4 \times \mathbb{C}P^3$ has been reproduced. In ref. [35] the free energy in the M-theory limit has been obtained using some ansatz for the eigenvalue distribution. In ref. [38] the genus expansion at strong 't Hooft coupling has been considered and a resummed form was obtained in terms of the Airy function by using the holomorphic anomaly equation [41]. The obtained simple form was claimed to be valid to all orders in the genus expansion up to the worldsheet instanton effect. In ref. [40], the free energy in the M-theory regime at small k has been calculated by the Fermi gas approach, and the result turns out to be given by the Airy function obtained in ref. [38] with some extra terms. These results, if correct, would enable us to shed light on the dynamical aspects of M-theory and to test the AdS/CFT duality including the string loop effect by studying the gravity side further.

In this thesis we show that the ABJM matrix model can be rewritten in a form suitable for Monte Carlo simulations [42, 43], which enables simple calculation of the partition function and BPS operators for arbitrary values of the rank N and the level k from first principles. In particular, we calculate the partition function explicitly for various N and k, which is supposed to contain the nonperturbative effects corresponding to the worldsheet instantons in string theory neglected in refs. [34, 38]. We find the well-known constant map contribution

[41, 44, 45] is also correctly reproduced.

We pursue this direction further and study the supersymmetric Wilson loops in the ABJM theory. Recently, Klemm, Mariño, Schiereck and Soroush proposed a beautiful analytic formula for the expectation value of the supersymmetric Wilson loop at finite N and finite k, which should hold in the strong coupling region up to the instanton corrections [46]. We calculate the full expectation value including the instanton corrections and test their proposal. We explore the whole parameter region and see how their formula and the perturbative formula are interpolated. By taking the difference of our full result and the analytic formula of Klemm *et al.*, we extract the instanton contribution.

This thesis is organized as follows. In chapter 1 we introduce the novel ABJM theory [15] as a leading candidate of such a theory. In chapter 2 we introduce the localization method [29] and apply the method to general 3d $\mathcal{N} = 2$ supersymmetric field theory on S^3, which includes the ABJM theory as a specific case. This chapter is essentially a review of refs [32, 47, 48]. In chapter 3 we show our numerical results of the free energy [42, 43]. In chapter 4 we present our (preliminary) numerical result of the supersymmetric Wilson loop. Chapter 5 is devoted to summary and discussions.

1 Low energy effective theory of multiple M2-branes

M2-brane has been considered as one of fundamental object in M-theory. While D-branes [49] in superstring theory are well described by DBI action at low energy scale, effective description of M2-branes has been considered to be more nontrivial. In this chapter, we introduce the novel ABJM theory [15] as a leading candidate of such a theory. This chapter is organized as follows. In section 1.1 we briefly review expected properties of M-theory. In section 1.2 we study an effective theory of single M2-brane and investigate its property. In section 1.3 we consider AdS/CFT correspondence for M2-branes and give properties of multiple M2-branes theory if we assume the correspondence. In section 1.4 we introduce ABJM theory.

1.1 M-theory

M-theory has been proposed as a strong coupling limit of the type IIA superstring theory [50]. Here we briefly introduce M-theory. First we will give a relation between the type IIA supergravity (IIA SUGRA) and the eleven-dimensional supergravity (11d SUGRA), which has been considered as a low energy limit of the M-theory. Next we will investigate black brane solutions in the 11d SUGRA, which is identified with M2- and M5-branes in the M-theory. Finally we discuss that various objects in the type IIA superstring theory can be consistently explained from the M-theory.

1.1.1 Type IIA supergravity and Eleven-dimensional supergravity

As ten-dimensional supergravity is a low-energy limit of superstring theory, the eleven-dimensional supergravity [51] has been considered as a low-energy limit of M-theory as we will see below. Here we motivate existence of M-theory by providing a relation between the IIA and 11d SUGRA. As a result, the IIA SUGRA can be understood as a Kaluza-Klein (KK) reduction of the 11d SUGRA [52, 53, 50].

Eleven-dimensional supergravity

Let us start with the 11d SUGRA. It is widely believed that consistent supergravity can exist up to eleven dimension [54]. As well known, the 11d SUGRA action is uniquely determined up to second derivative. The field content is quite simple. It consists of the gravition G_{MN} ($M, N = 0, 1, \cdots, 10$), gravitino $\psi_{M,\alpha}$ ($\alpha = 1, 2, \cdots, 32$) and anti-symmetric 3-form C_{MNP}. The 3-form field is needed to compensate the difference of the on-shell degrees of freedom between the gravition and gravitino: $(\frac{10\times 9}{2} - 1) - \frac{8\times 32}{2} = -84 = -{}_9C_3$. The bosonic part of the action is given by[1]

$$2\kappa_{11}^2 S_{11\mathrm{d}} \;=\; \int d^{11}x\sqrt{-G}\Big[R-\frac{1}{2}|F^{(4)}|^2\Big]-\frac{1}{6}\int C\wedge F^{(4)}\wedge F^{(4)}, \tag{1.2}$$

where κ_{11} is the eleven-dimensional gravitational coupling constant related to the Newton constant G_{11} and Planck length l_p as

$$16\pi G_{11}=2\kappa_{11}^2=\frac{1}{2\pi}(2\pi l_p)^9. \tag{1.3}$$

$F^{(4)}=dC$ is the field strength of C and $|F^{(4)}|^2=\frac{1}{4!}F^{(4)}_{MNPQ}F^{(4)MNPQ}$. The full action is invariant under the following local supersymmetric transformation[2]:

$$\begin{aligned}
\delta E_M^{\ A} &= \frac{i}{2}\bar\epsilon\Gamma^A\psi_M,\\
\delta C_{MNP} &= -\frac{3i}{2}\bar\epsilon\Gamma_{[MN}\psi_{P]},\\
\delta\psi_M &= 2\nabla_M(\hat\omega)\epsilon+\frac{1}{144}\left(\Gamma^{PQRS}{}_M+8\Gamma^{QRS}\delta_M^{\ P}\right)\hat F^{(4)}_{PQRS}\epsilon,
\end{aligned} \tag{1.4}$$

where Γ^M satisfies the Clifford algebra: $\{\Gamma^M,\Gamma^N\}=2G^{MN}$ and the symbol $\Gamma^{M_1\cdots M_n}$ stands for

$$\Gamma^{M_1\cdots M_n}=\frac{1}{n!}\sum_\sigma\Gamma^{M_{\sigma(1)}\cdots M_{\sigma(n)}}, \tag{1.5}$$

with permutation σ. The covariant derivative $\nabla_M(\hat\omega)$ is given by

$$\nabla_M(\hat\omega)\psi_N=\partial_M\psi_N-\frac{1}{4}\hat\omega_{MAB}\Gamma^{AB}\psi_N. \tag{1.6}$$

The spin connection $\hat\omega$ is slightly different from the usual Levi-Civita spin connection $\omega^{(0)}$ in terms of the vielbein $E_M^{\ A}$. This is defined by

$$\begin{aligned}
\hat\omega_{MAB} &= \omega_{MAB}-\frac{i}{16}\bar\psi_N\Gamma_{MAB}{}^{NP}\psi_P,\\
\omega_{MAB} &= \omega^{(0)}_{MAB}+\frac{i}{16}\Big[\bar\psi_N\Gamma_{MAB}{}^{NP}\psi_P-2(\bar\psi_M\Gamma_B\psi_A-\bar\psi_M\Gamma_A\psi_B+\bar\psi_B\Gamma_N\psi_A)\Big].
\end{aligned} \tag{1.7}$$

[1]Although the fermionic part of the action is irrelevant in this thesis, this is concretely given by

$$\begin{aligned}
2\kappa_{11}^2 S^{(F)}_{11\mathrm{d}} &= \int d^{11}x\sqrt{-G}\Bigg[-\frac{i}{2}\bar\psi_M\Gamma^{MNP}\nabla_N\left(\frac{\omega+\hat\omega}{2}\right)\psi_p\\
&\quad -\frac{i}{384}\left(\bar\psi_M\Gamma^{MNABCD}\psi_N+12\bar\psi^A\Gamma^{BC}\psi^D\right)\left(F^{(4)}_{ABCD}+\hat F^{(4)}_{ABCD}\right)\Bigg],
\end{aligned} \tag{1.1}$$

where each symbol is defined below.

[2]We mainly follow the notation of [55]. This notation can be obtained from the notation of the original paper [51] by rescaling $\Gamma_M\to i\Gamma_M, \Gamma^M\to i\Gamma^M, \partial^M\to-\partial^M, \bar\psi_M\to i\bar\psi_M$.

$\hat{F}^{(4)}$ is defined in terms of $F^{(4)}$ and Ψ_M as

$$\hat{F}^{(4)}_{MNPQ} = F^{(4)}_{MNPQ} + \frac{3i}{2}\bar{\psi}_M \Gamma_{NP} \psi_Q. \tag{1.8}$$

Presence of the 3-form field implies existence of electrically coupled 2-dimensional object and magnetically coupled 5-dimensional object as we will see later. In sec. 1.1.2 we find so-called black M2- and M5-brane solutions [56, 57] as Bogomolny-Prasad-Sommerfield (BPS) solutions of this theory.

Kaluza-Klein reduction

Now let us compactify the eleventh dimension x^{10} as

$$x^M = (x^\mu, x^{10}), \quad x^{10} \sim x^{10} + 2\pi R_{11} \quad (\mu = 0, 1, \cdots, 9). \tag{1.9}$$

In an appropriate choice of coordinate, the eleven-dimensional vielbein $E_M^{\ A}$ reduces as [52, 53, 50]

$$E_M^{\ A} = \begin{pmatrix} e^{-\phi/3} e_\mu^{\ a} & e^{2\phi/3} A^{(1)}_\mu \\ 0 & e^{2\phi/3} \end{pmatrix}, \quad E_A^{\ N} = \begin{pmatrix} e^{\phi/3} e_a^{\ \nu} & -e^{\phi/3} A^{(1)}_a \\ 0 & e^{-2\phi/3} \end{pmatrix}, \tag{1.10}$$

where $e_\mu^{\ a}$, $A^{(1)}_\mu$ and ϕ are the ten-dimensional vielbein, 1-form field and scalar field, respectively. From this expression, G_{MN} is decomposed as

$$G_{MN} = e^{-2\phi/3} \begin{pmatrix} g_{\mu\nu} + e^{2\phi} A^{(1)}_\mu A^{(1)}_\nu & e^{2\phi} A^{(1)}_\mu \\ e^{2\phi} A^{(1)}_\nu & e^{2\phi} \end{pmatrix}, \tag{1.11}$$

where $g_{\mu\nu}$ is the ten-dimensional metric. The 3-form is also reduced as

$$C_{\mu\nu\rho} = A^{(3)}_{\mu\nu\rho}, \quad C_{\mu\nu 10} = B^{(2)}_{\mu\nu}, \tag{1.12}$$

in terms of the 3-form $A^{(3)}_{\mu\nu\rho}$ and 2-form fields $B^{(2)}_{\mu\nu}$. Dropping derivative terms along the eleventh direction, we obtain the following ten-dimensional action

$$\begin{aligned} S_{10\mathrm{d}} \;=\; & \frac{2\pi R_{11}}{2\kappa_{11}^2} \left[\int d^{10}x \sqrt{-g} \left\{ e^{-2\phi} \left(\tilde{R} + |d\phi|^2 - \frac{1}{2}|H^{(3)}|^2 \right) - \frac{1}{2}|F^{(2)}|^2 - \frac{1}{2}|G^{(4)}|^2 \right\} \right. \\ & \left. -\frac{1}{2} \int B^{(2)} \wedge G^{(4)} \wedge G^{(4)} \right], \end{aligned} \tag{1.13}$$

where $\tilde{R}$ is the ten-dimensional scalar curvature. The field strengths $H^{(3)}$, $F^{(2)}$ and $G^{(4)}$ are defined by

$$H^{(3)} = dB^{(2)}, \quad F^{(2)} = dA^{(1)}, \quad G^{(4)} = dA^{(3)} + A^{(1)} \wedge H^{(3)}. \tag{1.14}$$

If we identify $\phi, B^{(2)}, A^{(1)}$ and $A^{(3)}$ with the dilaton, B-field, Ramond-Ramond (R-R) 1-form and R-R 3-form, we can find that this is nothing but the bosonic action of the IIA SUGRA in the string frame up to overall constant[3]. This overall constant can agree with the one of IIA SUGRA if we impose

$$\frac{2\pi R_{11}}{2\kappa_{11}^2} = \frac{1}{2\kappa_{10}^2} = \frac{2\pi}{(2\pi l_s)^8 g_s^2}, \tag{1.15}$$

where κ_{10}, l_s and g_s are the ten-dimensional gravitational coupling constant, string length and string coupling, respectively. This matching and eq. (1.11) imply that a physical distance L in unit of l_p and l_s are related with each other by

$$\frac{L}{l_p} = e^{-\phi/3}\frac{L}{l_s}. \tag{1.16}$$

Recalling the string coupling g_s is given as the vacuum expectation value of the dilaton, we find

$$l_p = g_s^{1/3} l_s. \tag{1.17}$$

Combining this with (1.15) leads us to

$$R_{11} = g_s^{2/3} l_p = g_s l_s. \tag{1.18}$$

Thus we have seen that the 11d SUGRA compactified on S^1 with the appropriate radius is identical to the IIA SUGRA. While the eleventh dimension is almost shrunk in weak string coupling regime, it opens in strong g_s region. So far we have discussed only at supergravity level. Then what will happen for the strong coupling limit of the type IIA superstring theory? This is the idea of the M-theory. Remaining of this section is devoted to arguments from the point of view of D-branes [49]. This motivates existence of M-theory.

1.1.2 Black brane solutions in eleven-dimensional supergravity

p-form gauge field naturally couples to $(p-1)$-dimensionally extended object. In the IIA SUGRA, these object appear as a kind of black hole (brane) solutions [58, 59], which have been identified with fundamental string, D-branes and NS5-brane in the type IIA superstring theory. It is natural to suspect that the 3-form and its magnetic dual in the 11d SUGRA imply black 2-brane and 5-brane solutions. Here we discuss that the 11d SUGRA indeed also have such solutions as BPS solutions [56, 57] corresponding to M2-brane and M5-brane in M-theory.

The BPS solutions of the 11d SUGRA satisfy

$$\delta\psi_M \;=\; 2\nabla_M(\omega^{(0)})\epsilon + \frac{1}{144}\left(\Gamma^{PQRS}{}_M + 8\Gamma^{QRS}\delta_M^{\ P}\right) F^{(4)}_{PQRS}\epsilon = 0, \tag{1.19}$$

where we set $\psi_M = 0 = \bar{\psi}_M$. We can show that the solutions for this equation also solves the equation of motion (EOM) in this theory. This solution is stable [60] thanks to the BPS bound [61, 62].

[3] Although we have seen the agreement only for the bosonic part, the fermionic part also agrees with the one of the IIA SUGRA up to the (same) overall constant.

M2-brane solution

Let us consider the black 2-brane solution [56]. If we expect parallel 2-brane on flat space as a simplest situation, then such a solution should have $SO(2,1) \times SO(8)$ Lorenz symmetry. Thus we consider the following ansatz:

$$\begin{aligned} ds^2 &= f_1(r)dx_\mu dx^\mu + f_2(r)dy^I dy^I, \\ F^{(4)} &= f_3(r)dx_0 \wedge dx_1 \wedge dx_2 \wedge dr, \quad \text{others} = 0, \end{aligned} \tag{1.20}$$

where we parametrize $x^M = (x^{\mu=0,1,2}, y^{I=1,\cdots,8})$ and $r^2 = y^I y^I$. Substituting this ansatz to eq. (1.19) and EOM, we find

$$f_1(r) = H_2(r)^{-2/3}, \quad f_2(r) = H_2(r)^{1/3}, \quad f_3(r) = -\frac{\partial}{\partial r}H_2(r)^{-1} \quad \text{with } H_2(r) = 1 + \frac{R_2^6}{r^6}, \tag{1.21}$$

where R_2 is a constant related to the electric charge as we will see below. In order to study the electric charge, we introduce the dual 7-form as

$$F^{(7)} = \star F^{(4)} - \frac{1}{2}C \wedge F^{(4)}, \tag{1.22}$$

where $\star$ denotes the Hodge dual. Here the second term is necessary for satisfying $dF^{(7)} = 0$ since we have the topological coupling $\int C \wedge F^{(4)} \wedge F^{(4)}$. Then the electric charge q_e of the 2-brane is given by

$$q_e = \int_{S^7} 4^{(7)} = 6R_2^6 V_{S^7} = 2\pi^4 R_2^6, \tag{1.23}$$

where the integration is performed over S^7 enclosing the 2-brane and $V_{S^7} = \pi^4/3$ is the volume of S^7.

R_2 can be denoted also by the 2-brane tension T_{M_2}. Let us consider the asymptotic infinity $r \gg 1$ and Newtonian limit $G_{00} \gg G_{MN}$ $(M, N \neq 0)$ with the static N branes contribution

$$T_{\mu\nu} = NT_{M_2}\delta^{(8)}(y_I)\eta_{\mu\nu}, \quad T_{IJ} = 0. \tag{1.24}$$

where T_{MN} is the energy-momentum tensor. Then we can approximate G_{00} as[4]

$$G_{00} = -\left(1 + \frac{R_2^6}{r^6}\right)^{-2/3} \simeq -1 + \frac{2}{3}\frac{R_2^6}{r^6}. \tag{1.26}$$

In this approximation, the Einstein equation

$$R_{MN} - \frac{1}{2}G_{MN}R = \kappa_{11}^2 NT_{MN} \quad \Longrightarrow \quad R = -\frac{2\kappa_{11}^2}{3}NT_{M_2}\delta^{(8)}(y_I) \tag{1.27}$$

reduces to

$$\nabla_I^2\left(\frac{1}{r^6}\right) = -\frac{2\kappa_{11}^2 NT_{M_2}}{R_2^6}\delta^{(8)}(y_I) \tag{1.28}$$

[4]Recall that the scalar curvature R at first order of the metric perturbation:$G_{MN} = \eta_{MN} + h_{MN}$ is given by

$$R = \nabla^M\nabla^N h_{MN} - \nabla^2(G^{MN}h_{MN}). \tag{1.25}$$

By using $\nabla_I^2 r^{-6} = -6V_{S^7}\delta^{(8)}(y_I)$, we obtain

$$R_2^6 = \frac{\kappa_{11}^2}{3V_{S^7}} T_{M_2} = 128\pi^4 l_p^9 N T_{M_2}. \tag{1.29}$$

M5-brane solution

Next we consider parallel N 5-branes on flat space [57]. Then the black 5-brane solution should have $SO(5,1)\times SO(5)$ Lorenz symmetry. Thus we consider the following ansatz:

$$\begin{aligned} ds^2 &= g_1(r)dx_\mu dx^\mu + g_2(r)dy^I dy^I, \\ \star F^{(4)} &= g_3(r)dx_0 \wedge dx_1 \wedge dx_2 \wedge dr, \quad \text{others} = 0, \end{aligned} \tag{1.30}$$

where we parametrize $x^M = (x^{\mu=0,1,\cdots,5}, y^{I=1,\cdots,5})$ and $r^2 = y^I y^I$ again. From this ansatz, eq. (1.19) and EOM, we obtain

$$g_1(r) = H_5(r)^{-1/3}, \quad g_2(r) = H_5(r)^{2/3}, \quad g_3(r) = -\frac{\partial}{\partial r} H_5(r)^{-1} \quad \text{with } H_5(r) = 1 + \frac{R_5^3}{r^3}, \tag{1.31}$$

where R_5 is a constant related to the magnetic charge of 5-brane by

$$q_m = \int_{S^4} \star F^{(4)} = 3R_5^3 V_{S^4} = 8\pi^2 R_5^3, \tag{1.32}$$

where S^4 enclose the 5-brane and the volume V_{S^4} of S^4 is given by $V_{S^4} = 8\pi^2/3$. Similarly for the 2-brane case, R_5 is given in terms of T_{M_5} by

$$R_5^3 = \frac{\kappa_{11}^2}{3V_{S^4}} N T_{M_5} = 32\pi^6 l_p^9 N T_{M_5}. \tag{1.33}$$

Moreover, the Dirac quantization condition [63]

$$\frac{1}{2\kappa_{11}^2} q_e q_m = 2\pi \mathbf{Z} \tag{1.34}$$

gives the important relation

$$T_{M_2} T_{M_5} = \frac{1}{(2\pi)^7 l_p^9}. \tag{1.35}$$

In next subsection we show that tensions of fundamental string, NS5-brane and D-branes in the type IIA superstring theory can be understood from M-theory if we assign

$$T_{M_2} = \frac{1}{(2\pi)^2 l_p^3}, \quad T_{M_5} = \frac{1}{(2\pi)^5 l_p^6}. \tag{1.36}$$

1.1.3 Type IIA superstring and M-theory

The type IIA superstring theory has fundamental string, NS5-brane and Dp-branes ($p = 0, 2, 4, 8$), whose tensions are given by

$$T_F = \frac{1}{2\pi l_s^2}, \quad T_{NS5} = \frac{1}{g_s^2 (2\pi)^5 l_s^6}, \quad T_{Dp} = \frac{1}{g_s (2\pi)^p l_s^{p+1}}, \tag{1.37}$$

respectively. Here we discuss that these tensions are consistently explained from the M-theory.

- Fundamental string = Wrapped M2-brane on the circle
  First of all, these tensions agree with each other:

$$2\pi R_{11} T_{M_2} = 2\pi g_s l_s \frac{1}{(2\pi)^2 (g_s^{1/3} l_s)^3} = \frac{1}{2\pi l_s^2} = T_F. \tag{1.38}$$

  As an additional check, such a wrapped M2-brane should couple to $C_{\mu\nu 10} \to B_{\mu\nu}^{(2)}$, which couples to the fundamental string. One of more direct evidences is that the Green-Schwarz action of the type IIA superstring can be derived from the classical supermembrane action [64] in eleven dimension by a simultaneous dimensional reduction along the worldvolume and space [65].

- D2-brane = Transverse M2-brane

$$T_{M_2} = \frac{1}{(2\pi)^2 (g_s^{1/3} l_s)^3} = \frac{1}{g_s (2\pi)^2 l_s^3} = T_{D2}. \tag{1.39}$$

  Associated with the compactification, the 3-form field $C_{\mu\nu\rho}$ coupled to the transverse M2-brane reduces to the R-R 3-form $A_{\mu\nu\rho}^{(3)}$ coupled to the D2-branes. In next subsection we will show that in a low energy limit, single M2-brane is identical to single D2-brane in strong coupling limit.

- D4-brane = Wrapped M5-brane on the circle

$$2\pi R_{11} T_{M_5} = 2\pi g_s l_s \frac{1}{(2\pi)^5 (g_s^{1/3} l_s)^6} = \frac{1}{g_s (2\pi)^4 l_s^5} = T_{D4}. \tag{1.40}$$

- NS5-brane = Transverse M5-brane

$$T_{M_5} = \frac{1}{(2\pi)^5 (g_s^{1/3} l_s)^6} = \frac{1}{g_s^2 (2\pi)^5 l_s^6} = T_{NS5}. \tag{1.41}$$

- D0-brane = KK momentum

$$\frac{1}{R_{11}} = \frac{1}{g_s l_s} = T_{D0}. \tag{1.42}$$

  The D0-brane couples to the R-R 1-form coming from the KK gauge field in M-theory.

- D6-brane = KK monopole
  The D6-brane couples to the magnetic dual of the R-R 1-form. The magnetic dual of the KK gauge field in the 11d SUGRA corresponds KK monopole [66, 67]:

$$\frac{1}{2\kappa_{11}^2}(2\pi R_{11})^2 = \frac{1}{g_s(2\pi)^6 l_s^7} = T_{D6}. \tag{1.43}$$

1.2 Single M2-brane

In this section we consider a single M2-brane action and investigate expected properties of an action for arbitrary number of M2-branes. If the number of M2-brane is one, we can write down the action as a summation of a (super-)Nambu-Goto action and minimal coupling to the 3-form C [64]. Let us start with the low-energy limit ($l_p \to 0$) of the action for the flat single M2-brane with $C = 0$ in a static gauge:

$$S_{\rm M2} = \int d^3\xi \left(-\frac{1}{2}\partial_\mu X^I \partial^\mu X^I + \frac{i}{2}\bar{\psi}^A \gamma^\mu \partial_\mu \psi^A\right), \tag{1.44}$$

where $\mu = 0, 1, 2$, $I = 1, \cdots, 8$ and $A = 1, \cdots, 8$. X^I, ψ^A and $\bar{\psi}^A$ are functions of the world-volume coordinate ξ^μ. This is the free field theory with $\mathcal{N} = 8$ supersymmetry, conformal symmetry and $SO(8)$ R-symmetry. Since the superpotential is trivial, its moduli space $\mathcal{M}$ is simply given by

$$\mathcal{M} = \mathbb{R}^8, \tag{1.45}$$

which corresponds to the single M2-brane on $\mathbb{R}^8$. This action have a relation with an action for single flat D2-brane coupled to a worldvolume gauge field A_μ as we will see below. The low-energy limit ($l_s \to 0$) is the three-dimensional $U(1)$ $\mathcal{N} = 8$ super Yang-Mills theory, whose action is

$$S_{\rm D2} = \frac{1}{g_{\rm YM}^2}\int d^3\xi \left(-\frac{1}{2}\partial_\mu X^i \partial^\mu X^i - \frac{1}{4}F_{\mu\nu}F^{\mu\nu} + \frac{i}{2}\bar{\psi}^A \gamma^\mu \partial_\mu \psi^A\right), \tag{1.46}$$

where $g_{\rm YM}$ is the gauge coupling, $i = 1, \cdots, 7$ and $F_{\mu\nu} = \partial_\mu A_\nu - \partial_\nu A_\mu$. As we already discussed in previous section, we expect that the D2-brane becomes the M2-brane in the strong string coupling limit. Recalling the relation

$$g_{\rm YM}^2 = \frac{g_s}{\sqrt{\alpha'}}, \tag{1.47}$$

such a limit corresponds to the strong gauge coupling limit $g_{\rm YM} \to \infty$.

Indeed we can show that the two theories (1.44) and (1.44) are identical to each other via abelian duality [68, 69]. By adding an auxiliary field B_μ and X^8, we consider the following equivalent Lagrangian:

$$\begin{aligned}
\mathcal{L}_{\rm D2} &= \frac{1}{g_{\rm YM}^2}\left(\frac{1}{2}\epsilon^{\mu\nu\lambda}B_\mu F_{\nu\lambda} - \frac{1}{2}B_\mu^2 + \frac{g_{\rm YM}}{2}X^8 \epsilon^{\mu\nu\lambda}\partial_\mu F_{\nu\lambda} - \frac{1}{2}\partial_\mu X^i \partial^\mu X^i + \frac{i}{2}\bar{\psi}^A \gamma^\mu \partial_\mu \psi^A\right) \\
&= \frac{1}{g_{\rm YM}^2}\left(\frac{1}{2}\epsilon^{\mu\nu\lambda}B_\mu F_{\nu\lambda} - \frac{1}{2}B_\mu^2 - \frac{g_{\rm YM}}{2}(\partial_\mu X^8)\epsilon^{\mu\nu\lambda}F_{\nu\lambda} - \frac{1}{2}\partial_\mu X^i \partial^\mu X^i + \frac{i}{2}\bar{\psi}^A \gamma^\mu \partial_\mu \psi^A\right).
\end{aligned}$$

$$(1.48)$$

Then the conjugate momentum of X^8 is quantized by a charge quantization condition as

$$p = -\frac{1}{g_{\rm YM}} \oint F = \frac{2\pi}{g_{\rm YM}} \mathbf{Z}. \tag{1.49}$$

This means that X^8 satisfies a periodicity condition

$$X^8 \sim X^8 + g_{\rm YM}. \tag{1.50}$$

The EOM of $F_{\nu\lambda}$ gives

$$B_\mu = g_{\rm YM} \partial_\mu X^8. \tag{1.51}$$

Rescaling $X^i \to g_{\rm YM} X^i$ and $\psi^A \to g_{\rm YM} \psi^A$ leads us to

$$S_{\rm D2} = \int d^3\xi \left(-\frac{1}{2} \partial_\mu X^I \partial^\mu X^I + \frac{i}{2} \bar{\psi}^A \gamma^\mu \partial_\mu \psi^A \right). \tag{1.52}$$

Although this is nothing but the classical action $S_{\rm M2}$ of the M2-brane, these are not quantum mechanically equivalent due to the periodicity condition (1.50) generically. This equivalence holds only in the strong coupling limit $g_{\rm YM} \to \infty$. Thus we have shown that the single D2-brane behaves as the single M2-brane in the strong g_s limit.

What do we expect for multiple M2-branes case? From the single M2-brane analysis, we desire the following properties for the low-energy effective theory of N M2-branes:

- Three dimensional conformal symmetry
- $\mathcal{N} = 8$ supersymmetry
- $SO(8)$ R-symmetry
- Moduli space:

  $$\mathcal{M} = \frac{(\mathbb{R}^8)^N}{S_N}, \tag{1.53}$$

  where S_N is a permutation group with degree N. This moduli space denotes indistinguishable N M2-branes on $\mathbb{R}^8$.
- Identical to the strong gauge coupling limit of the three dimensional $U(N)$ $\mathcal{N} = 8$ super Yang-Mills theory, which is the low-energy effective theory of N D2-branes.

In next section we will argue that the AdS/CFT correspondence for M2-branes also demands such properties and some additional constraints.

1.3 AdS/CFT correspondence for M2-branes

In this section we consider AdS/CFT correspondence [16, 17, 18, 19] for M2-branes. The basic idea of AdS/CFT correspondence is that there is a duality between low energy physics of

Superstring Theory or M Theory on a certain geometry by branes
and
Worldvolume theory of the branes.

Although this is still the conjecture, there are many indirect evidences. First we will consider D3-brane case as a most typical example. Next we will apply the idea to M2-brane case.

1.3.1 D3-brane case

Applying the basic idea to D3-brane case, the conjecture becomes

Low Energy Type IIB String Theory on the geometry by D3-branes
$\updownarrow$ dual
Low Energy Worldvolume theory of N coincident D3-branes.

In order to justify and make the correspondence more clearly, we investigate the low energy limit of each case concretely.

Low Energy Physics of D3-branes

Here we consider the same system from two points of view[5]:

1. Regarding D3-branes as end points of open strings
2. Regarding D3-branes as massive charged objects which act as a source for the various supergravity fields

First let us consider the former position in the framework of type IIB string theory, where D3-branes are extended in flat spacetime. There are two excitations which are of closed strings in the bulk and open strings on D3-branes. In the low energy limit $l_s \to 0$, only massless strings can be excited. The closed and open string massless state give the type IIB SUGRA and $\mathcal{N}=4$ $U(N)$ Super Yang-Mills theory (SYM) in the limit, respectively.

Complete effective action of these massless modes have the form

$$S_{\text{eff}} = S_{\text{bulk}} + S_{\text{brane}} + S_{\text{int}}. \tag{1.54}$$

S_{bulk} is the action of type IIB SUGRA with many higher derivative terms generically, which is suppressed in the low energy limit. S_{brane} is generally the action of $\mathcal{N}=4$ $SU(N)$ SYM plus many higher derivative terms, but this is just the action of $\mathcal{N}=4$ $SU(N)$ SYM in the

[5] This explanation follows to the excellent review [70].

low energy limit. $S_{\rm int}$ is interaction terms between the bulk modes and modes on D3-branes, which mainly include interactions obtained by the DBI action.

If we expand these action as power series of κ_{10} and take only $\mathcal{O}(\kappa_{10}^0)$ terms, we will find two decoupled systems: free gravity in the bulk and $\mathcal{N}=4$ SYM. It is easy to see that the leading order of $S_{\rm bulk}$ become the free gravity. For example, writing the metric as $g=\eta+\kappa_{10}h$, the Einstein-Hilbert term becomes

$$\frac{1}{2\kappa_{10}^2}\int\sqrt{-g}R\sim\int(\partial h)^2+\kappa_{10}(\partial h)^2h+\mathcal{O}(\kappa_{10}^2). \tag{1.55}$$

Other terms in the type IIB SUGRA action trivially can be expanded in similar way and higher derivative terms themselves is $\mathcal{O}(\kappa_{10})$. Namely $S_{\rm bulk}$ is the free gravity in the low energy limit. Since all interactions in $S_{\rm int}$ is $\mathcal{O}(\kappa_{10})$, this is also dropped out in the limit. $S_{\rm brane}$ just becomes $\mathcal{N}=4$ SYM since higher derivative terms is also $\mathcal{O}(\kappa_{10})$. Thus we have two decoupled systems in the low energy limit: the free massless particles in the bulk and $\mathcal{N}=4$ SYM.

Geometry made by D3-branes

Next we see the same system from the other point of view. In this point of view, we regard the D3-branes as massive charged objects, which act as a source for the various SUGRA fields. As a conclusion, we will have also two decoupled systems in the low energy limit as for the previous case.

Let us consider the geometry made by the D3-branes. In the extremal case, the geometry is described by the following black D3-brane solution

$$ds^2=A^{-1/2}(-dt^2+dx_1^2+dx_2^2+dx_3^2)+A^{1/2}(dr^2+r^2d\Omega_5^2)\ , \tag{1.56}$$

where

$$A\equiv 1+\frac{R_3^4}{r^4}\quad ,\quad R_3^4\equiv 4\pi g_s\alpha'^2N\ . \tag{1.57}$$

Since g_{tt} is not constant, the energy E_r of an object, which is located at a constant position r and measured by an observer at r, is related to the energy E_∞ of the object measured by an observer at infinity by the redshift factor as

$$E_\infty=f^{-1/4}E_r=\left(\frac{r^4}{r^4+R_3^4}\right)^{1/4}E_r \tag{1.58}$$

This means that the observer at infinity measures the energy of the same object around $r=0$ as very low.

If we take the low energy limit again, then we have two kinds of low energy excitations: massless particles propagating in the bulk with very large wavelength and any excitations in near horizon region. We can see that these two excitations are decoupled from each other in the limit again.

Let us consider the bulk massless particles. They are decoupled from near horizon region because the low energy absorption cross section σ behaves as [71]

$$\sigma\sim\omega^3R_3^8, \tag{1.59}$$

where ω is the incident energy. Similarly it is hard that the excitations around $r = 0$ climb the gravitational potential and escape to the asymptotic region. Namely the near horizon excitations are decoupled from the bulk massless particles.

Correspondence

So far, we have seen the same system from the two points of view and found that both cases have two decoupled systems in the low energy limit. In both cases, one of the decoupled systems is massless particles propagating in the bulk. Therefore it is natural to identify the second decoupled system in the both descriptions. Thus we can arrive at the conjecture that the four-dimensional $\mathcal{N} = 4$ $SU(N)$ Super Yang-Mills theory dimension is dual (or equivalent) to type IIB string theory on near horizon geometry of the extremal black D3-brane solution.

What is the near horizon geometry? If we take the near horizon limit $r \to 0$, the solution (1.56) becomes

$$ds^2 = \frac{R_3^2}{z^2}(-dx_0^2 + dx_1^2 + dx_2^2 + dx_3^2 + dz^2) + R_3^2 d\Omega_5^2 \ , \tag{1.60}$$

where $z \equiv R^2/r$. Note that the first term is the AdS_5 metric in the Poincare coordinate[6]. As a conclusion, the conjecture is

$$\begin{array}{c} \text{Four-dimensional } \mathcal{N} = 4 \ SU(N) \text{ SYM} \\ \updownarrow \ \text{ dual} \\ \text{Type IIB String theory on } AdS_5 \times S^5. \end{array}$$

Symmetry matching

If the conjecture is correct, both theories must have the same symmetries. Surprisingly, symmetries of both theories completely match to each other.

- Supersymmetry
  The number of preserved supercharges of Type IIB superstring theory on the $AdS_5 \times S^5$ background[7] is 32. The $\mathcal{N} = 4$ SYM has usual 16 Poincare supercharges usually called as "Q". However, since this theory is the conformal field theory [73, 74, 75, 76, 77], the $\mathcal{N} = 4$ SYM has more bonus 16 special supercharges, which we can construct by combining special conformal generators K with Poincare supercharges Q as

  $$S \simeq [K, Q] \,. \tag{1.61}$$

  Thus both theories have the same number of supercharges and this is consistent with the conjecture.

[6] We review properties of anti-de Sitter space in appendix A.

[7] Strictly speaking, the full extremal black D3-brane solution has only 16 supercharges. There is the enhancement of supersymmetry because of the near horizon limit. See [72] for detail.

- $SO(4,2)$ symmetry
  While the isometry of AdS_5 is $SO(4,2)$, the conformal symmetry group of $\mathcal{N}=4$ SYM is isomorphic to $SO(4,2)$ group. This is because the Lie algebra of d-dimensional conformal group is isomorphic to the Lie algebra of $SO(d,2)$ group. (See appendix B for detail).

- $SU(4) \sim SO(6)$ symmetry
  While the isometry of S^5 is $SO(6)$, $\mathcal{N}=4$ SYM has $SU_R(4)$ R-symmetry and $SU(4)$ is homomorphic to $SO(6)$.

Coupling Constant and Stringy corrections

We consider corresponding relations between both theories in detail. First, we discuss a relation between coupling constant of the SYM and stringy corrections of string theory. Let us consider natures of the coupling constant of the SYM. In order to see the specialty of D3-branes, we consider more generally coupling constant of the $(p+1)$-dimensional maximally supersymmetric Yang-Mills theory. By a simple dimensional analysis, the gauge coupling $g_{\rm YM}$ of $(p+1)$-dimensional SYM has the dimension[8]

$$[g_{\rm YM}^2] = [\text{mass}]^{3-p}. \tag{1.62}$$

Therefore, the dimensionless effective coupling of the SYM is

$$g_{\rm eff}^2(M) \sim g_{\rm YM}^2 M^{p-3} \tag{1.63}$$

where M is the energy scale of the theory. This shows the following dependence of the effective coupling on the energy scale:

- For $p<3$,

$$\begin{aligned} M \to \text{large} \quad &\Longrightarrow \quad g_{\rm eff}^2 \to \text{small} \\ M \to \text{small} \quad &\Longrightarrow \quad g_{\rm eff}^2 \to \text{large} \end{aligned}$$

- For $p>3$,

$$\begin{aligned} M \to \text{large} \quad &\Longrightarrow \quad g_{\rm eff}^2 \to \text{large} \\ M \to \text{small} \quad &\Longrightarrow \quad g_{\rm eff}^2 \to \text{small} \end{aligned}$$

For $p=3$, the effective coupling is independent of the energy scale M at least classically. Although this is not true quantum theoretically in general $(3+1)$-dimensional gauge theories due to trace anomaly, this is exactly valid for the $\mathcal{N}=4$ SYM since the $\mathcal{N}=4$ SYM is a "quantum" conformal field theory!

How is this fact realized on the string theory side? g_{YM} is related to g_s due to open-closed duality by the relation

$$g_{YM}^2 = 4\pi g_s. \tag{1.64}$$

[8] Here we assign the dimension of gauge fields to $[\text{mass}]^1$.

Although the dilaton is not constant for general p, the dilaton for $p = 3$ is constant. This fact corresponds to that the β function of $\mathcal{N} = 4$ is zero. By using the relation (1.57) between AdS_5(or S^5) radius and string coupling, we obtain

$$\frac{R_3}{l_s} = \lambda^{\frac{1}{4}}. \tag{1.65}$$

This represents the relation between the radius and 'tHooft coupling.

- Weakly coupled: $\lambda \ll 1 \Longrightarrow R \ll l_s$
  In this case, since the near horizon geometry of extremal black D3-brane solution is

  $$ds^2 \sim R^2 \frac{dx \cdot dx + dz^2}{z^2} \tag{1.66}$$

  and (curvature) $\sim \frac{1}{R^2}$, the geometry of dual string theory is strongly curved and it is difficult analysis the system. To make matters worse, SUGRA approximation is not valid in this case since we cannot ignore the string length l_s compared with the scale length R.

- Strongly coupled: $\lambda \gg 1 \Longrightarrow R \gg l_s$
  In this case, we can ignore the string length and the geometry is weakly curved, that is, SUGRA approximation is quite valid in this region. Thus we expect that strong coupling regime in 4-dimensional $\mathcal{N} = 4$ SYM is described by type IIB SUGRA on weakly curved $AdS_5 \times S^5$.

Rank of Gauge Group and Quantum Gravity corrections

In addition, we can see below that quantum effect of gravity is suppressed for the large rank of the gauge group $N \gg 1$. As we discussed in sec 1.1.1, the string length l_s has to do with the Planck length l_p through the string coupling g_s by the relation

$$l_p = g_s^{\frac{1}{4}} l_s.$$

By using $\lambda = 4\pi g_s N$ and $R = \lambda^{\frac{1}{4}} l_s$, one finds

$$N = \frac{1}{4\pi} \frac{\lambda}{g_s} = \frac{1}{4\pi} \frac{R^4}{g_s l_s^4} = \frac{1}{4\pi} \left(\frac{R}{l_p} \right)^4. \tag{1.67}$$

Thus for $N \gg 1$, quantum (loop) effects are suppressed since $R \gg l_p$, namely, we see the physics in the low energy scale compared with the Planck scale. This means that the $\mathcal{N} = 4$ SYM for $\lambda \gg 1, N \gg 1$ is well described by the classical supergravity. Note that this is consistent with the relation between the genus and $1/N$ expansions [78].

Dictionary

We summarize the D3-brane case of the AdS/CFT correspondence in following

- Coupling:
$$g_{YM}^2 = 4\pi g_s.$$
g_{YM} independent of the energy scale $\iff$ dilaton=const.

- Symmetry
$$\begin{pmatrix} \text{4d conformal group} \simeq SO(4,2) \\ SU(4)_R \text{ symmetry} \end{pmatrix} = \begin{pmatrix} AdS_5 \times S^5 \text{ isometry group :} \\ SO(4,2) \times SO(6) \end{pmatrix}$$

- The relation between 't Hooft coupling $\lambda = g_{YM}^2 N$ and the AdS_5 radius R:
$$R = \lambda^{\frac{1}{4}} l_s.$$

1.3.2 M2-brane case

In the spirit of the D3-brane case, let us return to the black M2-brane solution:

$$ds^2 = H_2(r)^{-2/3} dx_\mu dx^\mu + H_2(r)^{1/3} dy^I dy^I, \quad \text{with } H_2(r) = 1 + \frac{R_2^6}{r^6}, \tag{1.68}$$

where we parametrize $x^M = (x^{\mu=0,1,2}, y^{I=1,\cdots,8})$ and $r^2 = y^I y^I$. If we take the near horizon limit again, then we obtain

$$ds^2 = \frac{R_2^2}{4z^2}\left(-dx_0^2 + dx_1^2 + dx_2^2 + dz^2\right) + R_2^2 d\Omega_7^2, \tag{1.69}$$

where $z = R_2^3/(2r^2)$. This spacetime is $AdS_4 \times S^7$, whose isometry group is $SO(3,2) \times SO(8)$. It is known that the 11d SUGRA on $AdS_4 \times S^7$ has 32 supercharges [72], which are twice of ones before the near horizon limit. Thus, if we the AdS/CFT correspondence is true, the low-energy effective theory of multiple M2-branes should also have the three-dimensional conformal symmetry, $SO(8)$ R-symmetry and 32 supersymmetries. This has been also expected from single M2-brane analysis in previous section. From this metric, we fin that the classical 11d SUGRA picture is quite good for $R_2 \gg l_p$. Since R_2 is given by

$$R_2^6 = 32\pi^2 l_p^6 N, \tag{1.70}$$

this region corresponds to $N \gg 1$. Hence, when N is not so large, quantum gravity effect is comparable.

1.4 Multiple M2-branes

From the single M2-brane analysis and implication of the AdS/CFT correspondence, we expect that the low energy effective theory for N M2-branes has the following properties:

- Three dimensional conformal symmetry

- $\mathcal{N} = 8$ supersymmetry

- $SO(8)$ R-symmetry
- Moduli space: $\mathcal{M} = (\mathbb{R}^8)^N/S_N$
- Identical to the three dimensional $U(N)$ $\mathcal{N}=8$ super Yang-Mills theory in the limit $g_{\rm YM} \to \infty$
- Dual to the classical 11d SUGRA on $AdS_4 \times S^7$ for $N \gg 1$.

Such a theory had not been found for long years. There are many reasons for this. One of most serious obstacle is difficulty of quantization of supermembrane [1] while there is a M(atrix) conjecture [2]. This prevents us from finding spectrum and something like a Chan-Paton factor for M2-branes. Another difficulty is that it is not easy to construct gauge theory with conformal and high supersymmetry except for four dimensions. Since Yang-Mills action is scale invariant only for four dimensions, we can use only Chern-Simons term of vector multiplet and marginal term of chiral multiplet for the construction. Indeed in 1990's, a maximal supersymmetric extension of Chern-Simons theory had been $\mathcal{N}=3$ [3, 4] (see also [5]).

Meanwhile the BLG theory [6, 7] based on the Lie 3-algebra $[X^a, X^b, X^c] = f^{abc}{}_d X^d$ appeared. If we take the structure constant f^{abcd} to be totally anti-symmetric, then the BLG theory generically has manifest $\mathcal{N}=8$ supersymmetry, $SO(8)$ R-symmetry and conformal symmetry. In spite of such successful structures, it is known that the only nontrivial solution for a generalized Jacobi identity is the A_4 algebra defined by $f^{abcd} = \epsilon^{abcd}$ [8, 9]. Then the resulting A_4 BLG theory can be rewritten as the $SU(2) \times SU(2)$ Chern-Simons matter theory[9] with a Chern-Simons level k [10]. Actually moduli space analysis of this theory [11, 12] implies that the interpretation as two indistinguishable M2-branes on $\mathbb{R}^8/\mathbf{Z}_k$ can be possible only for $k=1$ and $k=2$. After proposed the BLG theory, it has been found that $\mathcal{N}=4$ superconfomal Chern-Simons theory can be constructed by a type of quiver gauge theory [13, 14].

In 2008, Aharony, Bergman, Jafferis and Maldacena (ABJM) [15, 83] has proposed a $U(N) \times U(N)$ theory with Chern-Simons levels k and $-k$ coupled to bi-fundamental matters. The on-shell supersymmetric Lagrangian of the theory is given by

$$
\begin{aligned}
&\mathcal{L}_{U(N)\times U(N)} \\
&= k\,\mathrm{Tr}\Biggl[\frac{1}{2}\epsilon^{\mu\nu\rho}\left(-A_\mu\partial_\nu A_\rho - \frac{2}{3}A_\mu A_\nu A_\rho + \tilde{A}_\mu\partial_\nu\tilde{A}_\rho + \frac{2}{3}\tilde{A}_\mu\tilde{A}_\nu\tilde{A}_\rho\right) \\
&\qquad + \left(-D_\mu\bar{\Phi}^\alpha D^\mu\Phi_\alpha + i\bar{\Psi}^\alpha \not{D}\Psi_\alpha\right) - i\epsilon^{\alpha\beta\gamma\delta}\Phi_\alpha\bar{\Psi}_\beta\Phi_\gamma\bar{\Psi}_\delta + i\epsilon_{\alpha\beta\gamma\delta}\bar{\Phi}^\alpha\Psi^\beta\bar{\Phi}^\gamma\Psi^\delta \\
&\qquad + i\left(-\bar{\Psi}_\beta\Phi_\alpha\bar{\Phi}^\alpha\Psi^\beta + \Psi_\beta\bar{\Phi}_\alpha\Phi^\alpha\bar{\Psi}^\beta + 2\bar{\Psi}_\alpha\Phi_\beta\bar{\Phi}^\alpha\Psi^\beta - 2\Psi^\beta\bar{\Phi}^\alpha\Phi_\beta\bar{\Psi}_\alpha\right) \\
&\qquad + \frac{1}{3}\left(\Phi_\alpha\bar{\Phi}^\beta\Phi_\beta\bar{\Phi}^\gamma\Phi_\gamma\bar{\Phi}^\alpha + \Phi_\alpha\bar{\Phi}^\alpha\Phi_\beta\bar{\Phi}^\beta\Phi_\gamma\bar{\Phi}^\gamma\right.
\end{aligned}
$$

[9] Although this is actually the same as the $SU(2) \times SU(2)$ ABJM theory, the moduli space of this theory is different from expected one except for $k=2$. However, analysis by dual photon formulation and superconformal index [79] strongly support that a quotient of the BLG theory is isomorphic [80, 81, 82] to the $U(2) \times U(2)$ ABJM theory with some values of Chern-Simons level.

$$+4\Phi_\beta\bar{\Phi}^\alpha\Phi_\gamma\bar{\Phi}^\beta\Phi_\alpha\bar{\Phi}^\gamma - 6\Phi_\gamma\bar{\Phi}^\gamma\Phi_\beta\bar{\Phi}^\alpha\Phi_\alpha\bar{\Phi}^\beta\Big)\Bigg],$$

where A_μ and $\tilde{A}_\mu$ are $U(N)$ gauge fields, and Φ_α and Ψ_α ($\alpha = 1,2,3,4$) are bosonic and fermionic complex bi-fundamental fields, respectively. This theory has manifest $\mathcal{N} = 6$ supersymmetry for arbitrary integer k and the supersymmetry is enhanced to $\mathcal{N} = 8$ supersymmetry for $k = 1,2$ on quantum level [84]. The moduli space of this theory is given by

$$\mathcal{M} = \frac{(\mathbb{R}^8/\mathbf{Z}_k)^N}{S_N}, \tag{1.71}$$

which is the same as the moduli space of N M2-branes on $\mathbb{R}^8/\mathbf{Z}_k$. For $k = 1$, this is the desired moduli space.

Gravity dual

Let us consider the black 2-brane solution corresponding to N M2-branes on $\mathbb{R}^8/\mathbf{Z}_k$ in the 11d SUGRA. Such a solution is given by

$$\begin{aligned} ds_{11}^2 &= H(r)^{-2/3}(-dt^2 + dx_1^2 + dx_2^2) + H(r)^{1/3} ds^2_{\mathbb{R}^8/\mathbb{Z}_k}, \\ F^{(4)} &= dt \wedge dx_1 \wedge dx_2 \wedge dH^{-1}, \end{aligned} \tag{1.72}$$

where the harmonic function $H(r)$ is

$$H(r) = 1 + \frac{Q}{r^6}, \quad \text{with} \quad Q = 32\pi^2(kN)l_p^6. \tag{1.73}$$

If we take the near-horizon limit, then we obtain $AdS_4 \times S^7/\mathbf{Z}_k$ as

$$\begin{aligned} ds_{11}^2 &= \frac{R_k^2}{4z^2}\left(-dx_0^2 + dx_1^2 + dx_2^2 + dz^2\right) + R_k^2 ds^2_{S^7/\mathbf{Z}_k}, \\ F^{(4)} &= \frac{3}{8}R_k^2\epsilon_4. \end{aligned} \tag{1.74}$$

where $R_k = (2^5\pi^2 kN)^{1/6} l_p$ and ϵ_4 is the unit volume form on AdS_4.

Here we regard $S^7/\mathbf{Z}_k$ as the Hopf fibration of $\mathbf{C}P^3$,

$$ds^2_{S^7/\mathbf{Z}_k} = \frac{1}{k^2}(d\phi + k\omega)^2 + ds^2_{\mathbf{C}P^3} \tag{1.75}$$

where $\phi = 0 \sim \phi = 2\pi$ and $d\omega = J$. Since the radius of the eleventh circle in the unit of Planck length is

$$R_{11} = \frac{R_k}{kl_p} = \left(\frac{2^5\pi^2 N}{k^5}\right)^{1/6}, \tag{1.76}$$

we can trust the 11d SUGRA picture only for $k \ll N^{1/5}$.

For $k \gg N^{1/5}$, the M-theory circle shrinks to zero. Then the dimensional reduction of the solution (1.74):

$$ds_{10}^2 = \frac{R_k^3}{k}\left(\frac{1}{4}ds^3_{AdS_4} + ds^2_{\mathbf{C}P^3}\right), \quad e^{2\Phi} = \frac{R_k^3}{k^3} \quad , \quad F_2 = kJ \quad , \quad \tilde{F}_4 = \frac{3}{8}R^3\epsilon_4, \tag{1.77}$$

solves the equation of motion of the type IIA supergravity[10]. Since the curvature radius is given by

$$\sqrt{\frac{R_k^3}{k}} = \left(\frac{2^5\pi^2 N}{k}\right)^{1/4}, \tag{1.78}$$

the type IIA SUGRA picture should be valid only for $N^{1/5} \ll k \ll N$.

[10]Here we set $\alpha' = 1$.

2 Localization method

In this chapter we introduce the localization method [29] and apply the method to general 3d $\mathcal{N}=2$ supersymmetric field theory on S^3 [32, 47, 48]. which includes the ABJM theory as a specific case[11]. The method enables us to denote a class of supersymmetric observables in terms of a matrix model. This chapter is organized as follows. In section 2.1 we introduce the localization method with a simple example. In section 2.2 we construct $\mathcal{N}=2$ supersymmetric field theory with rigid supersymmetry. In section 2.3 we apply the localization to 3d $\mathcal{N}=2$ supersymmetric field theory on S^3. In section 2.4 we specify the argument to the ABJM theory.

2.1 Basic idea

Let us consider the partition function of a field theory,

$$Z=\int \mathcal{D}\Phi\ e^{-S[\Phi]}, \tag{2.1}$$

where Φ represents the collection of the components fields. Let us suppose that the action is invariant under an charge Q of a fermionic off-shell symmetry. If we assume the absence of the boundary term, this is equivalent to $QS[\Phi]=0$. Then the closure of the algebra requires $Q^2=\mathcal{L}_B$, where $\mathcal{L}_B$ is the generator of a bosonic symmetry the theory has. The first step of the localization method is to consider the deformation by a Q-exact term as

$$Z(t)=\int \mathcal{D}\Phi\ e^{-S[\Phi]-tQV[\Phi]}, \tag{2.2}$$

where V is any fermionic functional satisfying $\mathcal{L}_BV[\Phi]=0$. By taking the derivative with respect to t, we obtain

$$\begin{aligned}\frac{dZ(t)}{dt}=-\int \mathcal{D}\Phi\ (QV[\Phi])e^{-S[\Phi]-tQV[\Phi]} &= -\int \mathcal{D}\Phi\ Q\left(V[\Phi]e^{-S[\Phi]-tQV[\Phi]}\right)\\ &= \int (Q\mathcal{D}\Phi)\ V[\Phi]e^{-S[\Phi]-tQV[\Phi]}.\end{aligned} \tag{2.3}$$

If we assume the Q-invariance of the measure ($Q\mathcal{D}\Phi=0$), namely that Q is non-anomalous, then the deformed partition function $Z(t)$ should be independent of the parameter t. This implies that the original partition function Z can be written as

$$Z=\lim_{t\to+0}Z(t)=Z(t)=\lim_{t\to\infty}\int \mathcal{D}\Phi\ e^{-S[\Phi]-tQV[\Phi]}. \tag{2.4}$$

In this limit, the saddle point approximation around the classical solution to $QV=0$ becomes exact. Hence we obtain

$$Z=\sum_{\Phi_0}\exp(-S[\Phi_0])Z_{1-\mathrm{loop}}(\Phi_0), \tag{2.5}$$

[11] The localization of the ABJM theory and related theories on various spaces has also been considered: $S^1\times S^2$ [85, 86], squashed S^3 [87, 88], lens space [89, 90, 91] and Seifert manifold [92].

where Φ_0 is the 'localized' configuration determined by $(QV)[\Phi_0] = 0$. The summation $\sum_{\Phi_0}$ over the saddle points should be understood as an integration if the saddle points are labeled by continuous parameters. The one-loop determinant $Z_{1-\text{loop}}$ around Φ_0 is given by

$$Z_{1-\text{loop}} = \lim_{t\to\infty} \int \mathcal{D}(\delta\Phi)\ e^{-tQV[\Phi]}\Big|_{\Phi=\Phi_0+\delta\Phi}. \tag{2.6}$$

We can also use this method to calculate Q-invariant operators such as supersymmetric Wilson loops. Then the expectation value is formally written as

$$\langle \mathcal{O} \rangle = \frac{\sum_{\Phi_0} \mathcal{O}(\Phi_0) \exp(-S[\Phi_0]) Z_{1-\text{loop}}(\Phi_0)}{\sum_{\Phi_0} \exp(-S[\Phi_0]) Z_{1-\text{loop}}(\Phi_0)}. \tag{2.7}$$

Such a technique was applied [29] to 4d $\mathcal{N} = 4$ super Yang-Mills theory, and some conjecture on the half-BPS Wilson loops[12] [30, 31] has been confirmed.

Example: Zero-dimensional supersymmetric field theory

Let us consider the zero-dimensional field theory as a simple example whose action is given by

$$S(X, B, \psi_1, \psi_2) = \frac{1}{2}B^2 + iB(\partial_X h) - \left(\partial_X^2 h\right) \psi_1\psi_2, \tag{2.8}$$

where $h = h(X)$ is a degree-n polynomial of a real scalar X and $\psi_{1(2)}$ is the fermionic field. The action is invariant under the following supersymmetric transformations off-shell :

$$\begin{array}{rcl} \delta_1 X &=& \epsilon^1\psi_1 \\ \delta_1 B &=& 0 \\ \delta_1\psi_1 &=& 0 \\ \delta_1\psi_2 &=& -i\epsilon^1 B \end{array} \quad \text{and} \quad \begin{array}{rcl} \delta_2 X &=& -\epsilon^2\psi_2 \\ \delta_2 B &=& 0 \\ \delta_2\psi_1 &=& -i\epsilon^2 B \\ \delta_2\psi_2 &=& 0 \end{array}. \tag{2.9}$$

The partition function of the theory is exactly evaluated as

$$\begin{aligned} Z &= \frac{1}{2\pi}\int dXdBd\psi_1 d\psi_2\ e^{-\frac{1}{2}B^2 + iB(\partial_X h) + (\partial_X^2 h)\psi_1\psi_2} \\ &= \frac{1}{\sqrt{2\pi}}\int dX\ (\partial_X^2 h) e^{-\frac{1}{2}(\partial_X h)^2} \\ &= \frac{1}{\sqrt{2\pi}}\int dy\ e^{-\frac{1}{2}y^2} \quad (y = \partial_X h) \\ &= \begin{cases} 0 & \text{for } n : \text{odd} \\ \text{sign}\,(\partial_X^n h) & \text{for } n : \text{even} \end{cases}. \end{aligned} \tag{2.10}$$

We can also derive this result by using the localization method. From the supersymmetric transformations (2.9), we can easily show $\delta_{1(2)}^2 = 0$ and $[\delta_1, \delta_2] = 0$. This structure leads us to apply the localization method to the theory. Because the action is written as $\delta_1\delta_2$-exact as

$$\delta_1\delta_2\left(\frac{1}{2}\psi_1\psi_2 - h\right) = (\epsilon^1\epsilon^2)S = (\epsilon^1\epsilon^2)\left[\frac{1}{2}\left(B + i(\partial_X h)\right)^2 + \frac{1}{2}(\partial_X h)^2 - (\partial_X^2 h)\psi_1\psi_2\right], \tag{2.11}$$

[12]This formula is also reproduced by a numerical simulation in the large-N limit [26, 27].

we choose the action itself as QV. The localization configuration is given by

$$B + i\partial_X h = 0, \quad \partial_X h = 0, \quad \psi_1 = 0, \quad \psi_2 = 0. \tag{2.12}$$

If we consider the fluctuation $X \to x_0 + \frac{1}{\sqrt{t}}X, B \to \frac{1}{\sqrt{t}}B, \psi_1 \to \frac{1}{\sqrt{t}}\psi_1, \psi_2 \to \frac{1}{\sqrt{t}}\psi_2$ around the configuration, then the quadratic action over the fluctuation is given by

$$tQV|_{\text{Gaussian}} = \frac{1}{2}\left(B + ih''(x_0)(X - x_0)\right)^2 + \frac{1}{2}h''(x_0)(X - x_0)^2 - \frac{1}{2}h''(x_0)\psi_1\psi_2, \tag{2.13}$$

where x_0 is defined by $\partial_X h|_{X=x_0} = 0$. From the action we obtain the 1-loop determinant as

$$Z_{1-\text{loop}}(x_0) = 2\pi \frac{h''(x_0)}{|h''(x_0)|}. \tag{2.14}$$

Since the classical contribution is zero, the partition function via the localization method is

$$Z = \sum_{x_0} \frac{h''(x_0)}{|h''(x_0)|} = \; = \begin{cases} 0 & \text{for } n : \text{odd} \\ \text{sign}\left(\partial_X^n h\right) & \text{for } n : \text{even} \end{cases},$$

which is the same as the direct result (2.10).

2.2 3d $\mathcal{N} = 2$ supersymmetric field theory on S^3

In this section we construct 3d $\mathcal{N} = 2$ supersymmetric field theory on S^3 with rigid supersymmetry and investigate structures of the supersymmetry. We mainly follow the notation of [48].

2.2.1 Killing spinor and Killing vector on S^3

Let us consider the three-sphere with the radius l. We parametrize the unit S^3 as an element g of the Lie group $SU(2)$

$$\begin{aligned} g &= e^{i\alpha\gamma_3} e^{i\theta\gamma_2} e^{i\beta\gamma_3} && (2.15) \\ &= \begin{pmatrix} e^{i(\alpha+\beta)}\cos\theta & -e^{i(\alpha-\beta)}\sin\theta \\ -e^{-i(\alpha-\beta)}\sin\theta & e^{-i(\alpha+\beta)}\cos\theta \end{pmatrix}, && (2.16) \end{aligned}$$

where γ^a $(a = 1, 2, 3)$ are Pauli matrices and $0 \leq \theta \leq \frac{\pi}{2}, 0 \leq \alpha \leq \pi, 0 \leq \beta \leq 2\pi$. From the parametrization we define the left and right invariant 1-form $\mu, \tilde{\mu}$ in the following way:

$$g^{-1}dg = i\mu^a\gamma^a, \quad dgg^{-1} = i\tilde{\mu}^a\gamma^a \tag{2.17}$$

which satisfy the Maurer-Cartan equation

$$d\mu^a = \epsilon^{abc}\mu^b \wedge \mu^c, d\tilde{\mu}^a = -\epsilon^{abc}\tilde{\mu}^b \wedge \tilde{\mu}^c. \tag{2.18}$$

The 1-forms give the metric of S^3 as

$$ds^2 = \frac{1}{2}l^2 \text{tr}\left(dgdg^{-1}\right) = l^2\mu^a\mu^a = l^2\tilde{\mu}^a\tilde{\mu}^a$$

$$= \quad l^2\Big[d\theta^2 + \sin^2 2\theta d\alpha^2 + (d\beta + \cos 2\theta d\alpha)^2\Big]. \tag{2.19}$$

We use below the vielbein and spin connection in the left-invariant frame given by

$$e^a = e^a_\mu dx^\mu, \quad \omega^{ab} = \epsilon^{abc}\mu^c. \tag{2.20}$$

Since S^3 is curved, Killing spinors on S^3 are no longer constant. The Killing spinor equation on S^3 is given by (see [93] for example)

$$\nabla_\mu \epsilon \equiv \left(\partial_\mu + \frac{1}{4}\gamma^{ab}\omega^{ab}_\mu\right)\epsilon = \gamma_\mu \tilde{\epsilon}, \tag{2.21}$$

where $\gamma^{ab} = \frac{1}{2}[\gamma^a, \gamma^b] = i\epsilon^{abc}\gamma^c$ and $\tilde{\epsilon} = \frac{1}{3}\gamma^\mu \nabla_\mu \epsilon$. The solutions of this equation are

$$\begin{cases} \epsilon = \epsilon_0, & \tilde{\epsilon} = +\frac{i}{2l}\epsilon \\ \epsilon = g^{-1}\epsilon_0, & \tilde{\epsilon} = -\frac{i}{2l}\epsilon \end{cases}, \tag{2.22}$$

where ϵ_0 is a constant spinor. The first(second) solution is constant in the left(right)-invariant frame.

The Killing vector $\mathcal{R}^a = \mathcal{R}^{a\mu}\frac{\partial}{\partial x^\mu}$ generating the right action is determined by $\mathcal{R}^a g = ig\gamma^a$. This is proportional to the inverse of vielbein explicitly given by

$$\begin{aligned} \mathcal{R}^1 &= -\sin(2\beta)\frac{\partial}{\partial\theta} + \cos(2\beta)\left(\frac{1}{\sin(2\theta)}\frac{\partial}{\partial\alpha} - \cot(2\theta)\frac{\partial}{\partial\beta}\right) \\ \mathcal{R}^2 &= \cos(2\beta)\frac{\partial}{\partial\theta} + \sin(2\beta)\left(\frac{1}{\sin(2\theta)}\frac{\partial}{\partial\alpha} - \cot(2\theta)\frac{\partial}{\partial\beta}\right) \\ \mathcal{R}^3 &= \frac{\partial}{\partial\beta}. \end{aligned} \tag{2.23}$$

If we introduce $J^a = \frac{1}{2i}\mathcal{R}^a$ from the Killing vector, then J^a satisfies the $SU(2)$ commutation relation as

$$[J^a, J^b] = i\epsilon^{abc}J^c. \tag{2.24}$$

2.2.2 Actions and symmetries

We construct 3d $\mathcal{N}=2$ supersymmetric field theory on S^3 with off-shell supersymmetry. Note that we will take spinors in the Euclidean space, which cannot take reality condition contrary to the Minkowski signature. Although off-shell supersymmetry on S^3 recently has been understood from supergravity [94], we do not discuss the detail.

Yang-Mills part

We begin with the 3d $\mathcal{N}=2$ Super Yang-Mills theory (SYM) on S^3. Although the ABJM theory does not the Yang-Mills term, this part is important in the context of the localization as we will discuss below. The three-dimensional $\mathcal{N}=2$ vector multiplet consists of

$$(A_\mu, \sigma, D, \lambda, \bar{\lambda}), \tag{2.25}$$

where A_μ, σ, D are the gauge field, adjoint scalar and auxiliary field, respectively. λ and $\bar{\lambda}$ are the gauginos given by two-component spinors. The action of the $\mathcal{N}=2$ SYM on S^3 is given by

$$\begin{aligned} S_{\rm YM} &= \frac{1}{g_{\rm YM}^2}\int d^3x\sqrt{g}\ {\rm Tr}\Big[\frac{1}{4}F_{\mu\nu}^2+\frac{1}{2}(D_\mu\sigma)^2+\frac{1}{2}\left(D+\frac{\sigma}{l}\right)^2 \\ &\qquad +\frac{i}{2}\bar{\lambda}\gamma^\mu D_\mu\lambda+\frac{i}{2}\bar{\lambda}[\ \sigma,\lambda\ ]-\frac{1}{4l}\bar{\lambda}\lambda\Big], \end{aligned} \tag{2.26}$$

where $D_i(\cdot)=\partial_i(\cdot)-i[\ A_i,\cdot\ ]$. As a convention for the fermionic bilinear product, we take

$$\bar{\psi}\chi=\bar{\psi}^\alpha C_{\alpha\beta}\chi^\beta \tag{2.27}$$

for all spinors with the charge conjugation matrix C. In this convention, note that

$$\bar{\psi}\chi=\chi\bar{\psi},\quad \bar{\psi}\gamma^\mu\chi=-\chi\gamma^\mu\bar{\psi}. \tag{2.28}$$

The action is invariant under the following supersymmetric transformation:

$$\begin{aligned} \delta A_a &= -\frac{i}{2}(\bar{\epsilon}\gamma_a\lambda-\bar{\lambda}\gamma_a\epsilon) \\ \delta\sigma &= \frac{1}{2}(\bar{\epsilon}\lambda-\bar{\lambda}\epsilon) \\ \delta\lambda &= \frac{1}{2}\gamma^{ab}\epsilon F_{ab}-D\epsilon+i\gamma^a\epsilon D_a\sigma+\frac{2i}{l}\sigma\tilde{\epsilon} \\ \delta\bar{\lambda} &= \frac{1}{2}\gamma^{ab}\bar{\epsilon}F_{ab}+D\bar{\epsilon}-i\gamma^a\bar{\epsilon}D_a\sigma-\frac{2i}{l}\sigma\tilde{\bar{\epsilon}} \\ \delta D &= -\frac{i}{2}\bar{\epsilon}\gamma^a D_a\lambda-\frac{i}{2}D_a\bar{\lambda}\gamma^a\epsilon+\frac{i}{2}[\bar{\epsilon}\lambda+\bar{\lambda}\epsilon,\sigma]+\frac{i}{2l}(\tilde{\bar{\epsilon}}\lambda-\bar{\lambda}\tilde{\epsilon}). \end{aligned} \tag{2.29}$$

Again ϵ and $\bar{\epsilon}$ are independent of each other since we consider the spinors in the Euclidean space.

Next we consider the algebra generated by the supersymmery. Decomposing the transformation as $\delta=\delta_\epsilon+\delta_{\bar{\epsilon}}$, $[\delta_\epsilon,\delta_{\bar{\epsilon}}]$ for each field is given by

$$\begin{aligned} [\delta_\epsilon,\delta_{\bar{\epsilon}}]\,A_\mu &= \xi^\nu\partial_\nu A_\mu+\partial_\mu\xi^\nu A_\nu+D_\mu\Lambda \\ [\delta_\epsilon,\delta_{\bar{\epsilon}}]\,\sigma &= \xi^\mu\partial_\mu\sigma+i[\Lambda,\sigma]+\rho\sigma \\ [\delta_\epsilon,\delta_{\bar{\epsilon}}]\,\lambda &= \xi^\mu\partial_\mu\lambda+\frac{1}{4}\Theta_{\mu\nu}\gamma^{\mu\nu}\lambda+i[\Lambda,\lambda]+\frac{3}{2}\rho\lambda+\alpha\lambda \\ [\delta_\epsilon,\delta_{\bar{\epsilon}}]\,\bar{\lambda} &= \xi^\mu\partial_\mu\bar{\lambda}+\frac{1}{4}\Theta_{\mu\nu}\gamma^{\mu\nu}\bar{\lambda}+i[\Lambda,\bar{\lambda}]+\frac{3}{2}\rho\bar{\lambda}-\alpha\bar{\lambda} \\ [\delta_\epsilon,\delta_{\bar{\epsilon}}]\,D &= \xi^\mu\partial_\mu D+i[\Lambda,D]+2\rho D, \end{aligned} \tag{2.30}$$

where

$$\begin{aligned} \xi^\mu &= i\bar{\epsilon}\gamma^\mu\epsilon \\ \Theta^{\mu\nu} &= D^{[\mu}\xi^{\nu]}+\xi^\lambda\omega_\lambda^{\mu\nu} \\ \Lambda &= -A_\mu\bar{\epsilon}\gamma^\mu\epsilon L\sigma\bar{\epsilon}\epsilon \end{aligned}$$

$$\begin{aligned} \rho &= \frac{i}{3}\left(\bar{\epsilon}\gamma^{\mu}D_{\mu}\epsilon + (D_{\mu}\bar{\epsilon})\gamma^{\mu}\epsilon\right) \\ \alpha &= -\frac{i}{3}\left(\bar{\epsilon}\gamma^{\mu}D_{\mu}\epsilon - (D_{\mu}\bar{\epsilon})\gamma^{\mu}\epsilon\right). \end{aligned} \tag{2.31}$$

Here ξ^{μ}, $\Theta^{\mu\nu}$, Λ, ρ and α denote the parameters of translation, rotation, gauge transformation, dilatation and R-rotation, respectively. While this closes for superconformal field theory as in the ABJM theory, the dilatation hinders closure for non-conformal field theory. However, if we restrict the Killing spinors to the constant solution in the left-invariant frame (the first solution in eq. (2.22)), then the dilatation ρ vanishes and therefore the supersymmety closes also for non-CFT. Hence we use the restricted Killing spinor below.

Chern-Simons part

The ABJM theory has the Chern-Simons (CS) term. The Chern-Simons action for the $\mathcal{N}=2$ vector multiplet is given by

$$S_{CS} = -\frac{ik}{4\pi}\int \mathrm{Tr}\Big[A\wedge dA - \frac{2}{3}iA\wedge A\wedge A + (-\bar{\lambda}\lambda + 2\sigma D)\sqrt{g}d^3x\Big], \tag{2.32}$$

where k is the Chern-Simons level. This action is also invariant under the transformation (2.29). Most important property of the transformation in the context of the localization is that the Lagrangian $\mathcal{L}_{\mathrm{SYM}}$ of the SYM is written as $\delta_{\bar{\epsilon}}\delta_{\epsilon}$-exact:

$$\bar{\epsilon}\epsilon\mathcal{L}_{\mathrm{SYM}} = \delta_{\bar{\epsilon}}\delta_{\epsilon}\mathrm{Tr}\left(\frac{1}{2}\bar{\lambda}\lambda - 2D\sigma\right). \tag{2.33}$$

This fact enables us choose S_{SYM} as the deformation term QV. Then the localization states that $\delta_{\bar{\epsilon}}$ and δ_{ϵ}-invariant observables are independent of the YM coupling g_{YM} since $1/g_{\mathrm{YM}}^2$ plays role as the deformation parameter t in (2.2).

Matter part

The ABJM theory contains the two bi-fundamental and anti-bi-fundamental chiral multiplet. The action of the chiral multiplet with the representation $\mathcal{R}$ under the gauge group G is given by

$$S_{\mathrm{Matter}} = \int d^3x\sqrt{g}\left(\mathcal{L}_{\mathrm{kin}} + \mathcal{L}_{\mathrm{pt}}\right), \tag{2.34}$$

where $\mathcal{L}_{\mathrm{kin}}$ and $\mathcal{L}_{\mathrm{pt}}$ are a supersymmetric kinetic term and a superpotential term with higher powers[13] of the matter fields, respectively. $\mathcal{L}_{\mathrm{kin}}$ is given by

$$\begin{aligned} \mathcal{L}_{\mathrm{kin}} &= \mathrm{Tr}\Bigg[D_{\mu}\bar{\phi}D^{\mu}\phi + \bar{\phi}\sigma^2\phi + \frac{i(2q-1)}{l}\bar{\phi}\sigma\phi + \frac{q(2-q)}{l^2}\bar{\phi}\phi + i\bar{\phi}D\phi + \bar{F}F \\ &\qquad -i\bar{\psi}\gamma^{\mu}D_{\mu}\psi + i\bar{\psi}\sigma\psi - \frac{2q-1}{2l}\bar{\psi}\psi + i\bar{\psi}\lambda\phi - i\bar{\phi}\bar{\lambda}\psi\Bigg], \end{aligned} \tag{2.35}$$

[13] As we mentioned later, this term is irrelevant in the context of the localization method as long as we do not consider mass terms.

where q is the dimension and R-charge of ϕ, which is $1/2$ in the canonical assignment. Here we understand that for example $\bar{\phi}\sigma\phi$ means

$$\bar{\phi}\sigma\phi = \bar{\phi}\sigma^{\alpha}T_{\alpha}\phi, \tag{2.36}$$

where T_{α} is the generator of the gauge group G in the representation $\mathcal{R}$. The action is invariant under the supersymmetric transformation:

$$\begin{aligned}
\delta\phi &= \bar{\epsilon}\psi, \\
\delta\bar{\phi} &= \epsilon\bar{\psi}, \\
\delta\psi &= i\gamma^{a}\epsilon D_{a}\phi + i\epsilon\sigma_{AB}\phi + 2qi\tilde{\epsilon}\phi + \bar{\epsilon}F, \\
\delta\bar{\psi} &= i\gamma^{a}\bar{\epsilon}D_{a}\bar{\phi} + i\bar{\phi}\sigma_{AB}\bar{\epsilon} + 2qi\bar{\phi}\tilde{\bar{\epsilon}} + \bar{F}\epsilon, \\
\delta F &= \epsilon(i\gamma^{a}D_{a}\psi - i\sigma_{AB}\psi - i\lambda\phi) - \frac{i}{l}(2q-1)\tilde{\epsilon}\psi, \\
\delta\bar{F} &= \bar{\epsilon}(i\gamma^{a}D_{a}\bar{\psi} - i\bar{\psi}\sigma_{AB} - i\bar{\phi}\bar{\lambda}) - \frac{i}{l}(2q-1)\tilde{\bar{\epsilon}}\bar{\psi}.
\end{aligned} \tag{2.37}$$

From the transformation we obtain the supersymmetry algebra[14] as

$$\begin{aligned}
[\delta_{\epsilon}, \delta_{\bar{\epsilon}}]\,\phi &= \xi^{\mu}\partial_{\mu}\phi + i\Lambda\phi - q\alpha\phi \\
[\delta_{\epsilon}, \delta_{\bar{\epsilon}}]\,\bar{\phi} &= \xi^{\mu}\partial_{\mu}\bar{\phi} - i\bar{\phi}\Lambda + q\alpha\bar{\phi} \\
[\delta_{\epsilon}, \delta_{\bar{\epsilon}}]\,\psi &= \xi^{\mu}\partial_{\mu}\psi + \frac{1}{4}\Theta_{\mu\nu}\gamma^{\mu\nu}\psi + i\Lambda\psi + (1-q)\alpha\psi \\
[\delta_{\epsilon}, \delta_{\bar{\epsilon}}]\,\bar{\psi} &= \xi^{\mu}\partial_{\mu}\bar{\psi} + \frac{1}{4}\Theta_{\mu\nu}\gamma^{\mu\nu}\bar{\psi} - i\bar{\psi}\Lambda + (q-1)\alpha\bar{\psi} \\
[\delta_{\epsilon}, \delta_{\bar{\epsilon}}]\,F &= \xi^{\mu}\partial_{\mu}F + i\Lambda F + (2-q)\alpha F \\
[\delta_{\epsilon}, \delta_{\bar{\epsilon}}]\,\bar{F} &= \xi^{\mu}\partial_{\mu}\bar{F} - i\bar{F}\Lambda + (q-2)\alpha\bar{F},
\end{aligned} \tag{2.38}$$

which closes off-shell. One of important property of the transformation is that the matter Lagrangian $\mathcal{L}_{\text{kin}}$ is again written as

$$\bar{\epsilon}\epsilon\mathcal{L}_{\text{kin}} = \delta_{\bar{\epsilon}}\delta_{\epsilon}\text{Tr}\left(\bar{\psi}\psi - 2i\bar{\phi}\sigma\phi + \frac{2(q-1)}{l}\bar{\phi}\phi\right). \tag{2.39}$$

2.3 Localization of 3d $\mathcal{N}=2$ supersymmetric field theory on S^3

Here we apply the localization method to a general $\mathcal{N}=2$ supersymmetric field theory on S^3 [32, 47, 48] (see also [92] for equivariant localization). The action of such a theory is conventionally denoted as

$$S = S_{\text{CS}} + S_{\text{YM}} + S_{\text{Matter}}. \tag{2.40}$$

The localization method states that the partition function given by the original action (2.40) is the same as the "deformed" partition function given by the action

$$S(t) = S_{\text{CS}} + (1+t)S_{\text{YM}} + (1+t)S_{\text{Matter}}. \tag{2.41}$$

[14] Here we restrict the Killing spinor to the constant in the left-invariant frame. If we do not impose this restriction, the algebra contains the dilatation again.

Then we can exactly evaluate the original partition function by the saddle point method as

$$
\begin{aligned}
Z &= \lim_{t\to\infty}\int \mathcal{D}\Phi e^{-S_{\rm CS}[\Phi]-t(S_{\rm YM}[\Phi]+S_{\rm Matter}[\Phi])} && (2.42)\\
&= \sum_{\Phi_0} e^{-S_{\rm CS}[\Phi_0]} Z^{(\rm YM)}_{1-\rm loop}[\Phi_0] Z^{(\rm Matter)}_{1-\rm loop}[\Phi_0], && (2.43)
\end{aligned}
$$

where $Z^{(\rm YM)}_{1-\rm loop}[\Phi_0]$ and $Z^{(\rm Mat)}_{1-\rm loop}[\Phi_0]$ is the one-loop determinant from the gauge and Matter sector on the localized configuration Φ_0 satisfying $S_{\rm YM}[\Phi_0]+S_{\rm Mat}[\Phi_0]=0$, respectively.

2.3.1 Gauge sector

The action of the $\mathcal{N}=2$ SYM on S^3 is given by

$$
\begin{aligned}
S_{\rm YM} &= \frac{1}{g_{\rm YM}^2}\int d^3x\sqrt{g}\ {\rm Tr}\Big[\frac{1}{4}F_{\mu\nu}^2+\frac{1}{2}(D_\mu\sigma)^2+\frac{1}{2}\Big(D+\frac{\sigma}{l}\Big)^2\\
&\qquad +\frac{i}{2}\bar{\lambda}\gamma^\mu D_\mu\lambda+\frac{i}{2}\bar{\lambda}[\ \sigma,\lambda\ ]-\frac{1}{4l}\bar{\lambda}\lambda\Big].
\end{aligned}
$$

Imposing $S_{\rm YM}=0$, the localized configuration for the vector multiplet is determined by

$$F_{\mu\nu}=0,\quad D_\mu\sigma=0,\quad D=-\frac{\sigma}{l},\quad \lambda=0,\quad \bar{\lambda}=0. \qquad (2.44)$$

This is solved by[15]

$$A_\mu=0,\quad \sigma=\sigma_0,\quad D=-\frac{\sigma}{l},\quad \lambda=0,\quad \bar{\lambda}=0, \qquad (2.45)$$

up to gauge transformation. Here σ_0 is a constant matrix valued in the Lie algebra. At the localized configuration, the Chern-Simons action becomes

$$S_{\rm CS}=i\pi l^2 k{\rm Tr}\sigma_0^2. \qquad (2.46)$$

Before preceding to evaluation of the one-loop determinant, we should take care of gauge fixing omitted for simple explanation[16]. We introduce the gauge fixing term as The gauge-fixing action plus the ghost action is

$$\mathcal{L}_{\rm GF}=\delta_B{\rm Tr}(bG), \qquad (2.48)$$

where δ_B denotes the BRST transformation defined by

$$\delta_B A_\mu \;=\; D_\mu c \qquad (2.49)$$

[15]Here we assume absence of singularities. See [95, 96] for more general situation.

[16]Strictly speaking, we should first treat the BRST symmetry δ_B together with the supersymmetries $\delta_\epsilon,\delta_{\bar\epsilon}$ and consider deformation by "$\delta_\epsilon+\delta_B$" or "$\delta_{\bar\epsilon}+\delta_B$" exact term. However, we can show

$$\mathcal{L}_{\rm SYM}+\mathcal{L}_{\rm GF}\simeq(\delta_{\bar\epsilon}+\delta_B)(\delta_\epsilon+\delta_B){\rm Tr}\left(\frac{1}{2}\bar{\lambda}\lambda-2D\sigma\right)+(\delta_{\epsilon(\bar\epsilon)}+\delta_B){\rm Tr}(bG). \qquad (2.47)$$

Since the first term is gauge invariant, δ_B does not affect. Then although the term we need to worry is $\delta_{\epsilon(\bar\epsilon)}{\rm Tr}(bG)$, this can be absorbed by assigning $\delta_{\epsilon(\bar\epsilon)}b=0$ and an appropriate field redefinition of c.

$$
\begin{aligned}
\delta_B c &= ic^2 && (2.50)\\
\delta_B b &= B && (2.51)\\
\delta_B B &= 0. && (2.52)
\end{aligned}
$$

b, c and B are ghosts and Nakanishi-Lautrup field, respectively. If we choose the gauge fixing function G as

$$
G = \nabla^\mu A_\mu, \tag{2.53}
$$

the gauge fixing action becomes

$$
\mathcal{L}_{\rm GF} = B\nabla^\mu A_\mu - b\nabla^\mu D_\mu c. \tag{2.54}
$$

Note that the addition of this action does not change the localized configuration (2.45).

Expanding the fields around

$$
\sigma \to \sigma_0 + \frac{1}{\sqrt{t}}\sigma, \quad D \to -\frac{\sigma_0}{l} + \frac{1}{\sqrt{t}}D, \quad \text{(Other fields)} \to \frac{1}{\sqrt{t}}\text{(Other fields)}, \tag{2.55}
$$

we obtain the quadratic action as

$$
\begin{aligned}
& t(S_{\rm YM} + S_{\rm GF})|_{\rm Gaussian} \\
= & \int d^3x\sqrt{g}{\rm Tr}\Big[\frac{1}{4}f_{\mu\nu}^2 + \frac{1}{2}(\partial_\mu\sigma)^2 - \frac{1}{2}[A_\mu, \sigma_0]^2 + \frac{1}{2}\Big(D + \frac{\sigma}{l}\Big)^2 \\
& + \frac{i}{2}\bar{\lambda}\gamma^\mu\nabla_\mu\lambda + \frac{i}{2}\bar{\lambda}[\ \sigma_0, \lambda\ ] - \frac{1}{4l}\bar{\lambda}\lambda + B\nabla^\mu A_\mu - b\nabla^\mu\partial_\mu c\Big],
\end{aligned} \tag{2.56}
$$

where $f_{\mu\nu} = \nabla_\mu A_\nu - \nabla_\nu A_\mu$. Since the integration over D is trivial, we omit the forth term below. In order to simplify the integration over A_μ, we decompose the gauge field into a divergenceless part plus divergence part [97] as

$$
A_\mu = \partial_\mu a + B_\mu, \tag{2.57}
$$

with $\nabla^\mu B_\mu = 0$. Then integrating over B leads us to the gauge fixing condition

$$
\delta(-\nabla^2 a), \tag{2.58}
$$

which makes easy to integrate a out. Being careful to the Jacobian factor $\det(-\nabla^2)^{-1/2}$ associated with the delta function, we can easily find that integrating B, a, σ, b and c out gives just 1. Thus remaining nontrivial part is

$$
\begin{aligned}
& t(S_{\rm YM} + S_{\rm GF})|_{\rm Gaussian} \\
= & \int d^3x\sqrt{g}{\rm Tr}\Big[-\frac{1}{2}(\epsilon^{\mu\nu\tau}\nabla_\nu B_\tau)^2 - \frac{1}{2}[B_\mu, \sigma_0]^2 + \frac{i}{2}\bar{\lambda}\gamma^\mu\nabla_\mu\lambda + \frac{i}{2}\bar{\lambda}[\ \sigma_0, \lambda\ ] - \frac{1}{4l}\bar{\lambda}\lambda\Big].
\end{aligned} \tag{2.59}
$$

Next we make harmonic expansion as

$$
B_\mu = \sum_{\rho=\pm 1}\ \sum_{J=\frac{\rho(\rho-1)}{2}, 2J+1\in\mathbf{Z}}^{\infty}\ \sum_{m_L=-J-\frac{\rho(\rho+1)}{2}}^{J+\frac{\rho(\rho+1)}{2}}\ \sum_{m_R=-J-\frac{\rho(\rho-1)}{2}}^{J+\frac{\rho(\rho-1)}{2}} B_{Jm_Lm_R\rho}Y^\rho_{Jm_Lm_R\mu},
$$

$$\lambda_\alpha = \sum_{\kappa=\pm 1} \sum_{J=-\frac{\kappa-1}{4}}^{\infty} \sum_{m_L=-J-\frac{\kappa+1}{4}}^{J+\frac{\kappa+1}{4}} \sum_{m_R=-J+\frac{\kappa-1}{4}}^{J-\frac{\kappa-1}{4}} \lambda_{Jm_Lm_R\kappa} Y^{\kappa}_{Jm_Lm^R\alpha}, \tag{2.60}$$

where $Y_{Jm_Lm_R\rho\mu}$ and $Y_{Jm_Lm_R\rho\mu}$ are the vector and spinor spherical harmonics on S^3, respectively. Note that B_μ does not have the $\rho = 0$ mode since $\nabla^\mu B_\mu = 0$. Important properties of these harmonics here are

$$\begin{aligned}
&\epsilon^{\mu\nu\tau}\nabla_\nu Y^{\rho}_{Jm_Lm_R\tau} = -2\rho(J+1)Y^{\rho}_{Jm_Lm_R\mu}, \\
&(\gamma^\mu \nabla_\mu Y^{\kappa}_{Jm_Lm_R})_\alpha = i\kappa\left(2J+\frac{3}{2}\right)Y^{\kappa}_{Jm_Lm_R\alpha}, \\
&\int \frac{d\Omega_3}{2\pi^2}(Y^{\rho_1}_{J_1m^1_Lm^1_R\mu})^* Y^{\rho_2}_{J_2m^2_Lm^2_R\mu} = \delta_{\rho_1\rho_2}\delta_{J_1J_2}\delta_{m^1_Lm^2_L}\delta_{m^1_Lm^2_L}, \\
&\int \frac{d\Omega_3}{2\pi^2}(Y^{\kappa_1}_{J_1m^1_Lm^1_R\alpha})^* Y^{\kappa_2}_{J_2m^2_Lm^2_R\alpha} = \delta_{\kappa_1\kappa_2}\delta_{J_1J_2}\delta_{m^1_Lm^2_L}\delta_{m^1_Lm^2_L}.
\end{aligned} \tag{2.61}$$

Then the quadratic action becomes

$$\begin{aligned}
&t(S_{\rm YM}+S_{\rm GF})|_{\rm Gaussian} \\
=& \sum_{\rho,J,m_L,m_R} {\rm Tr}\Big[\frac{4(J+1)^2}{2l^2}B^\dagger_{Jm_Lm_R\rho}B_{Jm_Lm_R\rho} - \frac{1}{2}[B^\dagger_{Jm_Lm_R\rho},\sigma_0][B_{Jm_Lm_R\rho},\sigma_0]\Big] \\
&+\sum_{\kappa,J,m_L,m_R} {\rm Tr}\Big[\frac{1}{2l}\left(-\kappa\left(2J+\frac{3}{2}\right)-\frac{1}{2}\right)\bar{\lambda}^\dagger_{Jm_Lm_R\kappa}\lambda_{Jm_Lm_R\kappa} + \frac{i}{2}\bar{\lambda}^\dagger_{Jm_Lm_R\kappa}[\,\sigma_0,\lambda_{Jm_Lm_R\kappa}]\Big].
\end{aligned} \tag{2.62}$$

Finally we introduce the Cartan-Weyl basis $(H_i, E_\alpha, E_{-\alpha})$ satisfying

$$\begin{aligned}
&[\,H_i,H_j\,]=0, \quad [\,H_i,E_\alpha\,]=\alpha_i\cdot E_\alpha, \quad [\,E_\alpha,E_{-\alpha}\,]=\frac{2}{|\alpha|^2}\alpha_iH_i \\
&E^\dagger_\alpha = E_{-\alpha}, \quad {\rm Tr}(E_\alpha E_\beta)=\delta_{\alpha+\beta,0}.
\end{aligned} \tag{2.63}$$

If we expand each field in terms of the basis as

$$X = X_iH_i + \sum_{\alpha\in\Delta_+}(X^\alpha E_\alpha + X^{-\alpha}E_{-\alpha}) \tag{2.64}$$

and choose the gauge taking σ_0 as the Cartan values, then we obtain

$$\begin{aligned}
&t(S_{\rm YM}+S_{\rm GF})|_{\rm Gaussian} \\
=& \sum_{\alpha\in\Delta}\sum_{\rho,J,m_L,m_R}\frac{1}{2}\left\{\frac{4(J+1)^2}{l^2}+(\alpha\cdot\sigma)^2\right\}B^{-\alpha}_{Jm_Lm_R\rho}B^{\alpha}_{Jm_Lm_R\rho} \\
&+\sum_{\alpha\in\Delta}\sum_{\kappa,J,m_L,m_R}\frac{1}{2}\left\{\frac{-\kappa\left(2J+\frac{3}{2}\right)-\frac{1}{2}}{l}+i(\alpha\cdot\sigma)\right\}\bar{\lambda}^{-\alpha}_{Jm_Lm_R\kappa}\lambda^{\alpha}_{Jm_Lm_R\kappa}.
\end{aligned} \tag{2.65}$$

Thus the one-loop determinant from the vector multiplet is given by

$$
\begin{aligned}
Z^{(\mathrm{YM})}_{1-\mathrm{loop}}(\sigma_0) &= \prod_{\alpha\in\Delta} \frac{\prod_{J=0,2J+1\in\mathbf{Z}}^{\infty}\left[\frac{-2J-2}{l}+i(\alpha\cdot\sigma)\right]^{(2J+1)(2J+2)}}{\prod_{J=0,2J+1\in\mathbf{Z}}^{\infty}\left[\frac{4(J+1)^2}{l^2}+(\alpha\cdot\sigma)^2\right]^{\frac{(2J+1)(2J+3)}{2}}} \\
&\quad\times\frac{\prod_{J=-\frac{1}{2},2J+1\in\mathbf{Z}}^{\infty}\left[\frac{2J+1}{l}+i(\alpha\cdot\sigma)\right]^{(2J+1)(2J+2)}}{\prod_{J=-1,2J+1\in\mathbf{Z}}^{\infty}\left[\frac{4(J+1)^2}{l^2}+(\alpha\cdot\sigma)^2\right]^{\frac{(2J+1)(2J+3)}{2}}} \\
&= \prod_{\alpha\in\Delta}(\alpha\cdot\sigma)\left(\frac{1}{l^2}+(\alpha\cdot\sigma)^2\right)^2 \\
&\quad\times\prod_{J=0,2J+1\in\mathbf{Z}}^{\infty}\frac{\left[\frac{-2J-2}{l}+i(\alpha\cdot\sigma)\right]^{(2J+1)(2J+2)}\left[\frac{2J+2}{l}+i(\alpha\cdot\sigma)\right]^{(2J+2)(2J+3)}}{\left[\frac{4(J+1)^2}{l^2}+(\alpha\cdot\sigma)^2\right]^{(2J+1)(2J+3)}} \\
&= \prod_{\alpha\in\Delta_+}(\alpha\cdot\sigma)^2\left(\frac{1}{l^2}+(\alpha\cdot\sigma)^2\right)^2\prod_{J=0,2J+1\in\mathbf{Z}}^{\infty}\frac{\left[\frac{4(J+1)^2}{l^2}+(\alpha\cdot\sigma)^2\right]^{2(2J+2)^2}}{\left[\frac{4(J+1)^2}{l^2}+(\alpha\cdot\sigma)^2\right]^{2(2J+1)(2J+3)}} \\
&= \prod_{\alpha\in\Delta_+}(\alpha\cdot\sigma)^2\prod_{n=0}^{\infty}\left[\frac{(n+1)^2}{l^2}+(\alpha\cdot\sigma)^2\right]^2 \\
&= \prod_{\alpha\in\Delta_+}\left[\frac{2\sinh\left(\pi l(\alpha\cdot\sigma)\right)}{(\alpha\cdot\sigma)}\right]^2,
\end{aligned}
\tag{2.66}
$$

where we used some formulas of infinite products:

$$
\prod_{n=1}^{\infty}\frac{n^2+x^2}{n^2}=\frac{\sinh(\pi x)}{\pi x},\qquad \prod_{n=1}^{\infty}n^2=e^{2\zeta'(0)}=2\pi,\qquad \prod_{n=1}^{\infty}c=e^{\zeta(0)\log c}=\frac{1}{\sqrt{c}}. \tag{2.67}
$$

Note that the factor $\prod_{\alpha\in\Delta_+}\frac{1}{(\alpha\cdot\sigma)^2}$ is canceled with the factor coming from the residual gauge fixing of σ_0.

2.3.2 Matter sector

Next we consider the matter part whose Lagrangian is

$$
\begin{aligned}
S_{\mathrm{Mat}} &= \int d^3x\sqrt{g}\mathrm{Tr}\Bigg[D_\mu\bar{\phi}D^\mu\phi+\bar{\phi}\sigma^2\phi+\frac{i(2q-1)}{l}\bar{\phi}\sigma\phi+\frac{q(2-q)}{l^2}\bar{\phi}\phi+i\bar{\phi}D\phi \\
&\qquad +\bar{F}F-i\bar{\psi}\gamma^\mu D_\mu\psi+i\bar{\psi}\sigma\psi-\frac{2q-1}{2l}\bar{\psi}\psi+i\bar{\psi}\lambda\phi-i\bar{\phi}\bar{\lambda}\psi\Bigg].
\end{aligned}
$$

We can easily find that the localized configuration except for σ and D is trivial:

$$
\phi=\bar{\phi}=F=\bar{F}=\psi=\bar{\psi}=0. \tag{2.68}
$$

If we expand the fields around the configuration, we obtain the quadratic action as

$$
\begin{aligned}
tS_{\rm Mat}|_{\rm Gaussian} &= \int d^3x\sqrt{g}{\rm Tr}\Bigg[\partial_\mu\bar{\phi}\partial^\mu\phi + \bar{\phi}\sigma_0^2\phi + \frac{i(2q-2)}{l}\bar{\phi}\sigma_0\phi + \frac{q(2-q)}{l^2}\bar{\phi}\phi \\
&\qquad -i\bar{\psi}\gamma^\mu\nabla_\mu\psi + i\bar{\psi}\sigma_0\psi - \frac{2q-1}{2l}\bar{\psi}\psi\Bigg], \qquad (2.69)
\end{aligned}
$$

where we omit the trivial term $\bar{F}F$. We make harmonic expansion again as

$$
\begin{aligned}
\phi &= \sum_{J=0,2J+1\in\mathbf{Z}}^{\infty}\sum_{m_L=-J}^{J}\sum_{m_R=-J}^{J}\phi_{Jm_Lm_R}Y_{Jm_Lm_R}, \\
\psi_\alpha &= \sum_{\kappa=\pm1}\sum_{J=-\frac{\kappa-1}{4}}^{\infty}\sum_{m_L=-J-\frac{\kappa+1}{4}}^{J+\frac{\kappa+1}{4}}\sum_{m_R=-J+\frac{\kappa-1}{4}}^{J-\frac{\kappa-1}{4}}\psi_{Jm_Lm_R\kappa}Y^{\kappa}_{Jm_Lm^R\alpha}, \qquad (2.70)
\end{aligned}
$$

where $Y_{Jm_Lm_R}$ is the scalar spherical harmonics satisfying

$$
\begin{aligned}
&\nabla^2 Y_{Jm_Lm_R} = -4J(J+1)Y_{Jm_Lm_R}, \\
&\int\frac{d\Omega_3}{2\pi^2}(Y_{J_1m_L^1m_R^1})^*Y_{J_2m_L^2m_R^2} = \delta_{J_1J_2}\delta_{m_L^1m_L^2}\delta_{m_L^1m_L^2}. \qquad (2.71)
\end{aligned}
$$

Then the quadratic action is

$$
\begin{aligned}
tS_{\rm Mat}|_{\rm Gaussian} &= \sum_{J,m_L,m_R}{\rm Tr}\left[\bar{\phi}^\dagger_{Jm_Lm_R}\left\{\frac{4J(J+1)+q(2-q)}{l^2}+\sigma_0^2+\frac{i(2q-2)}{l}\sigma_0\right\}\phi_{Jm_Lm_R}\right] \\
&\quad + \sum_{\kappa,J,m_L,m_R}{\rm Tr}\left[\bar{\psi}^\dagger_{Jm_Lm_R\kappa}\left\{\frac{\kappa(2J+3/2)-q+1/2}{l}+i\sigma_0\right\}\psi_{Jm_Lm_R\kappa}\right]. (2.72)
\end{aligned}
$$

Thus the one-loop determinant from the matter sector is

$$
\begin{aligned}
Z_{\rm 1-loop}^{\rm (Mat)} &= \prod_{\rho\in\mathcal{R}}\frac{\prod_{J=0,2J+1\in\mathbf{Z}}^{\infty}\left[\frac{2J+2-q}{l}+i(\rho\cdot\sigma)\right]^{(2J+1)(2J+2)}}{\prod_{J=0,2J+1\in\mathbf{Z}}^{\infty}\left[\frac{4J(J+1)+q(2-q)}{l^2}+(\rho\cdot\sigma)^2+\frac{i(2q-2)}{l}(\rho\cdot\sigma)\right]^{(2J+1)^2}} \\
&\quad\times\prod_{J=-\frac{1}{2},2J+1\in\mathbf{Z}}^{\infty}\left[\frac{-2J-1-q}{l}+i(\rho\cdot\sigma)\right]^{(2J+1)(2J+2)} \\
&= \prod_{\rho\in\mathcal{R}}\prod_{J=0,2J+1\in\mathbf{Z}}^{\infty}\frac{\left[\frac{2J+2-q}{l}+i(\rho\cdot\sigma)\right]^{(2J+1)(2J+2)}\left[\frac{2J+1+q}{l}-i(\rho\cdot\sigma)\right]^{(2J+1)(2J+2)}}{\left[\frac{2J+2-q}{l}+i(\rho\cdot\sigma)\right]^{(2J+1)^2}\left[\frac{2J+q}{l}-i(\rho\cdot\sigma)\right]^{(2J+1)^2}} \\
&= \prod_{\rho\in\mathcal{R}}\prod_{n=1}^{\infty}\left(\frac{\frac{n+1-q}{l}+i(\rho\cdot\sigma)}{\frac{n-1+q}{l}-i(\rho\cdot\sigma)}\right)^n = \prod_{\rho\in\mathcal{R}}s_1(i-iq-l(\rho\cdot\sigma)) \qquad (2.73)
\end{aligned}
$$

where $s_b(z)$ is the double sine function introduced in appendix. C.

Thus we can write down formula for the partition function of general 3d $\mathcal{N}=2$ supersymmetric gauge theory on S^3: which is a Yang-Mills Chern-Simons gauge theory with arbitrary gauge group $G=G_1\times\cdots\times G_r$ and Chern-Simons levels coupled to arbitrary number of $\mathcal{N}=2$ chiral multiplets with arbitrary representations and R-charge assignment. Taking care of the residual gauge fixing term $\prod_{\alpha\in\Delta_+}(\alpha\cdot\sigma)^2$ and rescaling σ_0 as $2\pi l\sigma_0\to\sigma_0$, the partition function is obtained as

$$Z=\frac{1}{|W|}\int\frac{d^{\mathrm{rank}G_1}\sigma^{(1)}}{(2\pi)^{\mathrm{rank}G_1}}\cdots\frac{d^{\mathrm{rank}G_r}\sigma^{(r)}}{(2\pi)^{\mathrm{rank}G_r}}\prod_{a=1}^{r}\Delta_{\mathrm{Vec}}^{G_a}(\sigma^{(a)})\prod_{\alpha}\Delta_{\mathrm{Mat}}^{\mathcal{R}_\alpha}(\sigma;q_\alpha), \tag{2.74}$$

where $|W|$ is the order of the Weyl group of G, and $\sigma^{(a)}$ is the Cartan part of the adjoint scalar in the vector multiplet with the gauge group G_a at the localization point. $\Delta_{\mathrm{Vec}}^{G_a}(\sigma^{(a)})$ represents the contribution from the vector multiplet with the gauge group G_a given by

$$\Delta_{\mathrm{Vec}}^{G_a}(\sigma^{(a)})=\prod_{\alpha^{(a)}\in\Delta_+}\left[2\sinh\frac{\alpha^{(a)}\cdot\sigma^{(a)}}{2}\right]^2\cdot\exp\left[\frac{ik_a}{4\pi}\sigma^{(a)}\cdot\sigma^{(a)}\right], \tag{2.75}$$

where $\alpha^{(a)}$ labels the positive roots of G_a. $\Delta_{\mathrm{Mat}}^{\mathcal{R}_\alpha}(\sigma;q_\alpha)$ is the contribution from the chiral multiplet with the representation $\mathcal{R}_\alpha$ and R-charge q_α:

$$\Delta_{\mathrm{Mat}}^{\mathcal{R}_\alpha}(\sigma;q_\alpha)=\prod_{\rho_\alpha\in\mathcal{R}_\alpha}s_1\left(i-iq_\alpha-\frac{\rho_\alpha\cdot\sigma}{2\pi}\right), \tag{2.76}$$

where ρ_α is the weight vector of $\mathcal{R}_\alpha$. As a special case of a pair of chiral multiplets with the representation $\mathcal{R}$ and $\bar{\mathcal{R}}$ in the canonical R-charge assignment, which corresponds to the $\mathcal{N}=4$ hyper multiplet, the formula (2.76) reduces to the following simple form

$$\Delta_{\mathrm{Mat}}^{\mathcal{R}}(\sigma;1/2)\Delta_{\mathrm{Mat}}^{\bar{\mathcal{R}}}(\sigma;1/2)=\prod_{\rho\in\mathcal{R}}\frac{1}{2\cosh\frac{\rho\cdot\sigma}{2}}. \tag{2.77}$$

2.4 Localization of the $U(N)\times U(N)$ ABJM theory

Let us focus on the $U(N)\times U(N)$ ABJM theory. Since the ABJM theory is the $U(N)_k\times U(N)_{-k}$ Chern-Simons theory with two bi-fundamental and anti-bi-fundamental chiral multiples in the canonical R-charge assignment, the partition function is given by

$$\begin{aligned}Z(N,k) &= \frac{1}{(N!)^2}\int\frac{d^N\mu}{(2\pi)^N}\frac{d^N\nu}{(2\pi)^N}\\ &\qquad\frac{\prod_{i<j}\left[2\sinh\frac{\mu_i-\mu_j}{2}\right]^2\left[2\sinh\frac{\nu_i-\nu_j}{2}\right]^2}{\prod_{i,j}\left[2\cosh\frac{\mu_i-\nu_i}{2}\right]^2}\exp\left[\frac{ik}{4\pi}\sum_{i=1}^{N}(\mu_i^2-\nu_i^2)\right].\end{aligned} \tag{2.78}$$

We can also apply the localization method to BPS Wilson loops in the ABJM theory. The 1/6-BPS Wilson loop in the representation $\mathcal{R}$ [98, 99, 100], which keeps 4 of 24 supersymmetries,

$$W_{1/6}=\frac{1}{N}\mathrm{Tr}\,\mathrm{P}\exp\left[\int ds\left(iA_\mu\dot{x}^\mu+\frac{2\pi}{k}|\dot{x}|M_{IJ}\Phi^I\bar{\Phi}^J\right)\right], \tag{2.79}$$

where $M_{IJ} = \mathrm{diag.}\,(1,1,-1,-1)$ and $x^\mu(s)$ parametrize the great circle on S^3. This is dual to the smeared fundamental string in the dual supergravity background. Since only σ and D are nontrivial on the localized configurations (2.45) (2.68), the operator on the configuration naively seems to be trivial. However, the operator (2.79) is equivalent to the operator

$$\frac{1}{N}\mathrm{Tr}\,\mathrm{P}\exp\left[\int ds\,(iA_\mu \dot{x}^\mu + \sigma|\dot{x}|)\right], \tag{2.80}$$

after integrating σ out [101]. Thus we find that the expectation value reduces to

$$\langle W_{1/6}\rangle = \frac{1}{\mathrm{dim}\mathcal{R}}\left\langle \mathrm{Tr}_{\mathcal{R}} e^{\sigma_0}\right\rangle_{M.M.}, \tag{2.81}$$

where $\langle \cdots \rangle_{M.M.}$ represents an expectation value in the ABJM matrix model (2.78).

In ref. [102], the 1/2-BPS Wilson loop has also been constructed. It can be written as

$$W_{1/2} = \frac{1}{\mathrm{dim}\mathcal{R}}\mathrm{Tr}_{\mathcal{R}}\,\mathrm{P}\exp\left(\int ds\hat{L}\right), \tag{2.82}$$

where $\hat{L}$ is given by

$$\hat{L} = \begin{pmatrix} iA_\mu \dot{x}^\mu + \frac{2\pi}{k}|\dot{x}|M_{IJ}\Phi^I\bar{\Phi}^J & i\sqrt{\frac{2\pi}{k}}|\dot{x}(\tau)|\eta_I^\alpha(\tau)\bar{\psi}_\alpha^I \\ i\sqrt{\frac{2\pi}{k}}|\dot{x}(\tau)|\psi_I^\alpha \bar{\eta}_\alpha^I(\tau) & i\tilde{A}_\mu \dot{x}^\mu + \frac{2\pi}{k}|\dot{x}|\tilde{M}_{IJ}\bar{\Phi}^J\Phi^I \end{pmatrix}. \tag{2.83}$$

Here M_{IJ} and $\tilde{M}_{IJ}$ are again $M_{IJ} = \tilde{M}_{IJ} = \mathrm{diag.}\,(1,1,-1,-1)$ for the great circle and this is dual to the localized fundamental string in the gravity dual. The parameters $\eta_I^\alpha(\tau)$ and $\bar{\eta}_I^\alpha(\tau)$, which are determined by requiring supersymmetry, are irrelevant on the localization argument. By applying the localization method to the 1/2-BPS Wilson loop in the fundamental representation, the expectation value of the operator can be written as

$$\langle W_{1/2}\rangle = \frac{1}{\mathrm{dim}\mathcal{R}}\left\langle \mathrm{STr}_{\mathcal{R}}\begin{pmatrix} e^{\sigma_0} & 0 \\ 0 & -e^{\tilde{\sigma}_0}\end{pmatrix}\right\rangle_{M.M.}. \tag{2.84}$$

3 Free energy

In this chapter, we show numerical results of the free energy [42, 43]. This chapter is organized as follows. In section 3.1 we review the previous results for the free energy of the ABJM matrix model in various limits, which are obtained by analytical methods. In section 3.2 we describe our numerical method. In section 3.3 we present our results, and discuss the discrepancies from the analytical results. In section 3.4 we show that these discrepancies can be interpreted as the constant map contributions.

3.1 Previous analytical results for the free energy

In this section we summarize some known analytical results for free energy of the ABJM theory, which is defined in terms of the partition function (2.78) as

$$F(N,k) \;=\; \log Z(N,k)\,. \tag{3.1}$$

3.1.1 Perturbative results for all N

The free energy can be calculated by using a usual perturbative technique, and the result at the one-loop level is given as (See, for example, ref. [37].)

$$\begin{aligned} F_{\text{weak}} &= -N^2\log\frac{2N}{\pi\lambda} - N\log 2\pi + 2\log G_2(N+1) && (3.2)\\ &\overset{N\gg1}{=} N^2\left(\log 2\pi\lambda - \frac{3}{2} - 2\log 2\right) - \frac{1}{6}\log N + 2\zeta'(-1) + \sum_{g=2}^{\infty}\frac{B_{2g}}{g(2g-2)}N^{2-2g} && (3.3)\end{aligned}$$

where $G_2(x)$ is the Barnes G-function $G_2(x) \equiv \prod_{s=1}^{x-2} s!$. The $1/N$-expansion is shown in the second line with Riemann's zeta function $\zeta(x)$ and the Bernoulli numbers B_{2g}. The $\mathrm{O}(N^2)$ terms in (3.3) agree with the result (3.5) obtained in the planar limit. Note, however, that the expression (3.2) includes contributions to all orders in the $1/N$-expansion.

3.1.2 $N = 2$ with arbitrary k

An exact expression for $N = 2$ is obtained by Okuyama [39] as[17]

$$F(2,k) \;=\; \begin{cases} \log\left[\dfrac{1}{k}\displaystyle\sum_{s=1}^{k-1}(-1)^{s-1}\left(\frac{1}{2}-\frac{s}{k}\right)\tan^2\frac{\pi s}{k} + \frac{(-1)^{\frac{k-1}{2}}}{\pi}\right] - 4\log 2 & \text{for odd } k\\ \log\left[\dfrac{1}{k}\displaystyle\sum_{s=1}^{k-1}(-1)^{s-1}\left(\frac{1}{2}-\frac{s}{k}\right)^2\tan^2\frac{\pi s}{k}\right] - 4\log 2 & \text{for even } k\,. \end{cases} \tag{3.4}$$

This result has been obtained by direct integration of (3.17). Since the expressions for the odd and even k cases are different, the analyticity in k (when one regards k or equivalently

[17] Note that the normalization of the partition function adopted in ref. [39] differs from ours as $Z_{\text{Okuyama}} = 2^{2N}Z_{\text{ours}}$.

the 't Hooft coupling constant λ as a continuous variable) is not obvious a priori. However, as we will see in section 3.3, our numerical results suggest that the free energy is a smooth function of k. The analyticity is important in the context of the AdS/CFT correspondence, in which one assumes the analyticity on the gravity side. Also the analysis in the planar limit usually assumes the analyticity implicitly.

3.1.3 Planar limit ($N \to \infty$ with λ fixed)

The free energy in the planar limit ($N \to \infty$ with λ fixed) has been calculated by Drukker, Marino and Putrov (DMP) [34]. These results have been obtained by a standard matrix model technique after the analytic continuation [33] to the lens space $L(2,1) = S^3/\mathbb{Z}_2$ matrix model [103, 104], which is obtained from the pure Chern-Simons theory on $L(2,1)$. The validity of the analytic continuation is proved diagramatically in refs. [105, 106].

At weak coupling ($\lambda \ll 1$) the authors obtain

$$F_{\text{weak,planar}} = N^2 \left(\log 2\pi\lambda - \frac{3}{2} - 2\log 2 \right) \tag{3.5}$$

up to $\mathrm{O}(\lambda)$.

At strong coupling ($\lambda \gg 1$) the authors obtain

$$F_{\text{DMP}} = -\frac{\pi\sqrt{2}}{3} \frac{\hat{\lambda}^{3/2}}{\lambda^2} N^2 \qquad \text{where} \quad \hat{\lambda} = \lambda - \frac{1}{24} \tag{3.6}$$

to all orders of the $1/\lambda$ expansion. The leading behavior $F_{\text{DMP}} \simeq -\sqrt{2}\pi N^2/(3\sqrt{\lambda})$ agrees with the dual type IIA supergravity prediction [34, 107] including the overall coefficient. It has been claimed that the free energy (3.6) at strong coupling receives the correction of the form

$$\simeq \frac{N^2}{\lambda^2} \sum_{l \geq 1} e^{-2\pi l\sqrt{2\hat{\lambda}}} f_I^{(l)} \left(\frac{1}{\pi\sqrt{2\hat{\lambda}}} \right),$$

where $f_I^{(l)}(x)$ is a polynomial in x of degree $2l-3$ (for $l \geq 2$). This exponentially small correction has been interpreted in ref. [34] as the effect of the worldsheet instanton in the dual type IIA superstring, which corresponds to a string worldsheet wrapping a $\mathbb{C}P^1$ cycle in $\mathbb{C}P^3$ [108].

In section 3.3 we will show that another contribution of the order of $\mathrm{O}(N^2/\lambda^2)$ due to the constant map needs to be added in comparing with precise numerical analysis. Although this term does not affect the agreement with supergravity, it must be taken into account when one compares the finite λ corrections with the string α' corrections.

3.1.4 M-theory limit ($N \to \infty$ with k fixed)

In ref. [35], the free energy in the M-theory limit[18] ($N \to \infty$ with k fixed) has been calculated and confirmed the prediction

$$F_{\text{SUGRA}} = -\frac{\pi\sqrt{2k}}{3} N^{3/2} \tag{3.7}$$

from the dual eleven-dimensional supergravity, which shows the well-known $N^{3/2}$ scaling for the degrees of freedom in the theory of M2-branes [109]. Note also that (3.7) agrees with what one obtains formally from the leading large-λ behavior of the planar result (3.6) by replacing λ with N/k.

The result (3.7) was obtained by imposing an ansatz for the eigenvalue distribution

$$\mu_i = N^\alpha z_i + i w_i \,, \quad \nu_i = N^\alpha z_i - i w_i \quad (z_i, w_i \in \mathbb{R}) \,,$$

which is necessary for the cancellation of long-range forces, and is also suggested by numerical studies of the saddle point equation. The parameter α is chosen to be 1/2 by requiring that all the short-range forces contribute to the free energy at the same order of N in order to have nontrivial solutions.

3.1.5 $1/N$ expansion around the planar limit

Fuji, Hirano and Moriyama (FHM) [38] studied the free energy to all orders in the genus expansion neglecting the instanton contribution, which is of the order of $\mathrm{O}(e^{-2\pi\sqrt{\lambda}})$. Their proposal for a resummed form is given by

$$F_{\text{FHM}}(N, \lambda) \; = \; \log \left[\frac{1}{\sqrt{2}} \left(\frac{4\pi^2 N}{\lambda} \right)^{1/3} \text{Ai} \left[\left(\frac{\pi}{\sqrt{2}} \left(\frac{N}{\lambda} \right)^2 \lambda_{\text{ren}}^{3/2} \right)^{2/3} \right] \right] \,, \tag{3.8}$$

where $\text{Ai}(x)$ is the Airy function, and the "renormalized 't Hooft coupling" λ_{ren} is given by

$$\lambda_{\text{ren}} = \lambda - \frac{1}{24} - \frac{\lambda^2}{3N^2} \,. \tag{3.9}$$

The appearance of the Airy function [38] is also encountered in the context of M-theory flux compactification [110]. Note that the expression (3.8) reproduces (3.6) in the large-N limit as one can easily see by using the asymptotic formula $\log \text{Ai(x)} \sim -\frac{2x^{3/2}}{3}$ for $x \gg 1$. In section 3.3 we will show that (3.8) has another contribution, which is necessary for comparison with our numerical results.

The free energy at higher genus has been studied earlier [34, 36] by using a topological string technique after analytic continuation to the lens space matrix model. The analysis in ref. [38] has been performed by using the holomorphic anomaly equation [41], whose solution

[18] Strictly speaking, since the ABJM theory has been conjectured to be dual to the M-theory for $k \ll N^{1/5}$, the limit $N \to \infty$ with k fixed is merely a sufficient condition. In the following, however, we simply call it "the M-theory limit".

is the same as the one for the loop equation [111, 112] with some appropriate boundary conditions. In order to solve the holomorphic anomaly equation, one needs to provide some inputs such as the free energy at genus zero and one, which are taken to be

$$F^{(0)}_{\mathrm{FHM}} = \frac{4\sqrt{2}\pi^3}{3}\hat{\lambda}^{3/2} \quad \text{and} \quad F^{(1)}_{\mathrm{FHM}} = \frac{\pi}{3\sqrt{2}}\hat{\lambda}^{1/2} - \frac{1}{4}\log(8\hat{\lambda})\,.$$

In this way the authors have found a general solution, which gives the free energy at all genus up to the worldsheet instanton effect. The integration constants were determined by assuming the absence of non-perturbative corrections of the type $\sim O\left(e^{-1/g_s^2}\right)$. Strictly speaking, what one obtains in this way is the "weight zero" contribution to the free energy in the language of topological string theory. It is claimed that one can turn this result into the one including contributions from all weights by making a replacement $\lambda \to \lambda_{\mathrm{ren}}$, which is given in (3.9).

This "renormalized 't Hooft coupling" is different from the expectation from the gravity side [113]: $\lambda_{\mathrm{ren,grav}} = \lambda - 1/24 + \lambda^2/(24N^2)$. While it is possible that this disagreement may imply that the AdS/CFT does not hold at finite-N/quantum string level, we should definitely gain more understanding on both gauge theory and gravity sides. The additional contribution to the FHM result from the constant map should be important also from this point of view.

3.1.6 $N \gg 1$, small k

In ref. [40], the free energy with fixed small k has been calculated by using the Fermi gas approach neglecting the quantum mechanical instanton effect (worldsheet instanton) and the terms which are suppressed exponentially at large N (membrane instanton). In this approach, the partition function of the ABJM theory is regarded as an ideal Fermi gas system described by (3.15) with the Planck constant identified as $\hbar = 2\pi k$. The result is given by

$$F_{\mathrm{Fermi}} = \log\left[\frac{(4\pi^2 k)^{1/3}}{\sqrt{2}}\mathrm{Ai}\left[\left(\frac{\pi k^2}{\sqrt{2}}\right)^{2/3}\left(\frac{N}{k} - \frac{1}{24} - \frac{1}{3k^2}\right)\right]\right] + A(k) - \frac{1}{2}\log 2\,. \tag{3.10}$$

The leading large-N behavior reproduces eq. (3.7) exactly. The function $A(k)$ in (3.10) is given for $k \ll 1/(2\pi)$ as[19]

$$A(k) = \frac{2\zeta(3)}{\pi^2 k} - \frac{k}{12} - \frac{\pi^2 k^3}{4320} + \mathrm{O}(k^5)\,. \tag{3.11}$$

Since the first term in (3.10) can be obtained formally from the FHM result F_{FHM} in (3.8) by replacing λ with N/k, one can rewrite it as

$$F_{\mathrm{Fermi}} = F_{\mathrm{FHM}} + A(k) - \frac{1}{2}\log 2\,, \tag{3.12}$$

[19] Although the Chern-Simons level k must be integer in a physical setup, the integral (2.78) is itself well-defined also for non-integer k and we can actually obtain numerical results, which turn out to be a smooth function of k.

where $A(k)$ may be viewed as "quantum corrections" with the "Planck constant" $\hbar = 2\pi k$. Note that the first term in (3.12) is valid for all k although (3.11) is obtained at small k. The authors note that the second and third terms in (3.11) are given by

$$\begin{aligned} A(k) &= \frac{2\zeta(3)}{\pi^2 k} - \sum_{n=1}^{\infty} \frac{(-1)^{n-1} B_{2n}}{n(2n-1)(2n)!} \pi^{2n-2} k^{2n-1} \\ &= \frac{2\zeta(3)}{\pi^2 k} - \frac{2}{\pi} \int_0^{\pi k} \frac{d\xi}{\xi^2} \log\left[\frac{\sin(\xi/2)}{\xi/2}\right] \end{aligned} \tag{3.13}$$

for $n = 1, 2$. This is the power series with odd powers of k unlike the usual genus expansion around the planar limit. The authors suggest that $A(k)$ may encode the effect from D0-branes of the order of $\mathrm{O}\left(e^{-k}\right) \sim \mathrm{O}\left(e^{-1/g_s}\right)$.

Since this analysis for $A(k)$ assumes $k \ll 1/(2\pi)$, it is not clear a priori whether the result holds at physical values of k corresponding to integers. As we will see later, (3.11) and (3.13) are in reasonable agreement with our numerical result for small k such as $k = 1, 2, 3$, but not for larger k (including the planar limit).

3.2 Numerical methods for the ABJM matrix model at arbitrary N and k

In this section we discuss how we can study the ABJM matrix model at arbitrary N and k by applying a standard Monte Carlo method. For the readers who are not familiar with Monte Carlo methods in general, we review the basic ideas in Appendix D. For an earlier work on Monte Carlo simulation of a one-matrix model, see ref. [114].

3.2.1 Derivation of the sign-problem-free form of the ABJM matrix model

The ABJM matrix model in the form (2.78) is not suitable for Monte Carlo simulation since the integrand is not real positive.[20] However, as we review below in detail, one can rewrite the ABJM matrix model in a sign-free form. which was used in ref. [115, 39, 40] for a different purpose. Let us start with the ABJM matrix model (2.78). We are going to use the Cauchy identity[21]

$$\frac{\prod_{i<j}(u_i - u_j)(v_i - v_j)}{\prod_{i,j}(u_i + v_j)} = \sum_{\sigma} (-1)^{\sigma} \prod_i \frac{1}{u_i + v_{\sigma(i)}} . \tag{3.14}$$

Here σ runs through all permutations. By setting $u_i = e^{\mu_i}, v_i = e^{\nu_i}$, it becomes

$$\frac{\prod_{i<j}(e^{\mu_i} - e^{\mu_j})(e^{\nu_i} - e^{\nu_j})}{\prod_{i,j}(e^{\mu_i} + e^{\nu_j})} = \sum_{\sigma} (-1)^{\sigma} \prod_i \frac{1}{e^{\mu_i} + e^{\nu_{\sigma(i)}}} .$$

[20] One might think of simulating a system without the phase factor $\exp((ik/4\pi)(\mu_i^2 - \nu_i^2))$, and including its effect afterwards by reweighting. While it is possible to obtain results for the $k = 1$ case along this line, the calculation becomes more and more difficult for larger k due to the sign problem.

[21] See the appendix of ref. [115] for the proof of this identity.

From this, we obtain

$$\frac{\prod_{i<j}\left[2\sinh\left(\frac{\mu_i-\mu_j}{2}\right)\right]\left[2\sinh\left(\frac{\nu_i-\nu_j}{2}\right)\right]}{\prod_{i,j}\left[2\cosh\left(\frac{\mu_i-\nu_j}{2}\right)\right]} = \sum_\sigma(-1)^\sigma\prod_i\frac{1}{2\cosh\left(\frac{\mu_i-\nu_{\sigma(i)}}{2}\right)}.$$

Therefore, the partition function can be written as

$$\begin{aligned}
&Z(N,k)\\
=\;&\frac{1}{N!^2}\sum_{\sigma,\sigma'}(-1)^{\sigma+\sigma'}\int\frac{d^N\mu}{(2\pi)^N}\frac{d^N\nu}{(2\pi)^N}\prod_i\left[\frac{1}{2\cosh\frac{\mu_i-\nu_{\sigma(i)}}{2}\cdot 2\cosh\frac{\mu_i-\nu_{\sigma'(i)}}{2}}\right]e^{\frac{ik}{4\pi}\sum_{i=1}^N(\mu_i^2-\nu_i^2)}\\
=\;&\frac{1}{N!}\sum_{\sigma}(-1)^{\sigma}\int\frac{d^N\mu}{(2\pi)^N}\frac{d^N\nu}{(2\pi)^N}\prod_i\left[\frac{1}{2\cosh\left(\frac{\mu_i-\nu_i}{2}\right)\cdot 2\cosh\left(\frac{\mu_i-\nu_{\sigma(i)}}{2}\right)}\right]e^{\frac{ik}{4\pi}\sum_{i=1}^N(\mu_i^2-\nu_i^2)}.
\end{aligned}$$

By using the formula

$$\frac{1}{2\cosh p}=\frac{1}{\pi}\int dx\frac{e^{\frac{2i}{\pi}px}}{2\cosh x},$$

we obtain

$$\begin{aligned}
&\sum_\sigma(-1)^\sigma\prod_i\frac{1}{\left[2\cosh\left(\frac{\mu_i-\nu_i}{2}\right)\right]\left[2\cosh\left(\frac{\mu_i-\nu_{\sigma(i)}}{2}\right)\right]}\\
=\;&\sum_\sigma(-1)^\sigma\frac{1}{\pi^{2N}}\int d^Nxd^Ny\;\frac{\exp\left[\frac{i}{\pi}\sum_i(\mu_i-\nu_i)x_i+\frac{i}{\pi}\sum_i(\mu_i-\nu_{\sigma(i)})y_i\right]}{\prod_i 2\cosh x_i\cdot 2\cosh y_i}\\
=\;&\sum_\sigma(-1)^\sigma\frac{1}{\pi^{2N}}\int d^Nxd^Ny\;\frac{\exp\left[\frac{i}{\pi}\sum_i(\mu_i-\nu_i)x_i+\frac{i}{\pi}\sum_i(\mu_iy_i-\nu_iy_{\sigma(i)})\right]}{\prod_i 2\cosh x_i\cdot 2\cosh y_i}.
\end{aligned}$$

Therefore, the partition function becomes[22]

$$\begin{aligned}
&Z(N,k)\\
=\;&\frac{1}{N!}\sum_\sigma(-1)^\sigma\frac{1}{\pi^{2N}}\int d^Nxd^Ny\;\frac{1}{\prod_i 2\cosh x_i\cdot 2\cosh y_i}
\end{aligned}$$

[22]In the Fermi gas approach [40], the integrand is identified with a partition function for the ideal Fermi gas given by

$$Z(N,k) = \frac{1}{N!}\sum_\sigma(-1)^\sigma\int d^Nx\prod_{i=1}^N\rho(x_i,x_{\sigma(i)}), \tag{3.15}$$

where $\rho(x_1,x_2)$ is interpreted as the one-particle density matrix

$$\rho(x_1,x_2)=\frac{1}{2\pi k}\frac{1}{\left(2\cosh\frac{x_1}{2}\right)^{1/2}}\frac{1}{\left(2\cosh\frac{x_2}{2}\right)^{1/2}}\frac{1}{2\cosh\left(\frac{x_1-x_2}{2k}\right)}. \tag{3.16}$$

$$
\begin{aligned}
&\int \frac{d^N\mu}{(2\pi)^N}\frac{d^N\nu}{(2\pi)^N}\exp\Big[\frac{i}{\pi}\sum_i(\mu_i-\nu_i)x_i+\frac{i}{\pi}\sum_i(\mu_i y_i-\nu_i y_{\sigma(i)})+\frac{ik}{4\pi}\sum_i(\mu_i^2-\nu_i^2)\Big]\\
=\;& \frac{1}{N!}\sum_\sigma(-1)^\sigma\frac{1}{\pi^{2N}}\int d^Nxd^Ny\;\frac{1}{\prod_i 2\cosh x_i\cdot 2\cosh y_i}\int\frac{d^N\mu}{(2\pi)^N}\frac{d^N\nu}{(2\pi)^N}\\
&\exp\Big[\frac{ik}{4\pi}\sum_{i=1}^N\left(\mu_i+\frac{2}{k}(x_i+y_i)\right)^2-\frac{ik}{4\pi}\sum_{i=1}^N\left(\nu_i+\frac{2}{k}(x_i+y_{\sigma(i)})\right)^2\Big]\\
&\exp\Big[-\frac{i}{k\pi}\sum_{i=1}^N\left((x_i+y_i)^2-(x_i+y_{\sigma(i)})^2\right)\Big]\\
=\;& \frac{1}{N!}\sum_\sigma(-1)^\sigma\frac{1}{\pi^{2N}}\int d^Nxd^Ny\;\frac{1}{\prod_i 2\cosh x_i\cdot 2\cosh y_i}\int\frac{d^N\mu}{(2\pi)^N}\frac{d^N\nu}{(2\pi)^N}\\
&\exp\Big[\frac{ik}{4\pi}\sum_{i=1}^N\mu_i^2-\frac{ik}{4\pi}\sum_{i=1}^N\nu_i^2-\frac{2i}{k\pi}\sum_{i=1}^N x_i(y_i-y_{\sigma(i)})\Big]\\
=\;& \frac{1}{N!}\sum_\sigma(-1)^\sigma\frac{1}{k^N\pi^{2N}}\int d^Nxd^Ny\;\frac{1}{\prod_i 2\cosh x_i\cdot 2\cosh y_i}e^{-\frac{2i}{k\pi}\sum_{i=1}^N x_i(y_i-y_{\sigma(i)})}\\
=\;& \frac{1}{N!}\sum_\sigma(-1)^\sigma\frac{1}{(k\pi)^N}\int d^Ny\;\frac{1}{\prod_i 2\cosh\left(\frac{y_i-y_{\sigma(i)}}{k}\right)\cdot 2\cosh y_i}\\
=\;& \frac{1}{N!}\sum_\sigma(-1)^\sigma\int\frac{d^Nx}{(2\pi k)^N}\;\frac{1}{\prod_i 2\cosh\left(\frac{x_i}{2}\right)\cdot 2\cosh\left(\frac{x_i-x_{\sigma(i)}}{2k}\right)}.
\end{aligned}
\tag{3.17}
$$

We use the Cauchy identity again:

$$
\sum_\sigma(-1)^\sigma\prod_i\frac{1}{2\cosh\left(\frac{x_i-x_{\sigma(i)}}{2k}\right)}=\frac{\prod_{i<j}\Big[2\sinh\left(\frac{x_i-x_j}{2k}\right)\Big]^2}{\prod_{i,j}\Big[2\cosh\left(\frac{x_i-x_j}{2k}\right)\Big]}=\frac{1}{2^N}\prod_{i<j}\tanh^2\left(\frac{x_i-x_j}{2k}\right).
$$

Thus we arrive at the final expression

$$
Z(N,k)\;=\;\frac{1}{2^N N!}\int\frac{d^Nx}{(2\pi k)^N}\,\frac{\prod_{i<j}\tanh^2\left(\frac{x_i-x_j}{2k}\right)}{\prod_i 2\cosh\left(\frac{x_i}{2}\right)}, \tag{3.18}
$$

which does not have a sign problem. In the $k=1$ case, one may view this as a mirror description of the ABJM theory in terms of the 3d $U(N)$ $\mathcal{N}=4$ SYM with adjoint and fundamental hypermultiplets, which is isomorphic to 3d $U(N)$ $\mathcal{N}=8$ SYM in the low-energy limit [115]. The important point here is that the integrand is real positive, and we can perform Monte Carlo simulation in a straightforward manner as described in Appendix D.

We should also note that, while the level k should be an integer in the original 3d gauge theory, nothing prevents us from considering non-integer k in the integral (2.78). In what follows, we therefore extend the value of k to any real number.

3.2.2 Calculating the ratio of partition functions

In the previous section, we show that the ABJM matrix model is rewritten as

$$
\begin{aligned}
Z(N,k) &= C_{N,k}\, g(N,k)\,, \quad C_{N,k} = \frac{1}{(4\pi k)^N\, N!}\,, \\
g(N,k) &= \int d^N x \frac{\prod_{i<j} \tanh^2\left(\frac{x_i - x_j}{2k}\right)}{\prod_i 2\cosh(x_i/2)}\,.
\end{aligned} \tag{3.19}
$$

In order to calculate the free energy (3.1), which is the log of the partition function, we need to rewrite it in terms of expectation values of some quantities, which are directly calculable by Monte Carlo methods.[23] The basic idea in our case is to calculate the ratios of the partition functions for different k or N as expectation values. Since we know the results for $k = 0$ or $N = 1$, we can obtain results for arbitrary k and N by calculating an appropriate product of the ratios. Depending on whether we change k or N, we have the following two methods, which give the same result within statistical errors as we have checked for various k and N. The second method is particularly useful in studying the M-theory limit, which corresponds to the large N limit with fixed k.

Reweighting by different k

Let us consider a trivial identity

$$
\frac{g(N,k_2)}{g(N,k_1)} = \frac{\int d^N x\, e^{-S(N,k_2;x)}}{\int d^N x\, e^{-S(N,k_1;x)}} = \left\langle e^{-S(N,k_2;x)+S(N,k_1;x)} \right\rangle_{N,k_1}\,, \tag{3.20}
$$

where we have defined

$$
e^{-S(N,k;x)} = \frac{\prod_{i<j} \tanh^2(\frac{x_i - x_j}{2k})}{\prod_i 2\cosh(x_i/2)} \tag{3.21}
$$

and $\langle \cdots \rangle_{N,k}$ stands for the expectation value with respect to the action $S(N,k;x)$

$$
\langle \mathcal{O} \rangle_{N,k} = \frac{\int d^N x\, \mathcal{O}(x) e^{-S(N,k;x)}}{\int d^N x\, e^{-S(N,k;x)}}\,. \tag{3.22}
$$

The quantity (3.20) can be calculated easily by the standard Monte Carlo method as far as k_1 and k_2 are sufficiently close.[24] Therefore, we can calculate the free energy F as

$$
\begin{aligned}
F &= \log Z = \log C_{N,k} + \log g(N,k) \\
&= \log C_{N,k} + \sum_{i=1}^{l} \log \frac{g(N,k_i)}{g(N,k_{i-1})} + \log g(N,0)
\end{aligned}
$$

[23]For applications of such an idea on different supersymmetric systems, see refs. [116] and [117].

[24]As k_2 moves away from k_1, the quantity $e^{-S(N,k_2;x)+S(N,k_1;x)}$ fluctuate violently during the simulation of the system $S(N,k_1;x)$, which leads to larger statistical errors.

$$= \log C_{N,k} + \sum_{i=1}^{l} \log \left\langle e^{-S(N,k_i;x)+S(N,k_{i-1};x)} \right\rangle_{N,k_{i-1}} + N \log \pi \,, \tag{3.23}$$

where $0 = k_0 < k_1 < \cdots < k_l = k$ and we have used $g(N,0) = \int \frac{d^N x}{\prod_i 2\cosh(x_i/2)} = \pi^N$ in the last line. We have to make the adjacent values of k close enough for the reason mentioned above.

Reweighting by different N

Let us decompose N into $N = N_1 + N_2$ and consider the ratio

$$\begin{aligned} \frac{g(N,k)}{g(N_1,k)g(N_2,k)} &= \frac{\int d^N x \, e^{-S(N,k)}}{\int d^N x \, e^{-S(N_1,k;x_1,\cdots,x_{N_1})-S(N_2,k;x_{N_1+1},\cdots,x_N)}} \\ &= \left\langle e^{S(N_1,k;x_1,\cdots,x_{N_1})+S(N_2,k;x_{N_1+1},\cdots,x_N)-S(N,k)} \right\rangle_{N_1,N_2} \,, \end{aligned} \tag{3.24}$$

where the symbol $\langle \cdots \rangle_{N_1,N_2}$ denotes the expectation value with respect to the "action" $S(N_1,k;x_1,\cdots,x_{N_1}) + S(N_2,k;x_{N_1+1},\cdots,x_N)$. Note that

$$e^{S(N_1,k;x_1,\cdots,x_{N_1})+S(N_2,k;x_{N_1+1},\cdots,x_N)-S(N,k)} = \prod_{i=1}^{N_1} \prod_{J=N_1+1}^{N} \tanh^2\left(\frac{x_i - x_J}{2k}\right) , \tag{3.25}$$

due to the factorization of the potential terms. In order to calculate the right-hand side of (3.24) with good accuracy, it is necessary to take N_2 small enough to make sure that (3.25) does not fluctuate violently during the simulation. In actual calculation we use $N_2 = 1$. Then by calculating (3.24) for $N_1 = 1, 2, 3, \cdots$, and by using the $N = 1$ result

$$g(1,k) = \int \frac{dx}{2\cosh(x/2)} = \pi \,, \tag{3.26}$$

we can calculate the free energy for $N = 2, 3, 4, \cdots$ successively with a fixed value of k.

3.3 Results for the free energy

In this section we present our numerical result for the free energy of the ABJM theory. In order to test our code, we first study the $N = 2$ case and compare our result against the exact result (3.4) obtained by Okuyama [39]. As can be seen from fig. 1, our result reproduces the exact result very accurately. We have also obtained results for non-integer values of k, which are not obtained in ref. [39]. They are found to connect the results for integer k smoothly.

3.3.1 Planar limit

Next we consider the planar limit ($N \to \infty$ with $\lambda = N/k$ fixed), which is conjectured to be dual to the classical type IIA superstring on $AdS_4 \times \mathbb{C}P^3$. In fig. 2 we plot the normalized free energy F/N^2 against $1/N^2$ for various values of λ. Our results can be fitted well by

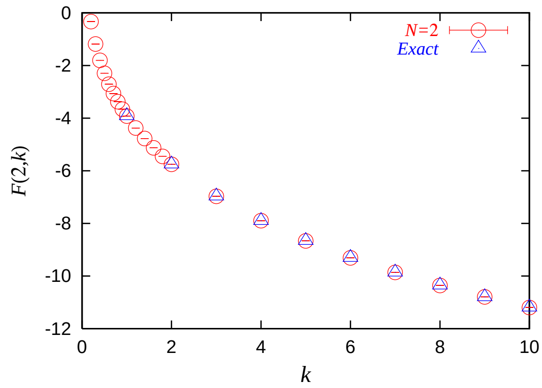

Figure 1: The free energy of the ABJM theory for $N = 2$ is plotted against the Chern-Simons level k. The circles and triangles represent our Monte Carlo result and the exact result (3.4), respectively.

$F(N,\lambda)/N^2 = f_0(\lambda) + f_1(\lambda)/N^2 - \frac{1}{6}\log N$ as theoretically expected[25]. In the left panel of fig. 3, we plot $f_0(\lambda) = \lim_{N\to\infty} F(N,\lambda)/N^2$ against $1/\sqrt{\lambda}$. The results seem to interpolate the DMP result (3.6) at strong coupling and the perturbative result (3.5) at weak coupling. However, by looking more carefully into the asymptotic behavior for large λ, we find certain discrepancies. This can be seen from the right panel of fig. 3, in which we plot the difference $\lim_{N\to\infty}(F - F_{\mathrm{DMP}})/N^2$, which is found to behave as

$$\lim_{N\to\infty} \frac{F - F_{\mathrm{DMP}}}{N^2} \overset{\lambda\gg 1}{\simeq} \frac{a_0}{\lambda^2} + b_0 \,, \tag{3.27}$$

$$a_0 = -0.015 \pm 0.001 \,, \qquad b_0 = -0.0006 \pm 0.0002 \tag{3.28}$$

instead of the behavior $\mathrm{O}(e^{-2\pi\sqrt{\lambda}})$ expected from the worldsheet instanton effect. We consider that b_0 is consistent with zero since the fitting error may well be slightly underestimated. Since the discrepancy (3.27) vanishes at $\lambda = \infty$ (assuming that b_0 in (3.27) is zero), it does not affect the agreement with the dual type IIA supergravity.

In section 3.4 we explain that this discrepancy can be understood as the constant map at genus 0. Similar discrepancies exist also in $1/N$ corrections around the planar limit as we will see.

3.3.2 M-theory limit

Next we consider the large-N limit with fixed k, which is conjectured to correspond to the eleven dimensional supergravity on $AdS_4 \times S^7/\mathbb{Z}_k$. Figure 4 shows that the free energy F grows in magnitude as $N^{3/2}$ with N, and $F/N^{3/2}$ behaves as $F(N,k)/N^{3/2} = h_0(k) + h_1(k)/N$, which enables us to obtain the M-theory limit $h_0(k) = \lim_{N\to\infty} F(N,k)/N^{3/2}$ reliably.

In fig. 5 we plot $h_0(k)$ against $\sqrt{k}$, which confirms the prediction (3.7) from eleven-dimensional supergravity for $k = 1, 2, \cdots, 10$ very precisely.

[25]The functions $f_0(\lambda)$ and $f_1(\lambda)$ defined here are related to $F_0(\lambda)$ and $F_1(\lambda)$, which are defined in (4.4), as $f_0(\lambda) = -F_0(\lambda)/4\pi^2\lambda^2$ and $f_1(\lambda) = F_1(\lambda)$.

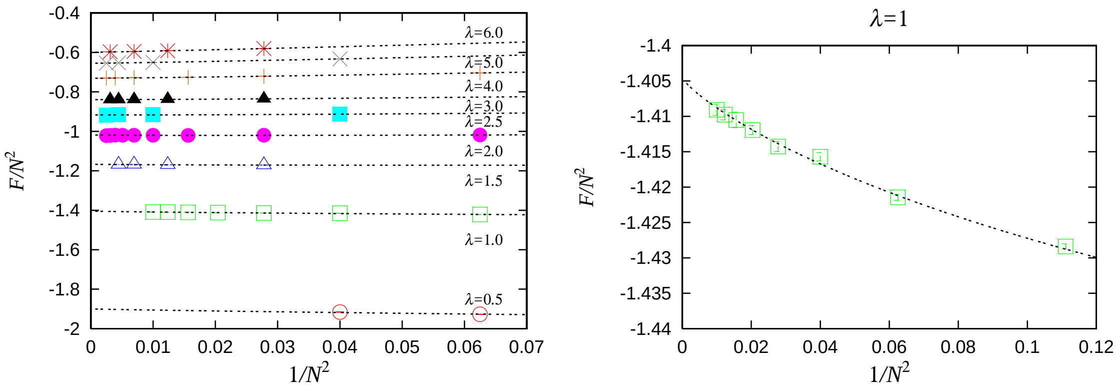

Figure 2: The normalized free energy F/N^2 is plotted against $1/N^2$ for various values of λ (Left). In the right panel, we zoom up the plot for $\lambda = 1$. The data can be nicely fitted to $F(N,\lambda)/N^2 = f_0(\lambda) + f_1(\lambda)/N^2 - \frac{1}{6}\log N$, which enables us to make a reliable extrapolation to the planar $N \to \infty$ limit.

3.3.3 Finite N effects

One of the important results on finite N effects in the free energy is that the $1/N$ corrections around the planar limit are resummed in a closed form (3.8) neglecting the worldsheet instanton effect. In fig. 6 we plot our results for $N = 4$ and $N = 8$ and compare them with the FHM result (3.8) and the DMP result (3.6). We find that both FHM and DMP are close to our data at strong coupling, but the difference between them is too small to see whether FHM is doing any better than DMP. This is simply because the term (3.7), which commonly exists in both results, is dominating over the difference. We therefore plot $F - F_{\text{SUGRA}}$ against N for $k = 1$ (Left) and $k = 8$ (Right) in fig. 7. The leading large-N behavior of the plotted quantity is $\frac{\pi}{\sqrt{2}}(\frac{1}{24} + \frac{1}{3k^2})k^{3/2}\sqrt{N}$ for FHM and $\frac{\pi}{24\sqrt{2}}k^{3/2}\sqrt{N}$ for DMP, where the difference comes from the $\lambda^2/(3N^2) = 1/(3k^2)$ term in (3.9). The difference becomes negligible for $k = 8$, but it is significant for $k = 1$, in which case our data are indeed closer to FHM than to DMP.

We also find some discrepancy between our result and FHM, which are almost independent of N. To see it more directly, we plot in fig. 8 the difference between our result and the FHM result for various k. It turns out that the discrepancies are indeed almost independent of N. This strongly suggests that the FHM result correctly incorporates the finite N effects except for a term which depends only on k. Note that this discrepancy cannot be explained by the worldsheet instanton effect $O(e^{-2\pi\sqrt{\lambda}})$, which is neglected in FHM. While this discrepancy does not affect the M-theory limit corresponding to the strict $N \to \infty$ limit for fixed k, it is non-negligible when one considers $1/N$ corrections. As we will see in section 3.4, this discrepancy coincides with $A(k) - \frac{1}{2}\log 2$ in eq. (3.12) by Fermi gas approach [40] for small k and with the constant map contribution for all k.

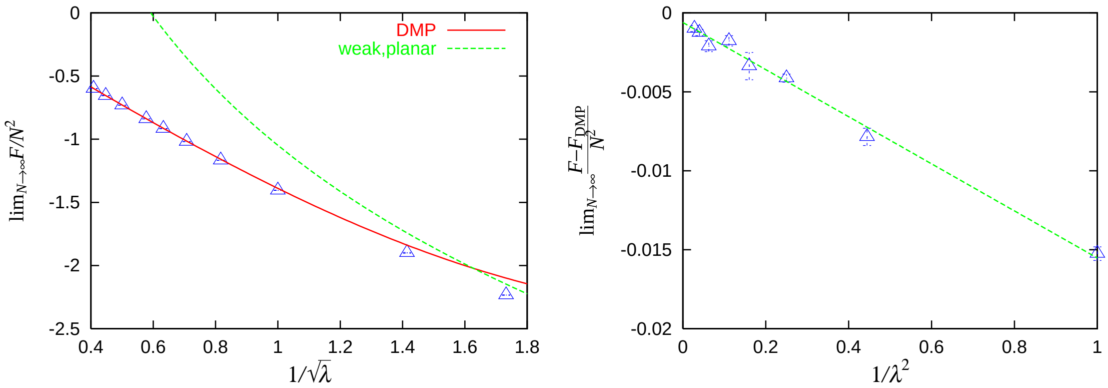

Figure 3: (Left) The free energy in the planar limit $f_0(\lambda) = \lim_{N\to\infty} F(N,\lambda)/N^2$ extracted from fig. 14 is plotted against $1/\sqrt{\lambda}$. Our results seem to interpolate the DMP result at strong coupling and the perturbative result at weak coupling. (Right) The difference between our result and the DMP result, i.e., $\lim_{N\to\infty}(F - F_{\rm DMP})/N^2$, is plotted against $1/\lambda^2$. The data points can be fitted to a straight line, which implies (3.27) and (3.28).

3.4 Interpretation of the discrepancies

In this section we provide an interpretation of the discrepancies between our data and the known analytical results, which we observe in the previous section.

3.4.1 Genus expansion

Let us consider the planar limit, in which $g_s N = 2\pi i N/k = 2\pi i\lambda$ is kept fixed. In that limit, the free energy can be expanded with respect to the genus as

$$\begin{aligned} F(g_s,\lambda) &= \sum_{g=0}^{\infty} F_g(\lambda) g_s^{2g-2} \\ &= -\frac{N^2}{(2\pi\lambda)^2} F_0(\lambda) + F_1(\lambda) - \frac{(2\pi\lambda)^2}{N^2} F_2(\lambda) + \cdots . \end{aligned} \tag{3.29}$$

Below we consider the free energy order by order in this expansion.

Planar contribution

The planar contribution $-k^2 F_0(\lambda)/(4\pi^2)$ can be studied by the saddle point method, and the $F_0(\lambda)$ can be determined by solving [33, 34, 37, 118]

$$\partial_\lambda F_0(\lambda) = \frac{\kappa}{4} G^{2,3}_{3,3}\left(\begin{array}{ccc} \frac{1}{2} & \frac{1}{2} & \frac{1}{2} \\ 0 & 0 & -\frac{1}{2} \end{array} \middle| -\frac{\kappa^2}{16} \right) + \frac{i\pi^2\kappa}{2} {}_3F_2\left(\frac{1}{2},\frac{1}{2},\frac{1}{2};1,\frac{3}{2};-\frac{\kappa^2}{16}\right), \tag{3.30}$$

$$\lambda(\kappa) = \frac{\kappa}{8\pi} {}_3F_2\left(\frac{1}{2},\frac{1}{2},\frac{1}{2};1,\frac{3}{2};-\frac{\kappa^2}{16}\right), \tag{3.31}$$

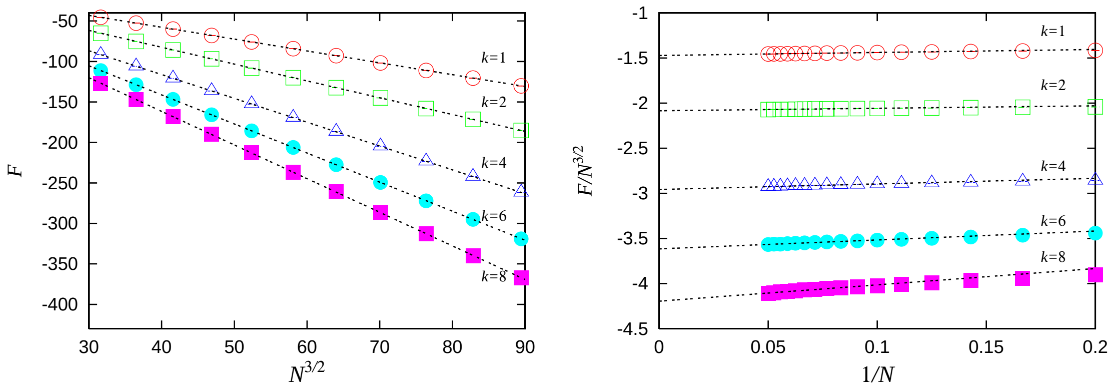

Figure 4: (Left) The free energy is plotted against $N^{3/2}$ for $k = 1, 2, 4, 6, 8$. The data points can be fitted to straight lines, which implies $F \sim N^{3/2}$ as N increases. (Right) The normalized free energy $F/N^{3/2}$ is plotted against $1/N$. The data can be nicely fitted to straight lines, which enables us to make extrapolations to the M-theory limit reliably.

where $G^{2,3}_{3,3}$ is the Meijer G-function[26] and ${}_3F_2$ is the hypergeometric function. Note that these equations are exact for arbitrary λ, and hence they fully incorporate the worldsheet instanton effect. One can obtain $F_0(\lambda)$ by carrying out the integration over λ as

$$F_0(\lambda) = F_0(0) + \int_0^\lambda d\lambda'\,\partial_{\lambda'}F_0(\lambda') = F_0(0) + \int_0^{\kappa(\lambda)} d\kappa'\,\frac{\partial\lambda'}{\partial\kappa'}\,\partial_{\lambda'}F_0(\lambda')\,. \tag{3.32}$$

At weak coupling $\lambda \ll 1$, in particular, one obtains

$$F_0(\lambda) = F_0(0) + \tilde{F}_0(\lambda) + \mathrm{O}(\lambda^9)\,, \tag{3.33}$$

$$\tilde{F}_0(\lambda) = 2\pi^2\lambda^2\left(3 - 2\log\frac{\pi\lambda}{2}\right) + \frac{4\pi^4\lambda^4}{9} - \frac{61\pi^6\lambda^6}{450} + \frac{12289\pi^8\lambda^8}{79380}\,. \tag{3.34}$$

By comparing this with the perturbative calculation (3.5), one finds $F_0(0) = 0$.

At strong coupling $\lambda \gg 1$, one obtains

$$F_0(\lambda) = c_0 + \hat{F}_0(\lambda) + \mathrm{O}\left(e^{-8\pi\sqrt{2\hat{\lambda}}}\right)\,, \tag{3.35}$$

$$\begin{aligned}\hat{F}_0(\lambda) = {} & \frac{4\pi^3\sqrt{2}}{3}\hat{\lambda}^{3/2} - e^{-2\pi\sqrt{2\hat{\lambda}}} + e^{-4\pi\sqrt{2\hat{\lambda}}}\left(\frac{9}{8} + \frac{1}{\pi\sqrt{2\hat{\lambda}}}\right) \\ & - e^{-6\pi\sqrt{2\hat{\lambda}}}\left(\frac{82}{27} + \frac{9\sqrt{2}}{4\pi\sqrt{\hat{\lambda}}} + \frac{1}{\pi^2\hat{\lambda}} + \frac{\sqrt{2}}{12\pi^3\hat{\lambda}^{3/2}}\right)\,,\end{aligned} \tag{3.36}$$

[26] The Meijer G-function is defined by

$$G^{m,n}_{p,q}\left(\begin{array}{ccc} a_1 & \cdots & a_p \\ b_1 & \cdots & b_q \end{array}\middle|\, x\right) = \frac{1}{2\pi i}\int_L \frac{\prod_{j=1}^m \Gamma(b_j - s)\prod_{j=1}^n \Gamma(1 - a_j + s)}{\prod_{j=m+1}^q \Gamma(1 - b_j + s)\prod_{j=n+1}^p \Gamma(a_j - s)} x^s ds\,,$$

where the path L is chosen in an appropriate way depending on the parameters.

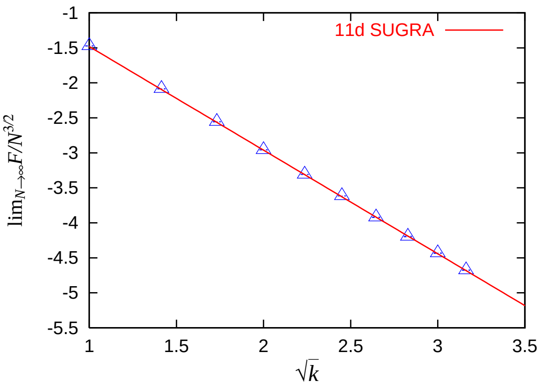

Figure 5: The M-theory limit of the free energy $\lim_{N\to\infty} F/N^{3/2}$ extracted from fig. 4 (Right) is plotted against $\sqrt{k}$. Our data are in good agreement with the result (3.7) predicted from eleven-dimensional supergravity, which is represented by the solid line.

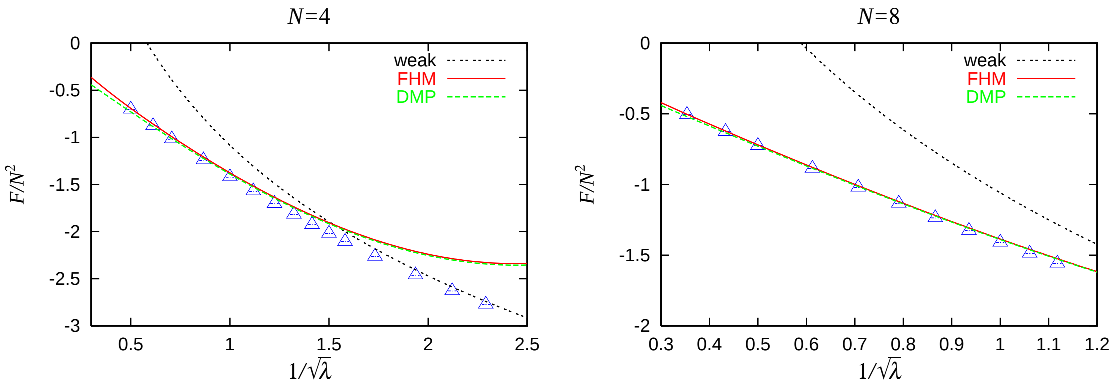

Figure 6: The free energy of the ABJM theory for $N = 4$ (Left) and $N = 8$ (Right) is plotted against $1/\sqrt{\lambda}$. The solid line and the dashed line represent the FHM result (3.8) and the DMP result (3.6), respectively. The dotted line represent the perturbative results (3.2).

where $\hat{\lambda} = \lambda - 1/24$. Here c_0 is an "integration constant", which has been set zero in the previous works, for instance, in ref. [34], which leads to eq. (3.6).

In fig. 9 we plot $c(\lambda) \equiv F_0(\lambda) - \hat{F}_0(\lambda)$, where $F_0(\lambda)$ is evaluated numerically by performing the integral (3.32) explicitly. As λ increases, we find that $c(\lambda)$ approaches a *nonzero* constant

$$c_0 \simeq 0.60103\,, \tag{3.37}$$

which coincides with $\zeta(3)/2 \simeq 0.601028$ obtained as the constant map contribution at genus zero [41, 44, 45]. The value of a_0 in (3.27) predicted from the above calculation is $a_0 = -c_0/4\pi^2 \simeq -0.015224$, which agrees well with the discrepancy (3.28) observed in the planar limit.

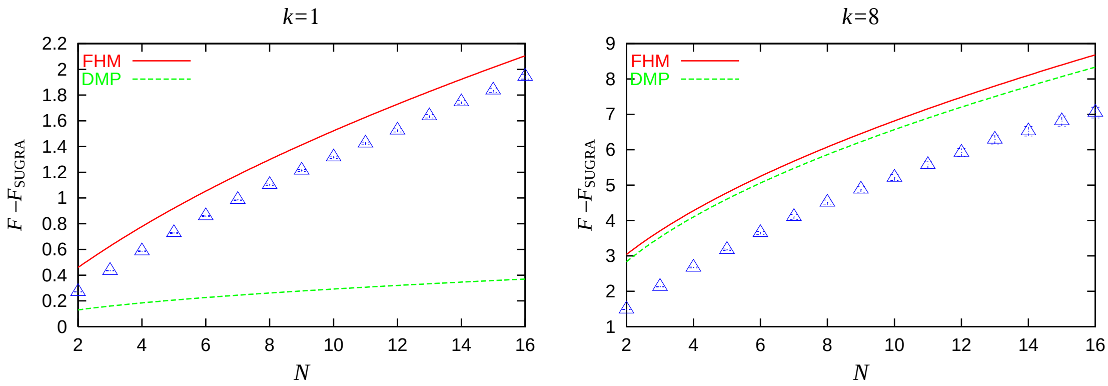

Figure 7: The free energy of the ABJM theory after subtraction of the dominant term (3.7) is plotted against N for $k = 1$ (Left) and $k = 8$ (Right). The solid line and the dashed line represent the FHM result (3.8) and the DMP result (3.6), respectively.

Higher genus contributions

Next we discuss the discrepancy at higher genus, which can be also interpreted as the constant map contributions as in the planar part. Let us note that the analytical results up to the constant map have been obtained for genus one and two in terms of modular forms as [34, 36, 112, 119]

$$F^{(1)}_{\rm modular}(\lambda) = -\log \eta(\tau)\,, \tag{3.38}$$

$$F^{(2)}_{\rm modular}(\lambda) = \frac{1}{432\vartheta_2^4\vartheta_4^8}\left(-\frac{5}{3}E_2^3 + 3\vartheta_2^4 E_2^2 - 2E_4E_2\right) + \frac{16\vartheta_2^{12} + 15\vartheta_2^8\vartheta_4^4 + 21\vartheta_2^4\vartheta_4^8 + 2\vartheta_4^{12}}{12960\vartheta_2^4\vartheta_4^8}\,, \tag{3.39}$$

where $\eta(\tau)$ is the Dedekind eta function, $E_n(\tau)$ is the Eisenstein series of weight n, $\vartheta_n(\tau)$ is the theta function, and $\tau(\lambda)$ is defined as

$$\tau(\lambda) = i\frac{K(\sqrt{1+\kappa^2/16})}{K(\frac{i\kappa}{4})} = 1 + \frac{i}{4\pi^3}\partial_\lambda^2 F_0(\lambda)\,, \tag{3.40}$$

where $K(x)$ is the complete elliptic integral of the first kind.

In fig. 10 we plot $F^{(1)}_{\rm modular} - \left(F^{(1)}_{\rm weak} + \frac{1}{6}\log k\right)$ (Left) and $F^{(2)}_{\rm modular} - F^{(2)}_{\rm weak}$ (Right) against λ, where we have defined the weak coupling results

$$F^{(1)}_{\rm weak}(\lambda) = -\frac{1}{6}\left(\log\lambda + \log k\right) + 2\zeta'(-1)\,, \tag{3.41}$$

$$F^{(2)}_{\rm weak}(\lambda) = -\frac{B_4}{16\pi^2\lambda^2}\,, \tag{3.42}$$

at genus one and two, respectively, as can be read off from (3.3). We find in both cases that the result approaches a constant as $\lambda \to 0$, which gives

$$c_1 \simeq 0.25558\,, \qquad c_2 \simeq 0.0027777\,, \tag{3.43}$$

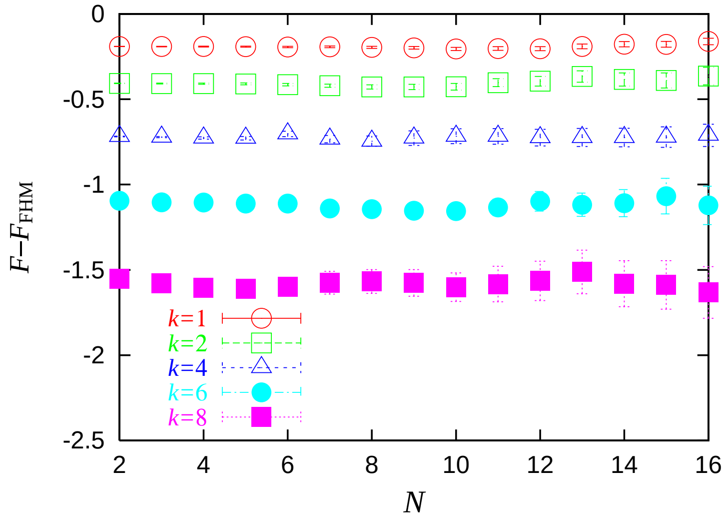

Figure 8: The difference $F - F_{\text{FHM}}$ is plotted against N for various values of k. It reveals non-negligible discrepancies for each k, which are almost independent of N.

respectively. This suggests that in the weak coupling region there are additional terms given by

$$\Delta F^{(1)} = -\frac{1}{6}\log k - c_1\,, \qquad \Delta F^{(2)} = -c_2\,, \tag{3.44}$$

which precisely coincide with the constant map contributions [41, 44, 45]

$$\begin{aligned} &\text{for genus } 1: && -\frac{1}{6}\log k + 2\zeta'(-1) + \frac{1}{6}\log\frac{\pi}{2}\,, \\ &\text{for genus } g \geq 2: && \frac{4^g B_{2g} B_{2g-2}}{4g(2g-2)(2g-2)!}\,. \end{aligned} \tag{3.45}$$

Since the FHM result (3.8) reproduces the previous results in the genus expansion, the FHM result must also have the additional contributions

$$F - F_{\text{FHM}} \simeq -c_0\frac{k^2}{4\pi^2} - \frac{1}{6}\log k - c_1 + c_2\frac{4\pi^2}{k^2} + \mathrm{O}(k^{-4})\,, \tag{3.46}$$

where the worldsheet instanton effect is neglected.

As we did in the case of planar contribution, we can test whether the discrepancy in the genus one contribution between our data and the previous analytical results can be explained by the additional terms identified above. In fig. 11 we extract the genus one contribution from our data in the following way. First we subtract from our data for the free energy, the planar contribution $g_s^{-2}F_0(\lambda)$, where $F_0(\lambda)$ is obtained by (3.32), and subtract also the term $-\frac{1}{6}\log k$ that appears in the weak coupling result (3.41). Then we plot the result after these subtractions against $1/N^2$ in fig. 11 (Left), which can be nicely fitted to straight lines. The intercepts give the values of the genus one contribution for each λ, which are plotted against λ in fig. 11 (Right). We find that the result is in good agreement with the genus one contribution of F_{FHM} after making a constant shift by $-c_1$ determined as (3.43).

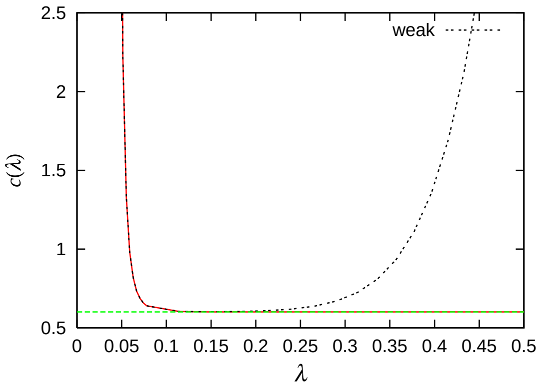

Figure 9: The solid line represents $c(\lambda) \equiv F_0(\lambda) - \hat{F}_0(\lambda)$, where $F_0(\lambda)$ is evaluated numerically by performing the integral (3.32) explicitly. The "integration constant" c_0 in (3.35) is obtained as (3.37) from the asymptotic value of $c(\lambda)$ at large λ. The dotted line represents $\tilde{F}_0(\lambda) - \hat{F}_0(\lambda)$, where $\tilde{F}_0(\lambda)$ is the result at weak coupling given by (3.34). The matching of the weak coupling result and the strong coupling result around $\lambda \sim 0.15$ also requires a similar value of c_0 in (3.35).

3.4.2 Finite N effects

Let us see how well the FHM result with the corrections (3.46) does at finite N. In fig. 12 we plot $F - F_{\mathrm{FHM}}$, i.e., the discrepancies between our result and the FHM result for $N = 2$ and $N = 10$ against k. At $k \gtrsim 1$, the $N = 2$ data and the $N = 10$ data are on top of each other as anticipated from fig. 8. In this regime, the discrepancies are in good agreement with the corrections (3.46) identified in section 3.4.1.

It is interesting to see what happens if we go to smaller k region in fig. 12 although non-integer k is not physical in the original gauge theory. Firstly we start to see some difference between $N = 2$ and $N = 10$, which implies that there is some N dependence which is not captured by the FHM result in this regime. We speculate that the N dependence is due to the membrane instanton effect [36, 120], which behaves as $\mathrm{O}(e^{-\pi\sqrt{2kN}})$, since the worldsheet instanton effect is negligible in this regime. Secondly, we find that the discrepancy between our result and the FHM result no longer agrees with (3.46) including corrections up to genus two. This is understandable since the higher genus terms become non-negligible as one goes to smaller k (larger g_s).

On the other hand, the free energy at small k is calculated by the Fermi gas approach as (3.12). We find that our data for $N = 10$ interpolate nicely the behavior (3.12) at small k and the behavior (3.46) at large k. This also supports our speculation that the difference between the $N = 2$ and $N = 10$ data at small k is due to the membrane instanton effect, which is neglected in the Fermi gas approach. Note, in particular, that the Fermi gas approach yields correction to the FHM result in odd powers of k, whereas the genus expansion yields even powers of $1/k$. Our data nicely interpolate the two asymptotic behaviors, which are smoothly connected around $k \sim 1$.

Finally let us consider the sum of the constant map contributions at all genus (3.45),

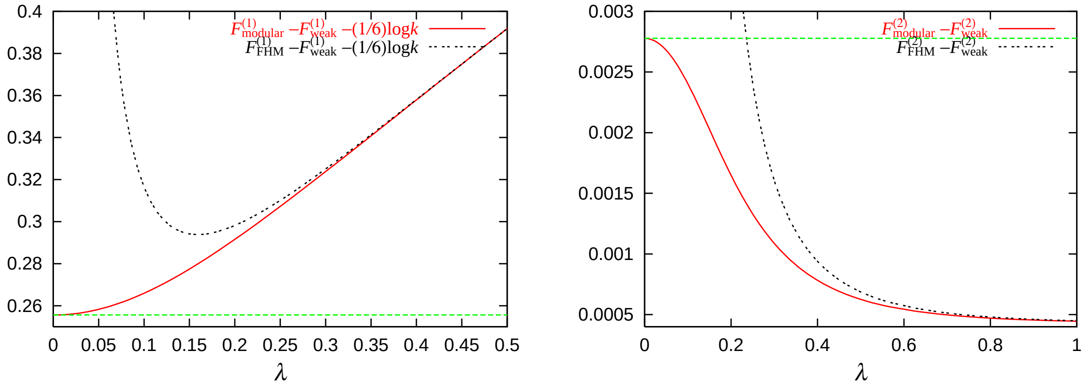

Figure 10: (Left) The solid line represents $F^{(1)}_{\rm modular} - \left(F^{(1)}_{\rm weak} + \frac{1}{6}\log k\right)$, which is the difference between the modular expression (3.38) and the weak coupling result for genus one. It approaches a constant smoothly for $\lambda \to 0$, which gives c_1 in (3.43). The dotted line represents $F^{(1)}_{\rm FHM} - \left(F^{(1)}_{\rm weak} + \frac{1}{6}\log k\right)$, which diverges as $\lambda \to 0$ since the FHM result neglects the worldsheet instanton effect. (Right) The solid line represents $F^{(2)}_{\rm modular} - F^{(2)}_{\rm weak}$, which is the difference between the modular expression (3.39) and the weak coupling result for genus two. It approaches a constant smoothly for $\lambda \to 0$, which gives c_2 in (3.43). The dotted line represents $F^{(2)}_{\rm FHM} - F^{(2)}_{\rm weak}$, which diverges as $\lambda \to 0$ since the FHM result neglects the worldsheet instanton effect. Here $F^{(2)}_{\rm FHM}$ is given by $F^{(2)}_{\rm FHM} = \frac{1}{144\sqrt{2}\pi}\hat{\lambda}^{-1/2} - \frac{1}{48\pi^2}\hat{\lambda}^{-1} + \frac{5}{96\sqrt{2}\pi^3}\hat{\lambda}^{-3/2}$.

which is given by[27]

$$
\begin{aligned}
F_{\rm const} \;&=\; -\frac{\zeta(3)}{8\pi^2}k^2 - \frac{1}{6}\log k + \frac{1}{6}\log\frac{\pi}{2} + 2\zeta'(-1) \\
&\quad -\frac{1}{3}\int_0^\infty dx\, \frac{1}{e^{kx}-1}\left(\frac{3}{x^3} - \frac{1}{x} - \frac{3}{x\sinh^2 x}\right) .
\end{aligned}
\tag{3.47}
$$

In fig. 12 we find that this function agrees well with the discrepancy between our result and the FHM result for the whole range of k investigated, including $k \lesssim 1$. Since the Fermi gas result (3.12) also gives accurate description there, it is natural to guess that they are actually the same. Indeed, as we show in appendix E, the sum of the constant map (3.47) can be expanded around $k = 0$ as

$$
\begin{aligned}
F_{\rm const} \;&=\; \frac{2\zeta(3)}{\pi^2 k} - \frac{1}{2}\log 2 + \sum_{n=1}^{\infty}\frac{(-1)^n}{(2n)!}B_{2n}B_{2n-2}\pi^{2n-2}k^{2n-1} \\
&=\; -\frac{1}{2}\log 2 + \frac{2\zeta(3)}{\pi^2 k} - \frac{k}{12} - \frac{\pi^2 k^3}{4320} + \frac{\pi^4 k^5}{907200} + \cdots ,
\end{aligned}
\tag{3.48}
$$

which exactly reproduces the result of the Fermi gas approach (3.12) to the k^3 term.[28] Remarkably, the constant map contribution (3.47) and the expansion (3.48) are equivalent

[27] An assumption is needed to obtain (3.47) and (3.48). For details, see appendix E.

[28] Note that the Fermi gas calculation has been done only to the k^3 term, and the higher order terms are just an educated guess. Calculations at higher orders would be an interesting future direction.

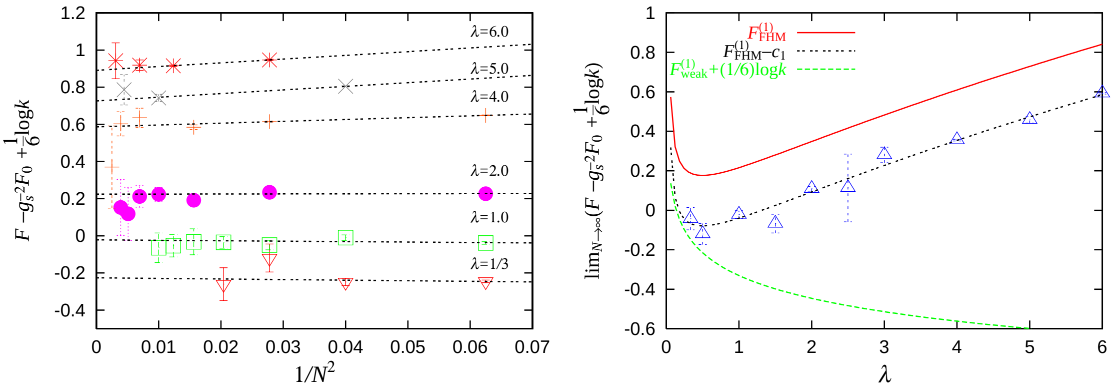

Figure 11: (Left) $F - g_s^{-2} F_0 + \frac{1}{6} \log k$ is plotted against $1/N^2$. The results are nicely fitted to straight lines, which enables us to extract the genus one contribution reliably. (Right) The genus one contribution extracted from the left panel is plotted against λ. The solid line represents the genus one contribution to $F_{\rm FHM}$, whereas the dotted line represents $F^{(1)}_{\rm FHM} - c_1$, where c_1 is given by (3.43). The dashed line represents the weak coupling behavior given by (3.41) with the $-\frac{1}{6} \log k$ term being subtracted.

at any k. Therefore, we expect that the result (3.48) is the all-order form of $A(k) - \frac{1}{2} \log 2$ in the Fermi gas approach. In other words, we expect that the expansions of the free energy around $k = \infty$ (the constant map contribution) and $k = 0$ (the Fermi gas approach) give the same answer after taking sums to all orders. In this sense the free energy around the planar and M-theory limits are smoothly connected with each other.

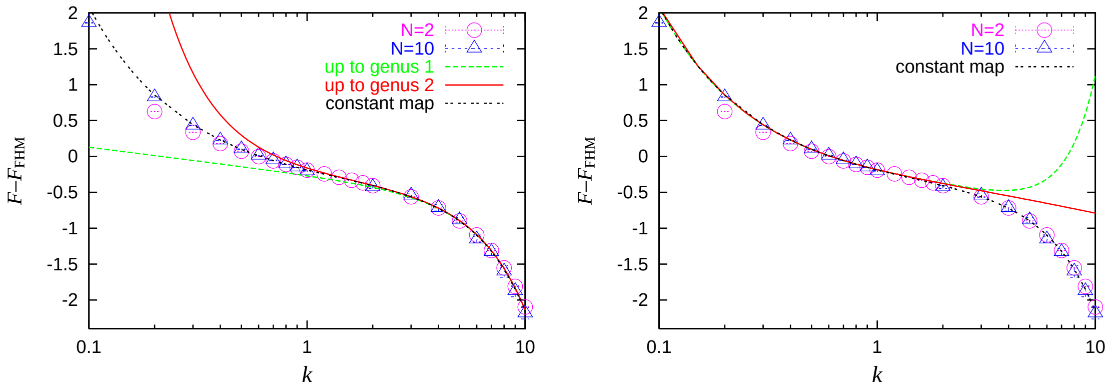

Figure 12: (Left) The discrepancy of the free energy between our data and the FHM result is plotted against k, and compared with the analytical results around the planar limit for $N = 2$ and $N = 10$. The dashed and the solid lines represent the correction (3.46) up to genus one term and up to genus two term, respectively. The dotted line represents the sum of the constant map contributions at all genus (3.47). (Right) The same as the left panel except that our data is compared with the result obtained by the Fermi gas approach. The dashed and the solid lines represent the analytical results (3.12) with $A(k)$ given by (3.11) and (3.13), respectively. The dotted line represents again the sum of the constant map contributions at all genus (3.47).

4 Supersymmetric Wilson loop

In this chapter we present our (preliminary) numerical result of the supersymmetric Wilson loop. This chapter is organized as follows. In Sec. 4.1 we introduce the supersymmetric Wilson loops of the ABJM theory and review analytic results which are compared with our numerical data. We will explain in what parameter region and up to what corrections the results should be valid. In Sec. 4.2 we present our numerical technique. Then in Sec. 4.3 we show the Monte Carlo data. By comparing them with the analytic expressions in various limits, we confirm the validity of the previous results, and furthermore, extract the instanton effects.

4.1 Supersymmetric Wilson loops in various limit

From (2.81) the expectation value of the 1/6-BPS Wilson loop in the fundamental representation is written as[29]

$$\left\langle W_{1/6} \right\rangle = \frac{1}{N} \sum_i \langle e^{\mu_i} \rangle_{M.M.} \,, \tag{4.1}$$

By applying the localization method to the 1/2-BPS Wilson loop in the fundamental representation, the expectation value of the operator is given by

$$\left\langle W_{1/2} \right\rangle = \frac{1}{N} \sum_i \langle e^{\mu_i} + e^{\nu_i} \rangle_{M.M.} \,. \tag{4.2}$$

from (2.84). Because $\langle e^{\nu_i} \rangle_{M.M.} = \langle e^{\mu_i} \rangle^*_{M.M.}$, this has the following simple relation to the expectation value of the 1/6-BPS Wilson loop as

$$\left\langle W_{1/2} \right\rangle = 2\mathrm{Re} \left\langle W_{1/6} \right\rangle . \tag{4.3}$$

Therefore we consider only $\left\langle W_{1/6} \right\rangle$ from now on.

The expectation value of the 1/6-BPS Wilson loop can be expanded with respect to the genus as

$$\begin{aligned} \left\langle W_{1/6} \right\rangle &= \sum_{g=0}^{\infty} g_s^{2g} \left\langle W_{1/6} \right\rangle_g \\ &= \left\langle W_{1/6} \right\rangle_{g=0} - \frac{(2\pi\lambda)^2}{N^2} \left\langle W_{1/6} \right\rangle_{g=1} + \frac{(2\pi\lambda)^4}{N^4} \left\langle W_{1/6} \right\rangle_{g=2} + \cdots \,, \end{aligned} \tag{4.4}$$

where $g_s = 2\pi i/k = 2\pi i\lambda/N$.

[29] In order to obtain the result in the trivial framing, we must multiply $e^{-\pi i\lambda}$, which is the inverse of so-called framing factor.

Planar limit ($N \to \infty$ with λ fixed) for all λ

In ref. [33], the single differential equation determining the planar expectation value of the Wilson loop had been obtained as

$$\frac{d}{d\kappa}\left[\lambda(\kappa)\left\langle W_{1/6}\right\rangle_{g=0}\right] = -\frac{1}{2\pi^2\sqrt{ab}(1+ab)}\left[aK(k) - (a+b)\Pi(n|k)\right]. \tag{4.5}$$

Here,

$$\begin{aligned}
\lambda(\kappa) &= \frac{\kappa}{8\pi}{}_3F_2\left(\frac{1}{2},\frac{1}{2},\frac{1}{2};1,\frac{3}{2};-\frac{\kappa^2}{16}\right), \\
a(\kappa) &= \frac{1}{2}\left(2+i\kappa+\sqrt{\kappa(4i-\kappa)}\right), \quad b(\kappa) = \frac{1}{2}\left(2-i\kappa+\sqrt{-\kappa(4i+\kappa)}\right), \\
n(\kappa) &= \frac{b(\kappa)}{a(\kappa)}\frac{a(\kappa)^2-1}{1+a(\kappa)b(\kappa)}, \quad k(\kappa) = \frac{\sqrt{(a(\kappa)^2-1)(b(\kappa)^2-1)}}{1+a(\kappa)b(\kappa)},
\end{aligned} \tag{4.6}$$

where ${}_3F_2$ is a generalized hypergeometric function. K and Π are the complete elliptic integrals of the first and third kind, respectively.

Perturbative results ($\lambda \ll 1/2\pi$) for all N

In the planar limit, perturbative calculations had been performed in refs. [98, 99, 100, 121]. Alternatively, one can obtain the weak coupling expression by solving the differential equation (4.5). The result is

$$\left\langle W_{1/6}\right\rangle_{g=0} = e^{\pi i\lambda}\left(1+\frac{5\pi^2}{6}\lambda^2 - \frac{i\pi^3}{2}\lambda^3 - \frac{29\pi^4}{120}\lambda^4 + \frac{i\pi^5}{12}\lambda^5 + \mathrm{O}(\lambda^6)\right). \tag{4.7}$$

Furthermore, by taking small λ expansion of eq. (4.1), one can calculate the expression to all order in $1/N$ [34]

$$\begin{aligned}
\left\langle W_{1/6}\right\rangle &= e^{\pi i\lambda}\Bigg[1+\left(\frac{5}{6}+\frac{1}{6N^2}\right)\pi^2\lambda^2 - \left(\frac{1}{2}-\frac{1}{2N^2}\right)i\pi^3\lambda^3 \\
&\qquad - \left(\frac{29}{120}-\frac{8}{9N^2}-\frac{7}{360N^4}\right)\pi^4\lambda^4 + \mathrm{O}(\lambda^5)\Bigg],
\end{aligned} \tag{4.8}$$

which is valid for all finite N and reduces to eq. (4.7) in the large-N limit.

Strong coupling in the planar limit ($N \to \infty$ and $\lambda \gg 1/2\pi$)

At the strong coupling region in the planar limit, the analytic expression is obtained by solving the equation (4.5) in the $\kappa \gg 1$ and $\lambda \gg 1$ limit [33], and given by

$$\left\langle W_{1/6}\right\rangle_{g=0} = \frac{1}{2\pi i\lambda}\left(-\frac{1}{2}\sqrt{2\hat{\lambda}}+\frac{1}{2\pi}+\frac{i}{4}\right)e^{\pi\sqrt{2\hat{\lambda}}} + \mathrm{O}(e^{-\pi\sqrt{2\hat{\lambda}}}), \tag{4.9}$$

where $\hat{\lambda} = \lambda - 1/24$. (For the derivation, see Appendix F.) This expression shows a perfect agreement with the dual gravity calculation. Exponentially small correction of the order $e^{-\pi\sqrt{2\hat{\lambda}}}$ had been interpreted in ref. [34] as the effect of the worldsheet instanton in the dual type IIA superstring, which corresponds to a string worldsheet wrapping a $\mathbb{C}P^1$ cycle in $\mathbb{C}P^3$ [108].

The $1/N^2$ correction to this expression had also been studied in ref. [34]. Then we can obtain the genus-1 contribution as

$$\left\langle W_{1/6} \right\rangle_{g=1} = \frac{1}{2\pi i \lambda} \left(\frac{1}{12}\sqrt{2\hat{\lambda}} - \frac{i}{24} - \frac{1}{12\pi} + \frac{i}{12\pi\sqrt{2\hat{\lambda}}} - \frac{i}{32\pi^2\hat{\lambda}} \right) e^{\pi\sqrt{2\hat{\lambda}}}, \tag{4.10}$$

up to $\mathrm{O}(e^{-\pi\sqrt{2\hat{\lambda}}})$. Note that the instanton correction becomes large as λ becomes small. Therefore, it is important to see how this strong-coupling expression and the weak coupling expression (4.7) are interpolated at the intermediate region $\lambda \sim 1/2\pi$.

All N and k, up to the instanton effects

In ref. [46], the Fermi gas approach [40] is applied to the Wilson loop with fixed k, neglecting the quantum mechanical instanton effect (worldsheet instanton effect) and the exponentially small corrections in the chemical potential of the gas (membrane instanton effect [120]). The result is

$$\left\langle W_{1/6} \right\rangle = -\frac{A_1(k)}{NC^{1/3}} \frac{\mathrm{Ai}'\left[C^{-1/3}\left(N - \frac{k}{24} - \frac{7}{3k}\right)\right]}{\mathrm{Ai}\left[C^{-1/3}\left(N - \frac{k}{24} - \frac{1}{3k}\right)\right]} + \frac{A_2(k)}{N} \frac{\mathrm{Ai}\left[C^{-1/3}\left(N - \frac{k}{24} - \frac{7}{3k}\right)\right]}{\mathrm{Ai}\left[C^{-1/3}\left(N - \frac{k}{24} - \frac{1}{3k}\right)\right]} \tag{4.11}$$

up to $\mathrm{O}(e^{-\pi\sqrt{2\hat{\lambda}}}, e^{-\pi\sqrt{2kN}})$. The parameters $A_1(k)$, $A_2(k)$ and C are given by

$$A_1(k) = \frac{i}{\pi k} \csc\frac{2\pi}{k}, \quad A_2(k) = \left(\frac{1}{4} - \frac{i}{k}\cot\frac{2\pi}{k}\right)\csc\frac{2\pi}{k}, \quad C = \frac{2}{\pi^2 k}. \tag{4.12}$$

Note that this expression is singular for $k = 1, 2$. The authors of ref. [46] concluded that the expression is not valid for these values of k. Therefore, it is important to look more closely what happens when $k = 1, 2$.

As we have explained before, the instanton correction becomes large at weak 't Hooft coupling, and hence this expression should cease to work at some point and should be interpolated to the weak coupling formulae (4.7) and (4.8).

4.2 Numerical methods for ABJM BPS Wilson loop

Let us consider the expectation value of an observable $\mathcal{O}(x)$:

$$\langle \mathcal{O} \rangle = \frac{\int d^N x \, \mathcal{O}(x) e^{-S(x)}}{\int d^N x \, e^{-S(x)}}. \tag{4.13}$$

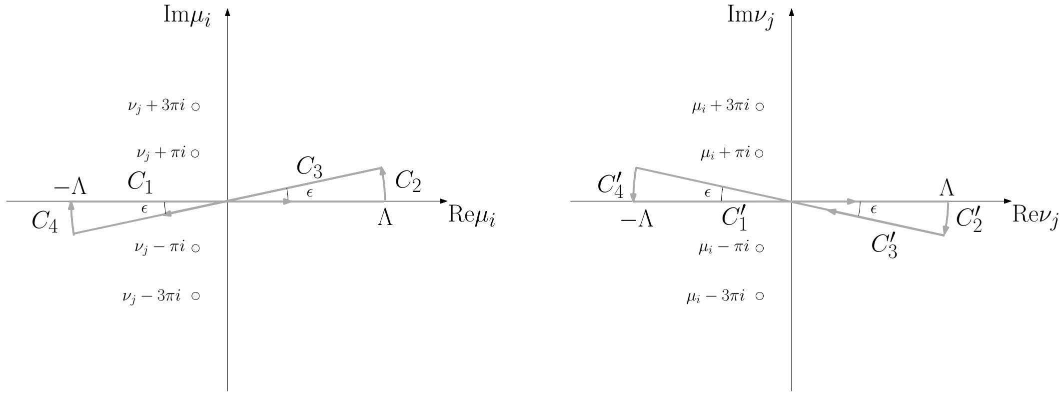

Figure 13: The contour deformation in eq. (4.18)

When $e^{-S(x)}$ is real and positive, one can use the Monte Carlo method to calculate it. (For the details, see Appendix A in ref. [42].) The partition function of the ABJM theory on S^3 (2.78) can be rewritten in the positive-definite form [39, 40, 115]

$$Z_{\text{ABJM}} = \frac{1}{2^N N!} \int \frac{d^N x}{(2\pi k)^N} \frac{\prod_{i<j} \tanh^2\left(\frac{x_i - x_j}{2k}\right)}{\prod_i 2\cosh\left(\frac{x_i}{2}\right)}, \tag{4.14}$$

so that the Monte Carlo method is applicable. Actually, in ref. [42], we performed the Monte Carlo simulation of the free energy by using this expression. In this section, we show the expectation value of 1/6-BPS Wilson loop can be also calculated by using this positive-definite expression. Moreover, we introduce an efficient simulation technique.

4.2.1 1/6-BPS Wilson loop in positive-definite form

The expectation value of 1/6-BPS Wilson loop (4.1) is written as

$$\begin{aligned} \left\langle W_{1/6} \right\rangle &= \frac{1}{Z_{\text{ABJM}}} \frac{1}{(N!)^2} \int \frac{d^N\mu}{(2\pi)^N} \frac{d^N\nu}{(2\pi)^N}\, e^{\mu_1} \frac{\prod_{i<j}\left(2\sinh\frac{\mu_i-\mu_j}{2}\right)^2 \left(2\sinh\frac{\nu_i-\nu_j}{2}\right)^2}{\prod_{i,j}\left(2\cosh\frac{\mu_i-\nu_j}{2}\right)^2} \\ &\quad \times \exp\left[\frac{ik}{4\pi}\sum_{i=1}^N(\mu_i^2 - \nu_i^2)\right]. \end{aligned} \tag{4.15}$$

By using the Cauchy identity (G.3), the integrand can be simplified:

$$\begin{aligned} \left\langle W_{1/6} \right\rangle &= \frac{1}{Z_{\text{ABJM}}} \frac{1}{N!} \sum_\sigma (-1)^\sigma \int \frac{d^N\mu}{(2\pi)^N} \frac{d^N\nu}{(2\pi)^N} \frac{e^{\mu_1}}{\prod_i 2\cosh\frac{\mu_i-\nu_i}{2} \cdot 2\cosh\frac{\mu_i - \nu_{\sigma(i)}}{2}} \\ &\quad \times \exp\left[\frac{ik}{4\pi}\sum_{i=1}^N(\mu_i^2 - \nu_i^2)\right]. \end{aligned} \tag{4.16}$$

As we will see below, this integral is divergent at small k. Therefore, in order to make the argument robust, we set the cutoff Λ for the integration domain and then remove it:

$$\langle W_{1/6} \rangle = \frac{\lim_{\Lambda\to\infty} W_\Lambda}{Z_{\text{ABJM}}} , \tag{4.17}$$

where we define

$$\begin{aligned} W_\Lambda \ &:= \ \frac{1}{N!}\sum_\sigma (-1)^\sigma \int_{-\Lambda}^{\Lambda} \frac{d^N\mu}{(2\pi)^N}\frac{d^N\nu}{(2\pi)^N} \frac{e^{\mu_1}}{\prod_i 2\cosh\frac{\mu_i-\nu_i}{2}\cdot 2\cosh\frac{\mu_i-\nu_{\sigma(i)}}{2}} \\ &\quad \times \exp\left[\frac{ik}{4\pi}\sum_{i=1}^N(\mu_i^2-\nu_i^2)\right]. \end{aligned} \tag{4.18}$$

Let us now change the integration contours as in Fig. 13 to make the convergence of integrand faster: $C_1 \to C_2 + C_3 + C_4$ and $C_1' \to C_2' + C_3' + C_4'$. We should take $|\epsilon| < \pi/\Lambda$, so that the values of integrations remain unchanged by the Cauchy's integration theorem. Since the integrations along C_2, C_4, C_2', C_4' are irrelevant[30] for the $\Lambda \to \infty$ limit, we drop these contributions below. Then, by using the Fourier transformation for $1/\cosh\frac{\mu-\nu}{2}$, W_Λ is rewritten as

$$\begin{aligned} W_\Lambda \ &= \ \frac{1}{N!}\sum_\sigma (-1)^\sigma \frac{1}{\pi^{2N}}\int d^N x d^N y \, \frac{e^{-\frac{i}{\pi k}\left((x_1+y_1-i\pi)^2-(x_1+y_{\sigma(1)})^2\right)-\frac{i}{\pi k}\sum_{i=2}^N\left((x_i+y_i)^2-(x_i+y_{\sigma(i)})^2\right)}}{\prod_i 2\cosh x_i\cdot 2\cosh y_i} \\ &\quad \times \int_{-\Lambda}^{\Lambda}\frac{d^N\mu}{(2\pi)^N}\frac{d^N\nu}{(2\pi)^N}\exp\left[\frac{ie^{2i\epsilon}k}{4\pi}\left(\mu_1+\frac{2e^{-i\epsilon}}{k}(x_1+y_1-i\pi)\right)^2\right. \\ &\qquad \left. +\frac{ie^{2i\epsilon}k}{4\pi}\sum_{i=2}^N\left(\mu_i+\frac{2e^{-i\epsilon}}{k}(x_i+y_i)\right)^2-\frac{ie^{-2i\epsilon}k}{4\pi}\sum_{i=1}^N\left(\nu_i-\frac{2e^{i\epsilon}}{k}(x_i+y_{\sigma(i)})\right)^2\right]. \end{aligned} \tag{4.19}$$

Then we can easily perform the integrations over $\mu_2, \cdots, \mu_N$ and ν_i by the usual Gauss integrations. The remaining integration over μ_1, however, is not so simple: we need to impose $\epsilon > 1/\Lambda^2$ in order to obtain the finite value of the Gauss integration.[31] By using again the Cauchy identity (G.6), we finally obtain

$$\begin{aligned} \langle W_{1/6}\rangle \cdot Z_{ABJM} &= \lim_{\Lambda\to\infty} W_\Lambda \\ &= \frac{e^{\frac{\pi}{k}i}}{2^N N!}\frac{1}{\cos\frac{\pi}{k}}\int\frac{d^N x}{(2\pi k)^N}\, e^{-\frac{x_1}{k}}\prod_{j=2}^N\left[\frac{\tanh\left(\frac{x_1-x_j-2\pi i}{2k}\right)}{\tanh\left(\frac{x_1-x_j}{2k}\right)}\right]\frac{\prod_{i<j}\tanh^2\left(\frac{x_i-x_j}{2k}\right)}{\prod_i 2\cosh\frac{x_i}{2}} . \end{aligned} \tag{4.20}$$

Therefore, $\langle W_{1/6}\rangle$ can be calculated as

$$\langle W_{1/6}\rangle = \frac{e^{\frac{\pi}{k}i}}{\cos\frac{\pi}{k}}\left\langle e^{-\frac{x_1}{k}}\prod_{j=2}^N\left[\frac{\tanh\left(\frac{x_1-x_j-2\pi i}{2k}\right)}{\tanh\left(\frac{x_1-x_j}{2k}\right)}\right]\right\rangle \tag{4.21}$$

[30] Here we must take $\text{sign}(\epsilon) = \text{sign}(k)$.

[31] More precisely, we require $\lim_{\Lambda\to\infty} e^{-\frac{k}{2\pi}\epsilon\Lambda^2} = 0$.

where the expectation value in the right hand side is evaluated by using the partition function (4.14).

When x_1 takes a large negative value, we see that

$$\text{(integrand of eq. (4.20))} \sim e^{(1/k-1/2)|x_1|} \tag{4.22}$$

and hence the integral is divergent for $k \leq 2$. This means that the expectation value of the Wilson loop $\langle W_{1/6} \rangle$ itself is divergent for $k \leq 2$ since the partition function of the ABJM matrix model is finite. This is consistent with the observation in ref. [46].

4.2.2 Simulation method

In the Monte Carlo simulation, it is not easy to evaluate a rapidly increasing operator like (4.21).[32] This difficulty becomes severe when k is close to 2 and/or λ is large. In order to avoid it, we consider

$$e^{-S_\alpha(N,k;x)} \quad := \quad \left| e^{-\frac{x_1}{k}} \prod_{j=2}^{N} \left[\frac{\tanh\left(\frac{x_1-x_j-2\pi i}{2k}\right)}{\tanh\left(\frac{x_1-x_j}{2k}\right)} \right] \right|^{\alpha} \frac{\prod_{i<j} \tanh^2\left(\frac{x_i-x_j}{2k}\right)}{\prod_i 2\cosh\frac{x_i}{2}}. \tag{4.23}$$

Then the expectation value of the Wilson loop can be written as

$$\langle W_{1/6} \rangle = \frac{e^{\frac{\pi}{k}i}}{\cos\frac{\pi}{k}} \cdot \langle phase \rangle_{S_{\alpha_\ell}} \cdot \prod_{i=0}^{\ell-1} \left\langle e^{-S_{\alpha_{i+1}}+S_{\alpha_i}} \right\rangle_{S_{\alpha_i}}, \tag{4.24}$$

where $\langle \cdots \rangle_{S_{\alpha_i}}$ is an expectation value with the weight $e^{-S_{\alpha_i}}$, *phase* is the phase factor $e^{-S_1}/|e^{-S_1}|$, and $0 = \alpha_0 < \alpha_1 < \cdots < \alpha_\ell = 1$. Then, by dividing the integral to sufficiently many steps $\ell \gg 1$ (i.e. by taking $\alpha_{i+1} - \alpha_i$ sufficiently small), each step can be calculated reliably and hence one can evaluate $\langle W_{1/6} \rangle$ accurately.

4.3 Simulation results

Now we show our Monte Carlo data. As we have seen in Sec. 4.1, nontrivial things which can be studied by the Monte Carlo simulation are:

- How the strong and weak coupling formulas are interpolated.
- The detail of the instanton correction.

In this section we study these points, after confirming the consistency of the data and analytic formulas. Note that we don't restrict k to integer; although it is quantized in the original ABJM theory, the matrix model obtained through the localization is well-defined also for non-integer k.

In the following, we denote $\langle W_{1/6} \rangle$ simply as $\langle W \rangle$. Remember that the expectation value of 1/2-BPS Wilson loop is given by the real part of that of 1/6-BPS Wilson loop as eq. (4.3).

[32] During the simulation, the fluctuation of the integrand in eq. (4.20) becomes very violent, so that the importance sampling fails in practice. More precisely, very sharp spikes appear due to the prefactor $e^{-\frac{x_1}{k}}$ in the integrand. Such spikes take 10^5 times or 10^{10} times or even bigger values compared to most samples.

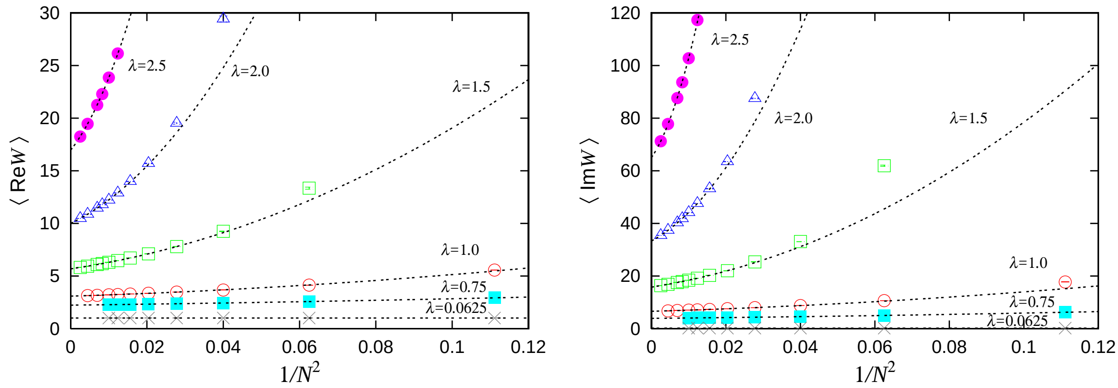

Figure 14: Plots of $\mathrm{Re}\,\langle W\rangle$ (left) and $\mathrm{Im}\,\langle W\rangle$ (right) for various values of λ as functions of $1/N^2$. The data can be fitted by $\mathrm{Re}\,\langle W\rangle = f_0^{(R)}(\lambda) + f_1^{(R)}(\lambda)/N^2 + f_2^{(R)}(\lambda)/N^4$ and $\mathrm{Im}\,\langle W\rangle = f_0^{(I)}(\lambda) + f_1^{(I)}(\lambda)/N^2 + f_2^{(I)}(\lambda)/N^4$.

4.3.1 Planar limit ($N \to \infty$ with $\lambda = N/k$ fixed)

First we consider the planar limit, which is conjectured to be dual to the classical type IIA superstring theory on $AdS_4 \times \mathbb{C}P^3$.

In fig. 14, we plot $\mathrm{Re}\,\langle W\rangle$ and $\mathrm{Im}\,\langle W\rangle$ for various fixed values of λ as functions of $1/N^2$. At sufficiently large N, the data can be fitted well by

$$\mathrm{Re}\,\langle W\rangle = f_0^{(R)}(\lambda) + \frac{f_1^{(R)}(\lambda)}{N^2} + \frac{f_2^{(R)}(\lambda)}{N^4} \tag{4.25}$$

and

$$\mathrm{Im}\,\langle W\rangle = f_0^{(I)}(\lambda) + \frac{f_1^{(I)}(\lambda)}{N^2} + \frac{f_2^{(I)}(\lambda)}{N^4}\,, \tag{4.26}$$

as expected from the usual $1/N$ counting. In the following, we study the properties of $f_g^{(R)}(\lambda)$ and $f_g^{(I)}(\lambda)$ determined by the numerical fit.

In fig. 15, we plot

$$\lim_{N\to\infty} \mathrm{Re}\,\langle W\rangle = f_0^{(R)}(\lambda) =: \mathrm{Re}\,\langle W\rangle_{g=0}\,, \qquad \lim_{N\to\infty} \mathrm{Im}\,\langle W\rangle = f_0^{(I)}(\lambda) =: \mathrm{Im}\,\langle W\rangle_{g=0} \tag{4.27}$$

against $\sqrt{\lambda}$. The solid lines are the strong coupling expression (4.9) obtained by Mariño and Putrov [33], while the dashed lines are the perturbative result (4.7) at weak coupling region. Our numerical data nicely interpolate these two expressions. The data agree well with the strong coupling expression at $\sqrt{\lambda} \gtrsim 0.6$.

In fig. 16, we plot the discrepancy between our data $\lim_{N\to\infty}\mathrm{Re}\,\langle W\rangle$, $\lim_{N\to\infty}\mathrm{Im}\,\langle W\rangle$ and eq. (4.9). This should be the contribution from the worldsheet instanton, which can be estimated analytically as

$$\langle W\rangle_{\mathrm{inst},g=0} = e^{\pi\sqrt{2\hat\lambda}} \sum_{l=2}^{9} w_l(\lambda) e^{-l\pi\sqrt{2\hat\lambda}} + \mathrm{O}(e^{-9\pi\sqrt{2\hat\lambda}}), \tag{4.28}$$

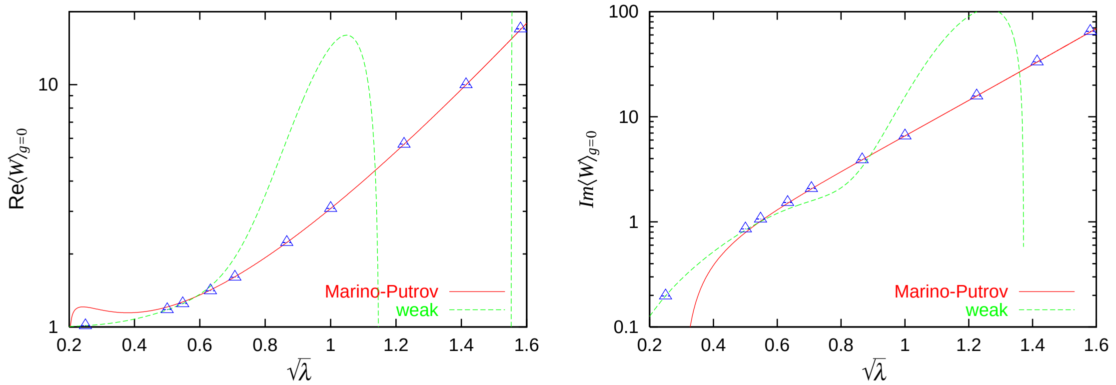

Figure 15: The real part in the planar limit Re $\langle W \rangle_{g=0}$ (left) and Im $\langle W \rangle_{g=0}$ (right) extracted from fig. 14.

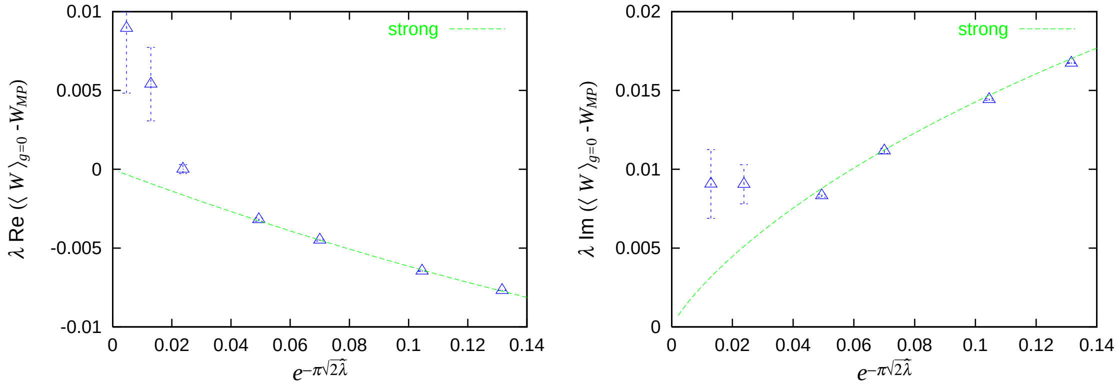

Figure 16: The difference between the numerical data and eq. (4.9) which we call $W_{\rm MP}$ here. The dashed lines are the analytical results of the worldsheet instanton contributions (4.28).

where $w_l(\lambda)$'s are explicitly given in eq. (F.6). We find that our data match the analytical expression within the statistical error. Therefore, we conclude that our numerical data nicely reproduce the previous analytical results including the worldsheet instanton effect in the planar limit.

4.3.2 Finite N

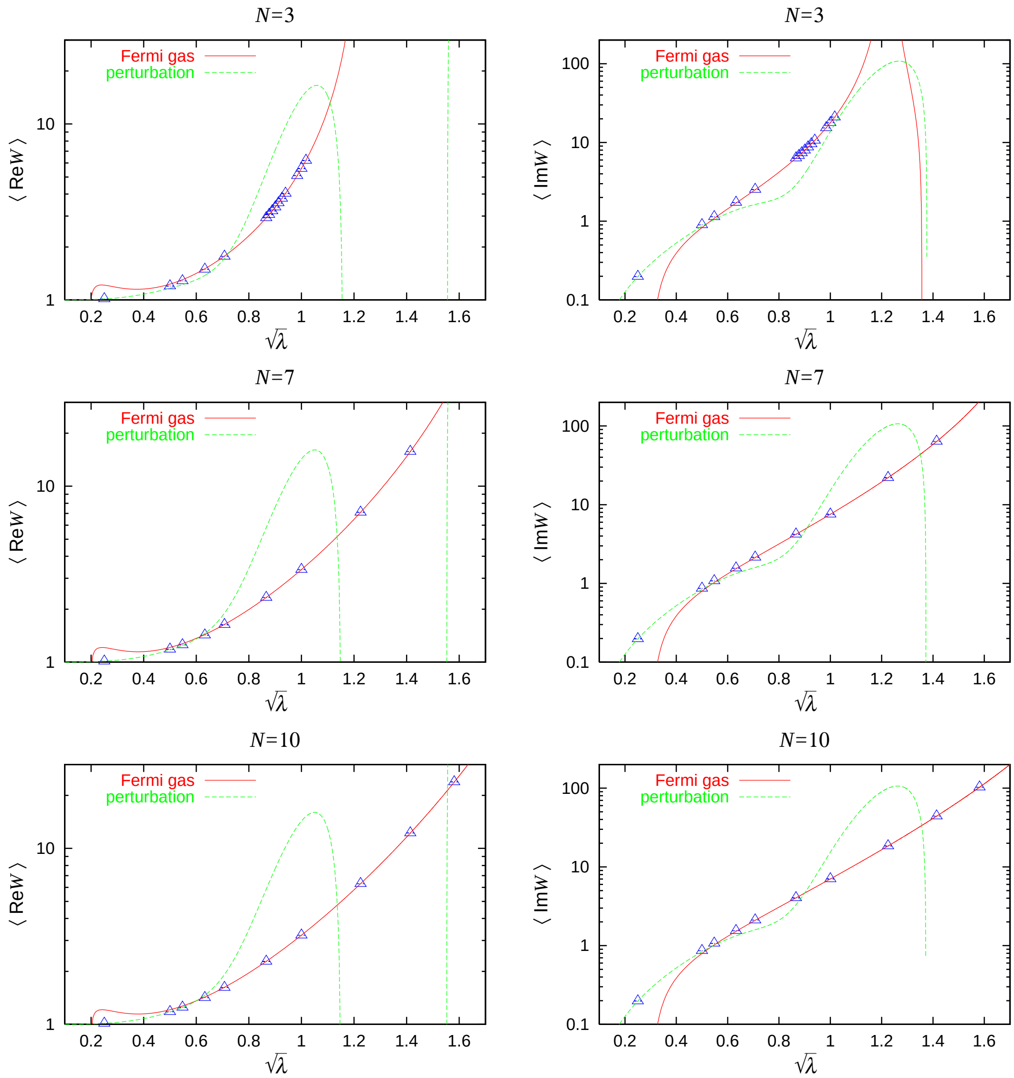

Figure 17: The numerical data for each N. The solid lines are Fermi gas result (4.11) for strong coupling region, while the dashed lines are perturbative result (4.8) for weak coupling region. The data agree with the strong coupling expression at $\sqrt{\lambda} \gtrsim 0.6$.

Finally we compare our full numerical data with the analytical results at finite N. In fig. 17, we plot $\mathrm{Re}\,\langle W \rangle$ and $\mathrm{Im}\,\langle W \rangle$ against $\sqrt{\lambda}$ for various values of N. The solid lines are the Fermi gas result (4.11), while the dashed lines are the perturbative result (4.8) to λ^4.

Our results successfully interpolate the perturbative result at weak coupling and the Fermi gas result at strong coupling.

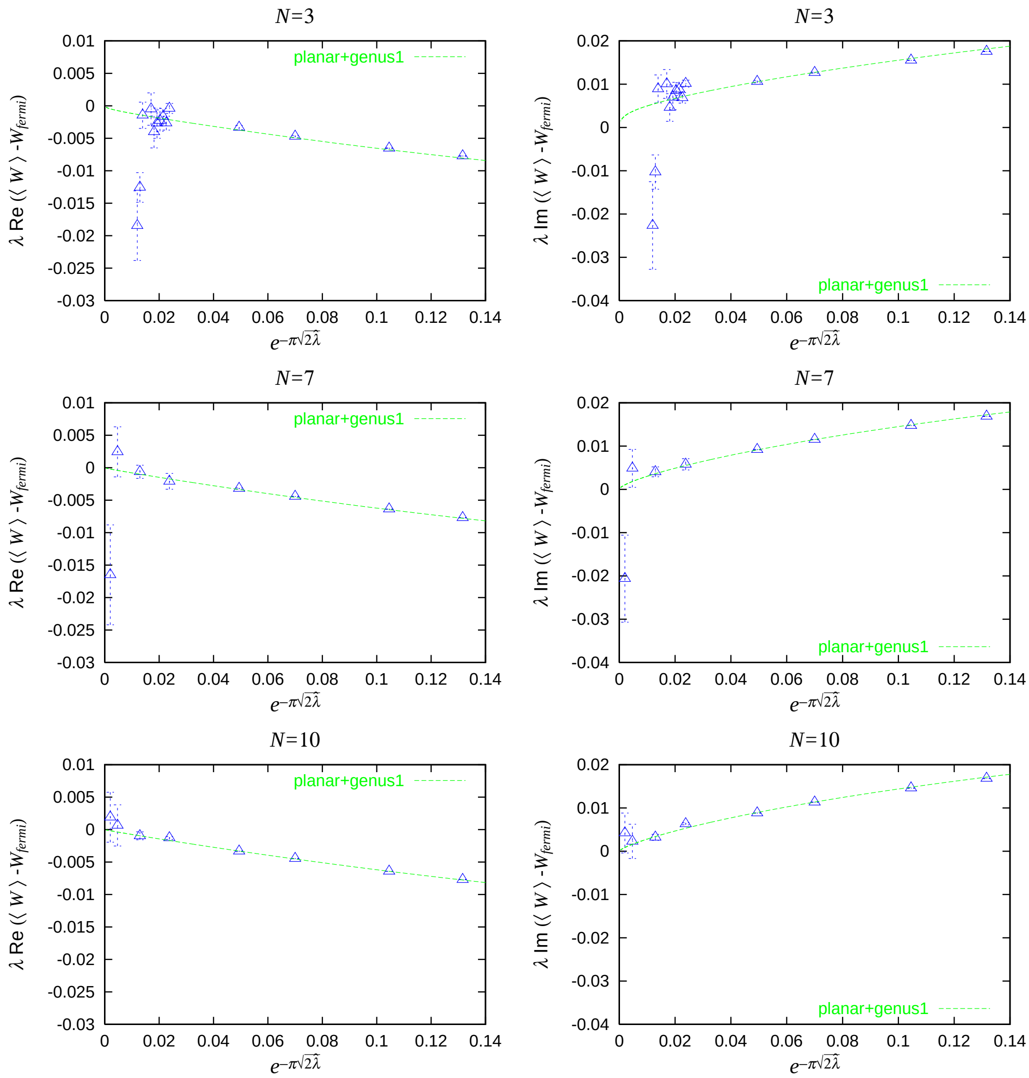

Figure 18: The difference between the full numerical data and Fermi gas result (4.11). The dashed lines are the fitting of data in the expression .

In fig. 18, we plot the discrepancy between our data $\mathrm{Re}\,\langle W\rangle$, $\mathrm{Im}\,\langle W\rangle$ and the Fermi gas result. This should correspond to the contribution from worldsheet instanton and membrane instanton. At sufficiently large N and/or small λ, the membrane instanton effect is exponentially suppressed as $\sim e^{-\pi\sqrt{2kN}} = e^{-\pi N\sqrt{2/\lambda}}$, so we should be able to see only the worldsheet instanton effect $\sim e^{-\pi\sqrt{2\hat{\lambda}}}$. In all the graphs, we can see such behavior at small λ. At small N and large λ, however, the both effects should be visible, so the behavior of the discrepancy becomes a little complicated. The graphs for $N = 3$ at large λ seem to be in this case.

5 Summary and discussions

We have established a simple numerical method for studying the ABJM theory on a three sphere for arbitrary rank N at arbitrary Chern-Simons level k. The crucial point is that we are able to rewrite the ABJM matrix model, which is obtained after applying the localization technique, in such a way that the integrand becomes positive definite. By using this method, we have confirmed from first principles that the free energy in the M-theory limit grows proportionally to $N^{3/2}$ as predicted from the eleven-dimensional supergravity. We have also found that the FHM formula with the additional terms describes the free energy of the ABJM theory in the type IIA superstring and M-theory regimes. Analytic form of the additional terms is discussed in detail, and beautiful agreement between planar and M-theory regions is found. These additional terms become important when we consider the quantum string effect in the AdS/CFT duality.

There are many issues worth being addressed by using our method. Most importantly from the conceptual point of view, we can use the free energy obtained for finite N and finite k to test the AdS/CFT duality at the quantum string level. At the tree level, or equivalently in the planar limit, there is strong evidence that the gauge theory correctly describes the string α' effect. For example, the D0-brane quantum mechanics reproduces the α' correction to the black 0-brane solution in type IIA superstring theory [122]. However, no definite conclusion is obtained for quantum string corrections so far. In fact, as pointed out in ref. [38], the FHM formula does not seem to agree with a prediction from the string theory side [113]. This disagreement is not solved even if we take into account of the corrections found in this paper. Some of the possible solutions to this puzzle includes: (i) one has to consider some different gauge theory such as $SU(N)_k \times SU(N)_{-k}$ theory, which gives different $1/N$ corrections, (ii) one has to refine the argument on the string theory side, and (iii) the AdS/CFT does not hold at the quantum string level. In particular, the scenario (i) can be tested straightforwardly by extending our method.

We consider it equally important to study *quantum* M-theory. While there is very little knowledge on it so far, we may hope to get some insight through intensive numerical studies of the ABJM theory. In fact similar attempts have been made recently [123, 124] using the BFSS matrix theory [2]. Numerical studies suggest that the prediction from the dual string theory for the scaling dimension of a certain class of operators continues to hold in the M-theory region. Similar or possibly more striking features of M-theory may show up by studying the ABJM theory numerically.

While we have focused on the free energy as the most fundamental quantity in the ABJM theory, our method can be used to calculate the expectation values of BPS operators. For instance, it is possible to calculate the expectation value of the circular Wilson loop for various representations. They are conjectured to be related to the string worldsheet area and the D-brane world-volume in the type IIA superstring region, respectively. It would be interesting to test this conjecture and to see the stringy corrections.

Our method can be also applied to other theories, which have recently attracted much attention in connection to the F-theorem and the entanglement entropy. For example, one can study the necklace-type quiver discussed in ref. [125]. We can also study other gauge groups such as $O(N)$ and $USp(N)$ studied in ref. [126, 127]. Detailed studies of these theories outside the planar limit, in particular, would be very interesting. For instance, the so-called orbifold equivalence, which is usually proven to hold only in the planar limit, can hold outside the planar limit in these models [128, 129]. Note also that the ABJM matrix model is related to the lens space matrix model, which appears in the context of the topological string theory. It is therefore conceivable that there might be some applications to the topological string theory as well.

We hope that the results of this work are convincing enough to show the power of the numerical approach, and that many more applications other than those listed above would reveal themselves as we proceed further.

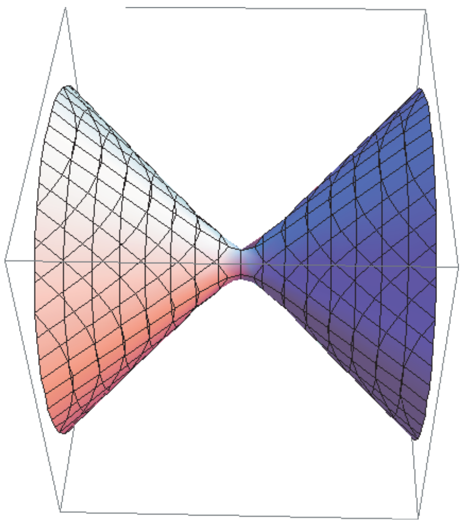

Figure 19: AdS_{d+1} is represented as the hyperboloid in $\mathbb{R}^{2,d-1}$.

A Anti-de Sitter space

In this appendix, we summarize properties of Anti-de Sitter spacetime (AdS). One of the most important fact in the context of AdS/CFT correspondence is that the boundary of AdS_{d+1} is the same as the conformal compactification of the d-dimensional Minkowski spacetime. For references about this appendix, see [130], [70] and section 12.3 of [131].

A.1 The definition of AdS

First, we give the definition of AdS. AdS_{d+1} has a constant negative curvature, and this is represented as certain hypersurface (fig.19):

$$-X_{-1}^2 - X_0^2 + \sum_{i=1}^{d} X_i^2 = -R^2 \tag{A.1}$$

in the $(d+2)-$dimensional flat space $\mathbf{R}^{d,2}$ with the metric

$$ds^2 = -dX_{-1}^2 - dX_0^2 + \sum_{i=1}^{d} dX_i^2, \tag{A.2}$$

where R is AdS radius. In the following, we fix R to unity for simplicity. By this construction, AdS_{d+1} has manifestly the isometry $SO(d,2)$ and its topology is

$$AdS_{d+1} \approx S^1 \times \mathbb{R}^d. \tag{A.3}$$

Note that AdS has a closed timelike curve (CTC) since the topology of the timelike direction is S^1.

A.2 Useful coordinates in AdS

Here we introduce various convenient coordinates of AdS_{d+1}.

Open chart : $(t, z^1, \cdots, z^d)$

The open chart is given by

$$X_{-1} = \sin t \quad , \quad X_j = \cos t z^j, \quad (j = 0, \cdots, d) \tag{A.4}$$

where

$$-(z^0)^2 + (z^1)^2 + (z^2)^2 + \cdots (z^d)^2 = -1. \tag{A.5}$$

Since

$$\begin{aligned} dX_{-1} &= \cos t dt, &\text{(A.6)} \\ -dX_0^2 + dX_1^2 + dX_2^2 + \cdots + dX_D^2 &= -\sin^2 t dt^2 + \cos^2 t(-(dz^0)^2 + (dz^i)^2), &\text{(A.7)} \end{aligned}$$

we find

$$ds^2 = -dt^2 + \cos^2 t(-(dz^0)^2 + (dz^i)^2). \tag{A.8}$$

In addition, by transforming as

$$\begin{array}{rcl} z^0 &=& \cosh\chi \\ (z^1, z^2, \cdots, z^d) &=& \sinh\chi \cdot d\mathbf{\Omega}_{d-1} \end{array}, \tag{A.9}$$

and using

$$-(dz^0)^2 + (dz^i)^2 = d\chi^2 + \sinh^2\chi d\Omega_{d-1}^2 , \tag{A.10}$$

one can find

$$ds^2 = -dt^2 + \cos^2 t(d\chi^2 + \sinh^2\chi d\Omega_{d-1}^2). \tag{A.11}$$

This corresponds to the open Robertson-Walker spacetime. Since this coordinate has singularity at $t = \pm\frac{1}{2}\pi$, the coordinate does not cover all of the AdS_{d+1}.

Static chart:$(\theta, r, \Omega_{d-1})$

The static chart is given by

$$\begin{array}{rcl} X_{-1} &=& \cosh r \sin\theta \\ X_0 &=& \cosh r \cos\theta. \\ (X_1, X_2, \cdots, X_d) &=& \sinh r \mathbf{\Omega}_{d-1} \end{array} \tag{A.12}$$

Since

$$-dX_{-1}^2 - dX_0^2 = -\sinh^2 r - \cosh^2 r d\theta^2 , \tag{A.13}$$

$$dX_i^2 = \cosh^2 r dr^2 + \sinh^2 r d\Omega_{d-1}^2 , \tag{A.14}$$

the line element is given by

$$ds^2 = -\cosh^2 r d\theta^2 + dr^2 + \sinh^2 r d\Omega_{d-1}^2. \tag{A.15}$$

This chart is static and spherically symmetric. Since this coordinate cover with all of the AdS_{d+1}, the static chart is the complete chart of AdS_{d+1}.

Poincare coordinate:(z, x^0, x^i)

The Poincare coordinate is given by

$$(z, x^0, x^i) = ((X_{-1} + X_d)^{-1}, X_0 z, X_i (X_{-1} + X_d)^{-1}). \tag{A.16}$$

This expression says that the Poincare coordinate has a discontinuous change between $X_{-1} + X_d > 0$ and $X_{-1} + X_d < 0$. Therefore we can not describe the AdS_{d+1} over $X_{-1} + X_d = 0$, namely, the Poincare coordinate is not the complete chart. Since

$$dz = -(X_{-1} + X_d)^{-2}(dX_{-1} + dX_d) \iff dX_{-1} + dX_d = -\frac{1}{z^2}dz, \tag{A.17}$$

$$dx^0 = zdX_0 + X_0 dz = zdX_0 + \frac{x^0}{z}dz \iff dX_0 = \frac{1}{z}(dx^0 - x^0 dz), \tag{A.18}$$

$$dx^i = zdX_i + \frac{x^i}{z}dz \iff dX_i = \frac{1}{z}dx^i - \frac{x^i}{z^2}dz, \tag{A.19}$$

we obtain

$$\begin{aligned} X_i^2 + X_d^2 - X_{-1}^2 - X_0^2 = -1 &\iff X_i^2 - (X_{-1} + X_d)(X_{-1} - X_d) - X_0^2 = -1 \\ &\iff (X_{-1} - X_d) = z\left[X_i^2 - X_0^2 + 1\right] = \frac{1}{z}(x_i^2 - x_0^2) + z. \end{aligned} \tag{A.20}$$

Moreover, since

$$d(X_{-1} - X_d) = -\frac{1}{z^2}(x_i^2 - x_0^2)dz + \frac{2}{z}(x^i dx^i - x^0 dx^0) + dz \ , \tag{A.21}$$

one can find

$$\begin{aligned} -dX_{-1}^2 + dX_d^2 &= -(dX_{-1} - dX_d)(dX_{-1} + dX_d) \\ &= \frac{1}{z^2}dz\left\{-\frac{1}{z^2}(x_i^2 - x_0^2)dz + \frac{2}{z}(x^i dx^i - x^0 dx^0) + dz\right\} \quad , \end{aligned} \tag{A.22}$$

$$dt_2^2 = \frac{1}{z^2}(dx^0 - x^0 dz)^2 \quad , \tag{A.23}$$

$$dy_i dy_i = \frac{1}{z^2}(dx^i - \frac{x^i}{z}dz)^2. \tag{A.24}$$

Thus we obtain the metric

$$\begin{aligned} ds^2 &= -dX_{-1}^2 - X_0^2 + dX_i dX_i + dX_d^2 \\ &= \frac{1}{z^2}(-(dx^0)^2 + dx^i dx^i + dz^2). \end{aligned} \tag{A.25}$$

The Poincare coordinate is quite useful for AdS/CFT correspondence since we can see d-dimensional Poincare symmetry manifestly.

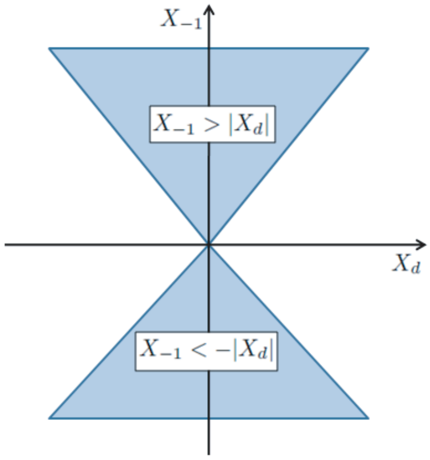

Figure 20: The region covered by AdS in the $X_{-1} - X_D$ plane.

A.3 Euclidenized AdS geometry

For later convenience, we consider the Euclideanized AdS : $EAdS$. Wick-rotating X_0, $EAdS_{d+1}$ is expressed as the hyper surface:

$$X_1^2 + \cdots + X_d^2 - X_{-1}^2 + X_0^2 = -1 \tag{A.26}$$

in the $d+2$-dimensional flat spacetime:

$$ds^2 = -dX_{-1}^2 + dX_0^2 + dX_1^2 + \cdots + dX_d^2. \tag{A.27}$$

It is trivial from the definition that $EAdS_{d+1}$ has the $SO(d+1,1)$ symmetry. Representing the Poincare coordinate, this becomes

$$ds^2 = \frac{1}{z^2}(dz^2 + (dx^2)_d) \tag{A.28}$$

where $(dx^2)_d$ is the line element of the d-dimensional Euclid space

$$(dx^2)_d \equiv dx_1^2 + \cdots + dx_d^2. \tag{A.29}$$

One of main difference between $EAdS$ and AdS is whether the Poincare coordinate is the complete chart or not. We show this in the following: We rewrite eq.(A.26) as follows

$$(X_{-1} + X_d)(X_{-1} - X_d) = X_1^2 + \cdots + X_d^2 + X_0^2 + 1. \tag{A.30}$$

Note that since the right hand side is always positive, the left hand side is also always positive:

$$\begin{array}{ccccc} X_{-1} + X_d > 0 & \Longrightarrow & X_{-1} - X_d > 0 & \Longleftrightarrow & X_{-1} > \ |X_d| \\ X_{-1} + X_d < 0 & \Longrightarrow & X_{-1} - X_d < 0 & \Longleftrightarrow & X_{-1} < -|X_d| \end{array}, \tag{A.31}$$

and since the right hand side is always nonzero, it holds

$$t_1 + y_d, t_1 - y_d \neq 0. \tag{A.32}$$

Although AdS covered the region $X_{-1} \leq |X_d| \cap X_{-1} \geq -|X_d|$ which is problematic in the Poincare coordinate, $EAdS$ does not cover the region. Therefore, the Poincare coordinate is the complete chart of $EAdS$.

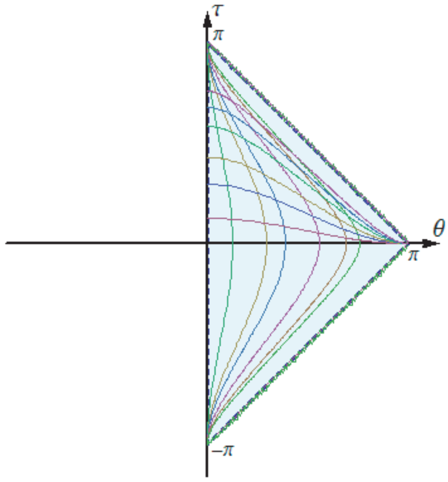

Figure 21: The Penrose diagram of Minkowski space.

A.4 The infinity structure of AdS_{d+1}

Let us investigate the infinity structure of AdS_{d+1}.

Minkowski spacetime

In order to compare the infinity structure of AdS with the conformal compactification of Minkowski space, we first consider the infinity structure of d-dimensional Minkowski spacetime. Let us start with the metric:

$$ds^2 = -dt^2 + dr^2 + r^2 d\Omega_{d-2}^2. \tag{A.33}$$

Putting $u_\pm = t \pm r$ and using $r = \frac{1}{2}(u_+ - u_-)$ and $dt^2 + dr^2 = -du_+ du_-$, we derive

$$ds^2 - du_+ du_- + \frac{1}{4}(u_+ - u_-)^2 d\Omega_{d-2}^2 \tag{A.34}$$

where $u_+ \geq u_-$ because of $r \geq 0$. Additionally transforming coordinates as $u_\pm = \tan \tilde{u}_\pm$ and using $du_\pm = d\tilde{u}_\pm / \cos^2 \tilde{u}_\pm$ and $(u_+ - u_-)^2 = \sin^2(\tilde{u}_+ - \tilde{u}_-)/\cos^2\tilde{u}_+ \cos^2 \tilde{u}_-$, the line element is

$$ds^2 = \frac{1}{\cos^2 \tilde{u}_+ \cos^2 \tilde{u}_-}\left(-d\tilde{u}_+ d\tilde{u}_- + \frac{1}{4}\sin^2(\tilde{u}_+ - \tilde{u}_-) d\Omega_{d-2}^2\right) \tag{A.35}$$

where $-\frac{\pi}{2} \leq \tilde{u}_\pm \leq \frac{\pi}{2}$ and $\tilde{u}_+ \geq \tilde{u}_-$. If we introduce the coordinates $\tau = \tilde{u}_+ + \tilde{u}_-$ and $\theta = \tilde{u}_+ - \tilde{u}_-$, we finally obtain the metric conformal to the Einstein's static universe:

$$ds^2 = \frac{1}{\cos^2 \tilde{u}_+ \cos^2 \tilde{u}_-}\left(-d\tau^2 + d\theta^2 + \sin^2\theta d\Omega_{d-2}^2\right) \tag{A.36}$$

where $-\pi \leq \tau \leq \pi$ and $0 \leq \theta \leq \pi$. This is the conformal embedding of the Einstein's static universe whose domain is $-\pi \leq \tau \leq \pi$ and $0 \leq \theta \leq \pi$ and therefore we can draw the Penrose diagram as fig.21. And the generator H of the τ translation is

$$H = \frac{1}{i}\frac{\partial}{\partial \tau}$$

$$
\begin{aligned}
&= \frac{1}{2i}(1+u_+^2)\frac{\partial}{\partial u_+} + \frac{1}{2i}(1+u_-^2)\frac{\partial}{\partial u_-} \\
&= \frac{1}{2i}\frac{\partial}{\partial t} + \frac{1}{2i}\left(-u_+u_-\frac{\partial}{\partial t} - 2*\left(-\frac{1}{2}\right)*(u_+ + u_-)\left(u_+\frac{\partial}{\partial u_+} + u_-\frac{\partial}{\partial u_-}\right)\right) \\
&= \frac{1}{2}(P_0 + K_0) = J_{0(-1)}.
\end{aligned} \tag{A.37}
$$

This corresponds to the $SO(2)$ part of the maximally symmetric subgroup $SO(2)\times SO(d)$ of $SO(2,d)$.

AdS

Transforming the coordinate as $v = \sinh r$ in the static chart (A.15), we obtain

$$ds^2 = -(1+v^2)d\theta^2 + \frac{dv^2}{1+v^2} + v^2 d\Omega_{d-1}^2. \tag{A.38}$$

In addition, the coordinate transformation $v = \tan\rho(-\pi/2 < \rho < \pi/2)$ leads to the line element which is given by

$$ds^2 = \frac{1}{\cos^2\rho}(-d\theta^2 + d\rho^2 + \sin^2\rho d\Omega_{d-1}^2). \tag{A.39}$$

Since (second term) + (third term) is conformal to the d-dimensional ball B_d, the topology is

$$\approx S^1 \times B_d \tag{A.40}$$

Therefore the topology of the boundary (spatial infinity) is

$$\approx S^1 \times S^{d-1}. \tag{A.41}$$

It is important that if we consider the universal covering space $CAdS_{d+1}$ of AdS_{d+1}, this is the same as the conformal-compactification of the d-dimensional Minkowski spacetime.

B Conformal group

We show that the Lie algebra of d-dimensional conformal group is isomorphic to the one of $SO(d,2)$ [33].

B.1 Conformal transformation

First, we define conformal transformation as coordinate transformation which change metric up to arbitrary scalar function:

$$g_{\mu\nu}(x\prime) \to \Omega^2(x) g_{\mu\nu}(x). \tag{B.1}$$

[33]Here, we consider only for $d \geq 3$ case.

Considering the infinitesimal transformation:

$$x^{\mu} \rightarrow x'^{\mu} = x^{\mu} + \epsilon^{\mu}(x) \ , \tag{B.2}$$

and since the transformation law of the metric tensor is

$$g_{\mu\nu}\prime(x\prime) = \frac{\partial x_{\mu}}{\partial x\prime_{\alpha}} \frac{\partial x_{\nu}}{\partial x\prime_{\beta}} g_{\alpha\beta}(x) \ , \tag{B.3}$$

we obtain

$$g\prime_{\mu\nu}(x\prime) = g_{\mu\nu}(x) - (\partial_{\mu}\epsilon_{\nu} + \partial_{\nu}\epsilon_{\mu}). \tag{B.4}$$

Because this is the conformal transformation, we can rewrite this in terms of a scalar function $f(x)$ as

$$\partial_{\mu}\epsilon_{\nu} + \partial_{\nu}\epsilon_{\mu} = f(x)g_{\mu\nu}. \tag{B.5}$$

Multiplying $g^{\mu\nu}$ and contracting lead to

$$f(x) = \frac{2}{d} g^{\mu\nu}\partial_{\mu}\epsilon_{\nu}. \tag{B.6}$$

In the following, let suppose for the flat spacetime $g_{\mu\nu} = \eta_{\mu\nu} = diag(-, +, \cdots, +)$. Then eq.(B.5) becomes

$$\partial_{\mu}\epsilon_{\nu} + \partial_{\nu}\epsilon_{\mu} = f(x)\eta_{\mu\nu}. \tag{B.7}$$

Differentiating both sides,

$$\partial_{\rho}\partial_{\mu}\epsilon_{\nu} + \partial_{\rho}\partial_{\nu}\epsilon_{\mu} = (\partial_{\rho}f)\eta_{\mu\nu}. \tag{B.8}$$

Replacing indices by $\rho \rightarrow \nu, \mu \rightarrow \rho, \nu \rightarrow \mu$,

$$\partial_{\nu}\partial_{\rho}\epsilon_{\mu} + \partial_{\nu}\partial_{\mu}\epsilon_{\rho} = (\partial_{\nu}f)\eta_{\rho\mu}. \tag{B.9}$$

Again, replacing the indices by $\rho \rightarrow \nu, \mu \rightarrow \rho, \nu \rightarrow \mu$,

$$\partial_{\mu}\partial_{\nu}\epsilon_{\rho} + \partial_{\mu}\partial_{\rho}\epsilon_{\nu} = (\partial_{\mu}f)\eta_{\nu\rho}. \tag{B.10}$$

Subtracting eq.(B.9) from eq.(B.8),

$$\partial_{\rho}\partial_{\mu}\epsilon_{\nu} - \partial_{\nu}\partial_{\mu}\epsilon_{\rho} = (\partial_{\rho}f)\eta_{\mu\nu} - (\partial_{\nu}f)\eta_{\rho\mu}. \tag{B.11}$$

bv Therefore, substituting this into eq.(B.10),

$$2\partial_{\mu}\partial_{\nu}\epsilon_{\rho} = (\partial_{\mu}f)\eta_{\nu\rho} - (\partial_{\rho}f)\eta_{\mu\nu} + (\partial_{\nu}f)\eta_{\rho\mu}. \tag{B.12}$$

Multiplying both sides by $\eta^{\mu\nu}$ and contracting,

$$\begin{aligned} 2\partial^2\epsilon_{\rho} &= \partial_{\rho} - d(\partial_{\rho}f) + \partial_{\rho}f \\ &= (2-d)\partial_{\rho}f. \end{aligned} \tag{B.13}$$

Differentiating both sides again,

$$\partial_{\sigma}\partial^2\epsilon_{\rho} = (2-d)\partial_{\sigma}\partial_{\rho}f$$

$$
\begin{aligned}
&\iff \partial^2(\partial_\sigma \epsilon_\rho + \partial_\rho \epsilon_\sigma) = (2-d)\partial_\sigma \partial_\rho f \\
&\iff \eta_{\rho\sigma}\partial^2 f = (2-d)\partial_\sigma \partial_\rho f
\end{aligned} \tag{B.14}
$$

Multiplying both sides by $\eta^{\rho\sigma}$ and contracting,

$$
d\partial^2 f = (2-d)\partial^2 f \quad \iff \quad (d-1)\partial^2 f = 0. \tag{B.15}
$$

Using this equation and eq. (B.14),

$$
\partial_\mu \partial_\nu f = 0. \tag{B.16}
$$

Since f is scalar, this leads to the limited form of f:

$$
f(x) = A + B_\mu x^\mu \tag{B.17}
$$

Substituting this into eq.(B.12),

$$
2\partial_{\mu\nu}\epsilon_\rho = B_\mu \eta_{\nu\rho} - B_\rho \eta_{\mu\nu} + B_\nu \eta_{\rho\mu} \tag{B.18}
$$

Therefore, $\partial_\mu \partial_\nu \epsilon_\rho$ is the constant tensor. This allowed form is

$$
\epsilon_\mu = a_\mu + b_{\mu\nu} x^\nu + c_{\mu\nu\rho} x^\nu x^\rho \ , \tag{B.19}
$$

where

$$
c_{\mu\nu\rho} = c_{\mu\rho\nu}. \tag{B.20}
$$

Substituting this into

$$
\partial_\mu \epsilon_\nu + \partial_\nu \epsilon_\mu = f \eta_{\mu\nu} \ , \tag{B.21}
$$

the equation :

$$
\begin{aligned}
f(x) &= \frac{2}{d}\eta^{\alpha\beta}\partial_\alpha \epsilon_\beta \\
&= \frac{2}{d}(b^\alpha{}_\alpha + 2\eta^{\alpha\beta} c_{\alpha\beta\gamma} x^\gamma) \\
&= \frac{2}{d} b^\alpha{}_\alpha - 2 b_\alpha x^\alpha \quad (b_\alpha \equiv -\frac{2}{d}\eta^{\beta\gamma} c_{\beta\gamma\alpha})
\end{aligned}
$$

leads to

$$
(b_{\nu\mu} + 2c_{\nu\mu\alpha}x^\alpha) + (b_{\mu\nu} + 2c_{\mu\nu\alpha}x^\alpha) = \left(\frac{2}{d} b^\alpha{}_\alpha - 2 b_\gamma x^\gamma\right)\eta_{\mu\nu}. \tag{B.22}
$$

Extracting $\mathcal{O}(x)$ terms from this equation,

$$
b_{\nu\mu} + b_{\mu\nu} = \frac{2}{d} b^\alpha{}_\alpha \eta_{\mu\nu} \ . \tag{B.23}
$$

Decomposing $b_{\mu\nu}$ into the symmetric part $s_{\mu\nu}$ and anti-symmetric part $\omega_{\mu\nu}$,

$$
b_{\mu\nu} = s_{\mu\nu} + \omega_{\mu\nu} \quad (s_{\mu\nu} = s_{\nu\mu}, \omega_{\mu\nu} = -\omega_{\nu\mu}). \tag{B.24}
$$

According to eq.(B.23),

$$s_{\mu\nu} = \frac{1}{d}(\mathrm{tr}b)\eta_{\mu\nu} \equiv \lambda\eta_{\mu\nu}, \tag{B.25}$$

we obtain

$$b_{\mu\nu} = \lambda\eta_{\mu\nu} + \omega_{\mu\nu}. \tag{B.26}$$

The infinitesimal transformation corresponding to this is

$$\delta x_\mu \sim b_{\mu\nu}x^\nu = \lambda x_\mu + \omega_{\mu\nu}x^\nu \tag{B.27}$$

where the first term represent the scale transformation and the second term represent the Lorentz transformation.

In addition, substituting eq.(B.19) into

$$2\partial_\mu\partial_\nu\epsilon_\rho = \eta_{\nu\rho}\partial_\mu f - \partial_{\mu\nu}\partial_\rho f + \eta_{\mu\rho}\partial_\nu f \ , \tag{B.28}$$

we get

$$c_{\rho\mu\nu} = -\eta_{\nu\rho}b_\mu + \eta_{\mu\nu}b_\rho - \eta_{\mu\nu}b_\rho - \eta_{\rho\mu}b_\nu. \tag{B.29}$$

Thus, the corresponding infinitesimal transformation corresponding is

$$\delta x_\rho \sim c_{\rho\mu\nu}x^{\mu\nu} = -2(b\cdot x)x_\rho + b_\rho x^2. \tag{B.30}$$

This represent the special conformal transformation. And since $\mathcal{O}(x^0)$ of ϵ_μ a_μ is not constrained, this represent the translation.

Let us summarize. The conformal transformation constitute from the following:

- Translation

$$x'^\mu = x^\mu + a^\mu \tag{B.31}$$

- Lorentz transformation

$$x'^\mu = \omega^\mu{}_\nu x^\nu \tag{B.32}$$

- Dilatation

$$x'^\mu = \lambda x^\mu \tag{B.33}$$

- Special conformal transformation

$$x'^\mu = \frac{x^\mu + b^\mu x^2}{1 + 2b^\nu x_\nu + b^2x^2} \tag{B.34}$$

B.2 Algebra

Denoting the generators of the conformal group as differential operators,

- Translation

$$P_\mu = -i\partial_\mu \tag{B.35}$$

- Lorentz transformation

$$M_{\mu\nu} = i(x_\mu\partial_\nu - x_\nu\partial_\mu) \tag{B.36}$$

- Dilatation

$$D = -ix^\mu \partial_\mu \tag{B.37}$$

- Special conformal transformation

$$K_\mu = -i(x^2\partial_\mu - 2x_\mu x^\nu \partial_\nu) \tag{B.38}$$

These satisfy the following commutation relations:

$$\begin{aligned}
[M_{\mu\nu}\ ,\ P_\rho] &= -i(\eta_{\mu\rho}P_\nu - \eta_{\nu\rho}P_\mu) && \text{(B.39)}\\
[M_{\mu\nu}\ ,\ K_\rho] &= -i(\eta_{\mu\rho}K_\nu - \eta_{\nu\rho}K_\mu) && \text{(B.40)}\\
[M_{\mu\nu}\ ,\ M_{\rho\sigma}] &= -i\eta_{\mu\rho}M_{\nu\sigma} \pm \text{(permutations)} && \text{(B.41)}\\
[M_{\mu\nu}\ ,\ D] &= 0 && \text{(B.42)}\\
[D\ ,\ K_\mu] &= iK_\mu && \text{(B.43)}\\
[D\ ,\ P_\mu] &= -iP_\mu && \text{(B.44)}\\
[P_\mu\ ,\ K_\nu] &= 2iM_{\mu\nu} - 2i\eta_{\mu\nu}D && \text{(B.45)}\\
\text{others} = 0 &
\end{aligned}$$

Putting[34]

$$J_{\mu\nu} \equiv M_{\mu\nu}\ ,\ J_{\mu d} \equiv \frac{1}{2}(K_\mu - P_\mu)\ ,\ J_{\mu(-1)} \equiv \frac{1}{2}(K_\mu + P_\mu)\ ,\ J_{(-1)d} \equiv D\ , \tag{B.46}$$

we obtain

$$\begin{aligned}
[J_{\mu\nu}\ ,\ J_{\rho d}] &= \frac{1}{2}[M_{\mu\nu}\ ,\ (K_\rho - P_\rho)]\\
&= \frac{1}{2}\{-i(\eta_{\mu\rho}K_\nu - \eta_{\nu\rho}K_\mu) - (-i)(\eta_{\mu\rho}P_\nu - \eta_{\nu\rho}P_\mu)\}\\
&= -i\eta_{\mu\rho}J_{\nu d} + i\eta_{\nu\rho}J_{\mu d} && \text{(B.47)}\\
\left[J_{\mu\nu}\ ,\ J_{\rho(-1)}\right] &= -i\eta_{\mu\rho}J_{\nu(-1)} + i\eta_{\nu\rho}J_{\mu(-1)} && \text{(B.48)}\\
\left[J_{\mu\nu}\ ,\ J_{(-1)d}\right] &= 0 && \text{(B.49)}\\
[J_{\mu d}\ ,\ J_{\nu d}] &= \frac{1}{4}[(K_\mu - P_\mu)\ ,\ (K_\nu - P_\nu)]\\
&= \frac{1}{2}\{+(iM_{\nu\mu} - i\eta_{\nu\mu}D) - (iM_{\mu\nu} - i\eta_{\mu\nu}D)\}\\
&= iJ_{\mu\nu} && \text{(B.50)}\\
\left[J_{\mu d}\ ,\ J_{(-1)d}\right] &= \frac{1}{2}[(K_\mu - P_\mu)\ ,\ D] = \frac{i}{2}(K_\mu + P_\mu)\\
&= iJ_{\mu(-1)} && \text{(B.51)}\\
\left[J_{\mu d}\ ,\ J_{\nu(-1)}\right] &= +i\eta_{\mu\nu}D\\
&= +i\eta_{\mu\nu}J_{(-1)d} && \text{(B.52)}\\
\left[J_{\mu(-1)}\ ,\ J_{(-1)d}\right] &= iJ_{\mu d} && \text{(B.53)}
\end{aligned}$$

[34]Other combination is taken as J is anti-symmetric.

$$\left[J_{\mu(-1)}\ ,\ J_{\nu(-1)}\right] = -iJ_{\mu\nu} \tag{B.54}$$
$$\left[J_{(-1)d}\ ,\ J_{(-1)d}\right] = 0 \tag{B.55}$$

Supposing $M, N = -1, 0, 1, \cdots d$,$\eta_{MN} = \mathrm{diag}(-1, -1, 1, \cdots, 1)$, we find that these are the $SO(d, 2)$ commutation relation.

C Double sine function

In this section we introduce double sine function.

C.1 Double Gamma function

Because the double sine function can be defined as a ratio of double gamma function, here we introduce the double gamma function. We define the double gamma function as

$$\begin{aligned}\log\Gamma_2(x|w_1, w_2) &= \frac{\partial}{\partial t}\sum_{n_1,n_2=0}^{\infty}(x + n_1w_1 + n_2w_2)^{-t}\Bigg|_{t=0} \\ &= -\sum_{n_1,n_2=0}^{\infty}\log(x + n_1w_1 + n_2w_2),\end{aligned} \tag{C.1}$$

or equivalently,

$$\Gamma_2(x|w_1, w_2) = \prod_{n_1,n_2=0}^{\infty}\frac{1}{(x + n_1w_1 + n_2w_2)}. \tag{C.2}$$

This satisfies the following relations:

$$\frac{\Gamma_2(x + w_1|w_1, w_2)}{\Gamma(x|w_1, w_2)} = \sqrt{2\pi}\frac{w_2^{\frac{1}{2}-\frac{x}{w_2}}}{\Gamma(x/w_2)}, \quad \frac{\Gamma_2(x + w_2|w_1, w_2)}{\Gamma(x|w_1, w_2)} = \sqrt{2\pi}\frac{w_1^{\frac{1}{2}-\frac{x}{w_1}}}{\Gamma(x/w_1)}. \tag{C.3}$$

If we specify to the case for $w_1 = b, w_2 = b^{-1}$, we obtain

$$\frac{\Gamma_2(x + b^{\pm1}|b, b^{-1})}{\Gamma(x|b, b^{-1})} = \sqrt{2\pi}\frac{b^{\mp(\frac{1}{2}-xb^{\pm1})}}{\Gamma(b^{\pm1}x)}, \quad \frac{\Gamma_2(x|b, b^{-1})}{\Gamma(x - b^{\pm1}|b, b^{-1})} = \sqrt{2\pi}\frac{b^{\mp(\frac{1}{2}-xb^{\pm1}+b^{\pm2})}}{\Gamma(b^{\pm1}x - b^{\pm2})}. \tag{C.4}$$

From the definition (C.1), we find that there are simple poles at $x = -mw_1 - nw_2$ with non-negative integer m, n.

C.2 Double sine function

In terms of the double gamma function, we define the double sine function as

$$s_b(z) = \frac{\Gamma_2(\eta + iz|b, b^{-1})}{\Gamma_2(\eta - iz|b, b^{-1})} = \prod_{p,q=0}^{\infty}\frac{bq + b^{-1}p + \eta - iz}{bp + b^{-1}q + \eta + iz}, \tag{C.5}$$

where $\eta = (b + b^{-1})/2$.

This function has the following properties:

- Self-duality
$$s_b(z) = s_{b^{-1}}(z) \tag{C.6}$$
- Functional equation
$$\frac{s_b(z + \frac{ib^{\pm 1}}{2})}{s_b(z - \frac{ib^{\pm 1}}{2})} = \frac{1}{2\cosh(\pi b^{\pm 1} z)} \tag{C.7}$$
- Reflection property
$$s_b(x)s_b(-x) = 1 \tag{C.8}$$
- Zeros
$$z = -i(\eta + mb + nb^{-1}) \quad \text{with non} - \text{negative } m, n \tag{C.9}$$
- Poles
$$z = +i(\eta + mb + nb^{-1}) \quad \text{with non} - \text{negative } m, n \tag{C.10}$$
- Asymptotics
$$s_b(z) \sim \begin{cases} e^{+\frac{i\pi}{2}(z^2 + \frac{1}{12}(b^2+b^{-2})} & \text{for} \quad |\arg z| < \frac{\pi}{2} \\ e^{-\frac{i\pi}{2}(z^2 + \frac{1}{12}(b^2+b^{-2})} & \text{for} \quad |\arg z| > \frac{\pi}{2} \end{cases} \tag{C.11}$$
- Simplification for $b = 1$ [47]
$$s_1(z) = \prod_{p,q=0}^{\infty} \left(\frac{p+q+1-iz}{p+q+1+iz} \right) = \prod_{n=1}^{\infty} \left(\frac{n-iz}{n+iz} \right)^n \tag{C.12}$$
$$= \exp\left[iz \log(1 - e^{2\pi z}) + \frac{i}{2}\left(-\pi z^2 + \frac{1}{\pi}\mathrm{Li}_2(e^{2\pi z}) \right) - \frac{i\pi}{12} \right] \tag{C.13}$$

D Basics and details of the Monte Carlo simulation

In this section we explain the basics and details of the Monte Carlo simulation[35]. Let us consider the action
$$S(N, k; x) = -\log \left(\frac{\prod_{i<j} \tanh^2((x_i - x_j)/2k)}{\prod_i 2\cosh(x_i/2)} \right). \tag{D.1}$$
(Below we abbreviate $S(N, k; x)$ as $S(x)$.) Let $\mathcal{O}(x)$ be an "observable", which is a function of $\{x_i\}$. In general, it is difficult to calculate the expectation value of $\mathcal{O}$ defined by
$$\langle \mathcal{O} \rangle = \frac{\int d^N x\, \mathcal{O}(x) e^{-S(x)}}{\int d^N x\, e^{-S(x)}}. \tag{D.2}$$
A brute force integration is not practical unless the number of variables N is very small such as $N \lesssim 5$. Monte Carlo simulation is a practical tool, which enables this calculation even for large N.

[35] There are many good references on Monte Carlo methods.

In Monte Carlo simulation, a series of configurations $\{x_i\}$

$$\{x_i^{(0)}\} \;\rightarrow\; \{x_i^{(1)}\} \;\rightarrow\; \{x_i^{(2)}\} \;\rightarrow\; \cdots \tag{D.3}$$

is generated in such a way that the probability with which a configuration $\{x_i\}$ appears approaches $e^{-S(x)}/Z$ as the number of configurations increases. More precisely, we require that the probability $w_k(\{x_i\})$ with which a configuration $\{x_i\}$ appears at M-th step converge to $e^{-S(x)}/Z$ as

$$\lim_{M\to\infty} w_M(\{x_i\}) = \frac{e^{-S(x)}}{Z}\,. \tag{D.4}$$

Then the expectation value can be obtained by simply taking an average over the configurations $\{x_i^{(n)}\}$ as

$$\langle \mathcal{O}(x)\rangle = \lim_{M\to\infty}\frac{1}{M}\sum_{n=1}^{M}\mathcal{O}(x_i^{(n)})\,. \tag{D.5}$$

This can be achieved by generating the series with a transition probability $P(\{x_i^{(n)}\} \rightarrow \{x_i^{(n+1)}\})$, which (neglecting a few technical details) satisfies following conditions.

- *Markov chain.* — The transition probability from $\{x_i^{(n)}\}$ to $\{x_i^{(n+1)}\}$ does not depend on previous configurations $\{x_i^{(l)}\}$ $(l < n)$.
- *Ergodicity.* — For any pair of configurations $\{x\}$ and $\{x'\}$, there is nonzero transition probability within finite steps.
- *Aperiodicity.* — The probability from $\{x_i\}$ to $\{x_i\}$ is always nonzero.
- *Positive state.* — All configurations have finite mean recurrence time[36].
- *Detailed balance.* — The following equality should hold for arbitrary pairs of configurations $\{x\}$ and $\{x'\}$.

$$e^{-S(x)}P(x\rightarrow x') = e^{-S(x')}P(x'\rightarrow x)\,. \tag{D.6}$$

There are many ways to satisfy these conditions. In this work we use the Hybrid Monte Carlo (HMC) method [132]. We introduce fictitious momentum variables p_i $(i = 1, 2, \cdots, N)$, which are conjugate to x_i, and consider a Hamiltonian

$$H = \sum_i \frac{p_i^2}{2} + S(x)\,. \tag{D.7}$$

Starting with an initial configuration $\{x_i^{(0)}\}$, we generate a series of configurations $\{x_i^{(n)}\}$ $(n = 1, 2, \cdots)$ by repeating the following steps:

[36] If $P_{ii}^{(n)}$ is the probability to get from $\{x\}$ to $\{x\}$ in n-steps of the Markov chain, without reaching this configuration at any intermediate step, then the mean recurrence time of $\{x\}$ is defined by $\tau_i = \sum_{n=1}^{\infty} nP_{ii}^{(n)}$.

- Generate $p_i^{(n-1)}$ randomly, with a probability weight $e^{-\left(p_i^{(n-1)}\right)^2/2}$.
- Starting with a configuration $\{x_i, p_i\} = \{x_i^{(n-1)}, p_i^{(n-1)}\}$, get a new configuration $\{x_i', p_i'\}$ by the "molecular dynamics" explained below.
- "Accept" the new configuration $\{x_i', p_i'\}$ (*i.e.* take $\{x_i^{(n)}\} = \{x_i'\}$) with a probability $\min\{1, e^{H-H'}\}$, where H and H' are the value of the Hamiltonian calculated with $\{x_i, p_i\}$ and $\{x_i', p_i'\}$, respectively. When the new configuration is rejected, we keep an old configuration, so that $\{x_i^{(n)}\} = \{x_i\} = \{x_i^{(n-1)}\}$.

The "molecular dynamics" is defined as follows. First we introduce a fictitious time τ and consider the time evolution according to the Hamilton equations

$$\frac{dx_i}{d\tau} = \frac{dp_i}{d\tau} = \frac{\partial H}{\partial p_i} = p_i\,, \qquad \frac{dp_i}{d\tau} = -\frac{\partial H}{\partial x_i} = -\frac{\partial S}{\partial x_i}\,. \tag{D.8}$$

If we solve the Hamilton equations exactly, the Hamiltonian is conserved. In practice, we solve them approximately by discretizing the differential equations, so the Hamiltonian is not conserved exactly. We denote the time step as $\Delta\tau$ and the number of steps as N_τ. Then $x_i' \equiv x_i(N_\tau\Delta\tau)$ and $p_i' \equiv p_i(N_\tau\Delta\tau)$ are calculated by using the following "leap-frog method", starting with $x_i(0) \equiv x_i$ and $p_i(0) \equiv p_i$.

- $x_i\left(\frac{\Delta\tau}{2}\right) = x_i(0) + p_i(0)\cdot\frac{\Delta\tau}{2}$
- $p_i(\Delta\tau) = p_i(0) - \left.\frac{\partial S}{\partial x_i}\right|_{\tau=\frac{\Delta\tau}{2}}\cdot\Delta\tau$
- $x_i\left(\frac{3}{2}\Delta\tau\right) = x_i\left(\frac{\Delta\tau}{2}\right) + p_i(\Delta\tau)\cdot\Delta\tau$
- $p_i(2\Delta\tau) = p_i(\Delta\tau) - \left.\frac{\partial S}{\partial x_i}\right|_{\tau=\frac{3}{2}\Delta\tau}\cdot\Delta\tau$
- $\cdots$
- $x_i((N_\tau - 1/2)\Delta\tau) = x_i((N_\tau - 3/2)\Delta\tau) + p_i((N_\tau - 1)\Delta\tau)\cdot\Delta\tau$
- $p_i(N_\tau\Delta\tau) = p_i((N_\tau - 1)\Delta\tau) - \left.\frac{\partial S}{\partial x_i}\right|_{\tau=(N_\tau-1/2)\Delta\tau}\cdot\Delta\tau$
- $x_i(N_\tau\Delta\tau) = x_i((N_\tau - 1/2)\Delta\tau) + p_i((N_\tau)\Delta\tau)\cdot\frac{\Delta\tau}{2}$

Note that the leap-frog method is designed so that the reversibility is satisfied. Namely, by starting with the final configuration $\{x_i'\}$ and $\{p_i'\}$ and reversing the time, the initial configuration $\{x_i\}$ and $\{p_i\}$ is reproduced. As a result, the detailed balance condition is satisfied.[37]

[37]For simplicity, let us assume $H > H'$. (The argument for the case with $H < H'$ is the same.) Because of the reversibility, the transition probabilities are

$$\begin{aligned} P(\{x_i\}\to\{x_i'\}) &= e^{-p^2/2}/\sqrt{\pi}\times\min\{1, e^{H-H'}\} && \text{(D.9)}\\ &= e^{-p^2/2}/\sqrt{\pi} && \text{(D.10)}\end{aligned}$$

In the simulation, N_τ and $\Delta\tau$ should be chosen so that a good approximation is achieved with fewer configurations. For that purpose, (i) the change at each transition should be sufficiently large, and (ii) the acceptance rate should be large. The first condition is achieved by taking $N_\tau\Delta\tau$ sufficiently large. However, if we fix $\Delta\tau$ and take larger N_τ, the Hamiltonian is not conserved at all, and the new configurations are hardly accepted. Therefore one has to take $\Delta\tau$ smaller so that the conservation of the Hamiltonian becomes better. In actual simulations (at $N = 20$ and $k = 5$, for example), we took $\Delta\tau \sim 0.1$ and $N_\tau \sim 200$, so that the acceptance rate is around 0.8. As an initial configuration, we choose $x_i^{(0)}$ to be a random number in $[-0.5, 0.5]$.

In Monte Carlo simulation, configurations with larger path-integral weight ("important samples") appear more often. For this reason it is called also the *importance sampling*. Since the region of configuration space, which gives dominant contribution to the path integral is typically quite limited, a good approximation can be achieved with a rather small number of important samples. This should be contrasted to the usual brute force integration, in which most of the CPU time is wasted for calculating the integrand for unimportant configurations.

In Monte Carlo simulation, as we have described above, configurations are generated with the *probability* e^{-S}/Z. Therefore, the Monte Carlo method works only if the path-integral weight e^{-S} is real and positive. If the measure e^{-S} is not real and positive, the model is said to suffer from the *sign problem* or the *phase problem*; here "sign" and "phase" mean the negative sign and the complex phase of the integration weight. In the original form of the ABJM matrix model (2.78), the partition function is given by an integration of a complex function. Therefore it suffers from the sign problem, and the Monte Carlo method is not applicable.

E The relation between the constant map and the Fermi gas result

In this appendix we show the correspondence between the constant map contribution and the Fermi gas result $A(k) - \frac{1}{2}\log 2$, which is derived by the large-k and small-k expansions, respectively.

As we mentioned earlier, the constant map contribution F_{const} is given by

$$F_{\text{const}} = \sum_{g=0}^{\infty} g_s^{2g-2} F_{\text{const}}^{(g)} \,, \tag{E.1}$$

---

and

$$\begin{aligned} P(\{x_i'\} \to \{x_i\}) &= e^{-p'^2/2}/\sqrt{\pi} \times \min\{1, e^{H'-H}\} & \text{(D.11)} \\ &= e^{-p^2/2+(S(x')-S(x))}/\sqrt{\pi}\,. & \text{(D.12)} \end{aligned}$$

Therefore,

$$\begin{aligned} e^{-S(x)} P(\{x_i\} \to \{x_i'\}) &= e^{-S(x)} \times e^{-p^2/2}/\sqrt{\pi} & \text{(D.13)} \\ &= e^{-S(x')} P(\{x_i'\} \to \{x_i\})\,. & \text{(D.14)} \end{aligned}$$

where the coefficients $F^{(g)}_{\rm const}$ are

$$F^{(0)}_{\rm const} = \frac{\zeta(3)}{2}, \quad F^{(1)}_{\rm const} = 2\zeta'(-1) + \frac{1}{6}\log\frac{\pi}{2k}\ , \quad F^{(g\geq 2)}_{\rm const} = 4^g \frac{B_{2g}B_{2g-2}}{(4g)(2g-2)(2g-2)!}\ . \tag{E.2}$$

We consider the following summation:

$$f(g_s) = \sum_{g=2}^{\infty} 4^g \frac{B_{2g}B_{2g-2}}{(4g)(2g-2)(2g-2)!} g_s^{2g-2} = 4g_s^2 \sum_{n=0}^{\infty} \frac{B_{2n+4}B_{2n+2}}{(n+2)(2n+2)(2n+2)!}(4g_s^2)^n \tag{E.3}$$

Since

$$\lim_{n\to\infty} \frac{\left|\frac{B_{2n+4}B_{2n+2}}{(n+2)(2n+2)(2n+2)!}\right|}{\left|\frac{B_{2n+6}B_{2n+4}}{(n+3)(2n+4)(2n+4)!}\right|} = \lim_{n\to\infty} \frac{(n+3)(2n+3)(2n+4)^2|B_{2n+2}|}{(n+2)(2n+2)|B_{2n+6}|} = 0, \tag{E.4}$$

the convergence radius is zero and therefore this series is divergent. We try to perform Borel summation. The Borel transformation of the series is

$$\mathcal{B}f(t) = 4g_s^2 \sum_{n=0}^{\infty} \frac{1}{n!} \frac{B_{2n+4}B_{2n+2}}{(n+2)(2n+2)(2n+2)!} t^n \tag{E.5}$$

This series is still divergent. We make Borel trans one more times:

$$\mathcal{B}^2 f(u) = 4g_s^2 \sum_{n=0}^{\infty} \frac{1}{(n!)^2} \frac{B_{2n+4}B_{2n+2}}{(n+2)(2n+2)(2n+2)!} u^n \tag{E.6}$$

This has a finite radius of convergence. But we do not know how to sum. This series is still divergent. We make Borel trans one more times:

$$\mathcal{B}^3 f(v) = 4g_s^2 \sum_{n=0}^{\infty} \frac{1}{(n!)^3} \frac{B_{2n+4}B_{2n+2}}{(n+2)(2n+2)(2n+2)!} v^n \tag{E.7}$$

This has infinite radius of convergence. In order to evaluate the summation more easily, we use the integral representation of the Bernoulli number,

$$B_{2g} = (-1)^{g-1} 4g \int_0^{\infty} \frac{x^{2g-1}}{e^{2\pi x}-1} dx \quad (g = 1, 2, \cdots)\ . \tag{E.8}$$

By using this representation, we obtain

$$\begin{aligned} \mathcal{B}^3 f(v) &= -32g_s^2 \sum_{n=0}^{\infty} \int_0^{\infty} \frac{x^{2n+3}}{e^{2\pi x}-1} dx \int_0^{\infty} \frac{y^{2n+1}}{e^{2\pi y}-1} dy\ \frac{1}{(n!)^3} \frac{1}{(2n+2)!} v^n \\ &= -32g_s^2 \int_0^{\infty} \frac{x^3}{e^{2\pi x}-1} dx \int_0^{\infty} \frac{y}{e^{2\pi y}-1} dy\ \sum_{n=0}^{\infty} \frac{1}{(n!)^3} \frac{1}{(2n+2)!} (x^2y^2v)^n \end{aligned} \tag{E.9}$$

The Borel summation ($z = 2g_s$) is

$$\begin{aligned}
&\int_0^\infty dvdudt\ e^{-v+u+t}\mathcal{B}^3 f(vutz) \\
=\ & -8z^2\int_0^\infty dvdudt\ e^{-v+u+t}\int_0^\infty dx\ \frac{x^3}{e^{2\pi x}-1}\int_0^\infty dy\ \frac{y}{e^{2\pi y}-1} \\
& \sum_{n=0}^\infty \frac{1}{(n!)^3}\frac{1}{(2n+2)!}(x^2y^2vutz)^n \\
=\ & -8z^2\int_0^\infty dx\ \frac{x^3}{e^{2\pi x}-1}\int_0^\infty dy\ \frac{y}{e^{2\pi y}-1}\sum_{n=0}^\infty \frac{1}{(2n+2)!}(x^2y^2z^2)^n \\
=\ & -8\int_0^\infty dx\ \frac{x}{e^{2\pi x}-1}\int_0^\infty dy\ \frac{y^{-1}}{e^{2\pi y}-1}(\cosh(xyz)-1) \\
=\ & -\frac{1}{3}\int_0^\infty dy\ \frac{y^{-1}}{e^{2\pi y}-1}\left(-1-\frac{12}{y^2z^2}+\frac{3}{\sin^2\frac{yz}{2}}\right) \\
=\ & -\frac{1}{3}\int_0^\infty dy\ \frac{y^{-1}}{e^{2\pi y}-1}\left(-1+\frac{3}{(2\pi y/k)^2}-\frac{3}{\sinh^2\frac{2\pi y}{k}}\right)
\end{aligned} \tag{E.10}$$

By changing the variable as $t = \frac{2\pi y}{k}$, we obtain a simpler form,

$$\int_0^\infty dvdudt\ e^{-v+u+t}\mathcal{B}^3 f(vutz) = -\frac{1}{3}\int_0^\infty dt\ \frac{t^{-3}}{e^{kt}-1}\left(3-t^2-\frac{3t^2}{\sinh^2 t}\right). \tag{E.11}$$

Although each term of the integrand is divergent at $t\sim 0$, this is canceled with each other, and therefore the integral gives a finite value. In order to make our analysis easier, we will apply the zeta-function regularization to the integral.

For later convenience, we decompose the integral as

$$\sum_{g=2}^\infty g_s^{2g-2}F^{(g)}_{\text{const}} = \int_0^\infty dt\ \frac{1}{e^{kt}-1}\left(-\frac{1}{t^3}+\frac{1}{3t}\right)+\frac{1}{k}\int_0^\infty dt\ \frac{kt}{e^{kt}-1}\frac{1}{t^2\sinh^2 t}. \tag{E.12}$$

Note that the first factor in the second term is the generating function of the Bernoulli number

$$\frac{x}{e^x-1} = \sum_{n=0}^\infty B_n\frac{x^n}{n!}. \tag{E.13}$$

Although this series also converges only for $|x|<2\pi$, we analytically continue it to the whole region and assume that this does not affect the result. Then by using the formula

$$\frac{1}{e^x-1} = \sum_{m=1}^\infty e^{-mx}, \quad \frac{1}{\sinh^2 x} = -\sum_{m=1}^\infty me^{-mx}, \tag{E.14}$$

the integral rewritten as

$$\sum_{g=2}^\infty g_s^{2g-2}F^{(g)}_{\text{const}} = \sum_{m=1}^\infty\int_0^\infty dt\ e^{-mkt}\left(-\frac{1}{t^3}+\frac{1}{3t}\right)+\frac{4}{k}\sum_{n=0}^\infty\frac{B_nk^n}{n!}\sum_{m=1}^\infty m\int_0^\infty dt\ t^{-2+n}e^{-2mt}.$$

$$(E.15)$$

The first integral is easily performed by using

$$\int_0^\infty dt\ e^{-st}t^{-1} = -\gamma - \log s, \quad \int_0^\infty dt\ e^{-st}t^{-3} = -\frac{1}{4}s^2(-3+2\gamma+2\log s)\ ,$$

where γ is the Euler-Mascheroni constant. We obtain

$$\begin{aligned}
&\sum_{m=1}^\infty \int_0^\infty dt\ e^{-mkt}\left(-\frac{1}{t^3}+\frac{1}{3t}\right) \\
&= \frac{k^2}{4}\sum_{m=1}^\infty n^2(-3+2\gamma+2\log(km)) + \frac{1}{3}\sum_{m=1}^\infty(-\gamma-\log(mk)) \\
&= \frac{k^2}{4}\left[(-3+2\gamma+2\log k)\zeta(-2)-2\zeta'(-2)\right] + \frac{1}{3}\left[(-\gamma-\log k)\zeta(0)+\zeta'(0)\right] \\
&= -\frac{k^2}{2}\zeta'(-2) + \frac{1}{6}\left[(\gamma+\log k)-\log(2\pi)\right]. \qquad (E.16)
\end{aligned}$$

Next we evaluate the second integral

$$\sum_{m=1}^\infty m\int_0^\infty dt\ t^{-2+n}e^{-2mt}\ .$$

- For $n=0$
  By using the formula

$$\int_0^\infty dt\ e^{-st}t^{-2} = s(-1+\gamma+\log s)\ , \qquad (E.17)$$

  we obtain

$$\sum_{m=1}^\infty m\int_0^\infty dt\ t^{-2}e^{-2mt} = -2\zeta'(-2)\ . \qquad (E.18)$$

- For $n=1$

$$\sum_{m=1}^\infty m\int_0^\infty dt\ t^{-1}e^{-2mt} = \frac{1}{12}(\gamma+\log 2)+\zeta'(-1)\ . \qquad (E.19)$$

- For $n\geq 2$
  By using the formula

$$\int_0^\infty dt\ e^{-st}t^{\lambda-1} = \Gamma(\lambda)\frac{1}{s^\lambda} \quad (Re(\lambda)>0)\ , \qquad (E.20)$$

  the integral becomes

$$\sum_{m=1}^\infty m\int_0^\infty dt\ t^{-2+n}e^{-2mt} = \frac{\Gamma(n-1)}{2^{n-1}}\zeta(n-2)\ . \qquad (E.21)$$

Thus the constant map contribution is rewritten as

$$
\begin{aligned}
F_{\rm const} &= -\frac{\zeta(3)}{8\pi^2}k^2 - \frac{1}{6}\log k + \frac{1}{6}\log\frac{\pi}{2} + 2\zeta'(-1) - \frac{k^2}{2}\zeta'(-2) + \frac{1}{6}\left(\gamma + \log k - \log(2\pi)\right) \\
&\quad + \frac{4}{k}\Bigg[-2B_0\zeta'(-2) + B_1 k\left(\frac{1}{12}(\gamma+\log 2) + \zeta'(-1)\right) \\
&\qquad + \sum_{n=1}^{\infty}\frac{B_{2n}}{(2n)!}k^{2n}\frac{\Gamma(2n-1)}{2^{2n-1}}\zeta(2n-2)\Bigg] \\
&= -\left(\frac{\zeta(3)}{8\pi^2} + \frac{\zeta'(-2)}{2}\right)k^2 + 2(1+2B_1)\zeta'(-1) + \frac{1}{6}(1+2B_1)\gamma + \frac{1}{3}(-1+B_1)\log 2 \\
&\quad -\frac{8}{k}B_0\zeta'(-2) + \sum_{n=1}^{\infty}\frac{B_{2n}}{(2n)(2n-1)2^{2n-3}}\zeta(2n-2)k^{2n-1} \ . \qquad \text{(E.22)}
\end{aligned}
$$

Since $B_0 = 1$, $B_1 = -\frac{1}{2}$, $\zeta'(-2) = -\frac{\zeta(3)}{4\pi^2}$ and $\zeta(2n) = (-1)^{n-1}\frac{2^{2n-1}\pi^{2n}}{(2n)!}B_{2n}$, we obtain

$$
\begin{aligned}
F_{\rm const} &= -\frac{1}{2}\log 2 + \frac{2\zeta(3)}{\pi^2 k} + \sum_{n=1}^{\infty}(-1)^n\frac{B_{2n}B_{2n-2}}{(2n)!}\pi^{2n-2}k^{2n-1} \qquad \text{(E.23)}\\
&= -\frac{1}{2}\log 2 + \frac{2\zeta(3)}{\pi^2 k} - \frac{k}{12} - \frac{\pi^2 k^3}{4320} + \frac{\pi^4 k^5}{907200} + \cdots \ , \qquad \text{(E.24)}
\end{aligned}
$$

which is the same as $A(k) - \frac{1}{2}\log 2$ derived by the Fermi gas approach [40] up to the order of $\mathrm{O}(k^5)$. Therefore, we expect that this is the all-order form in the Fermi gas picture if we calculate higher order of k.

Thus we conclude that the constant map contribution and the term $A(k) - \frac{1}{2}\log 2$ in the Fermi gas result are the asymptotic series expansions of the integral representation (E.11) around $k = \infty$ and $k = 0$, respectively, with the radius of convergence being finite. In other words, the two expansions are smoothly connected with each other by analytic continuation.

F Details of analytic studies

F.1 Planar limit

According to ref. [33], the expectation value of the 1/6-BPS Wilson loop at genus 0 is obtained by solving the differential equation (4.5). By using the asymptotic behavior at strong coupling, we obtain

$$
\begin{aligned}
\frac{d}{d\kappa}\left[\lambda(\kappa)\left\langle W_{1/6}\right\rangle_{g=0}\right] &= \frac{\pi - 2i\log\left(\frac{1}{\kappa}\right)}{8\pi^2} + \frac{i\left(\log\left(\frac{1}{\kappa}\right)+1\right)}{\pi^2\kappa^2} - \frac{i\left(18\log\left(\frac{1}{\kappa}\right)+29\right)}{2\pi^2\kappa^4} + \frac{8}{\pi^2\kappa^5} \\
&\quad + \frac{2i\left(150\log\left(\frac{1}{\kappa}\right)+299\right)}{3\pi^2\kappa^6} - \frac{168}{\pi^2\kappa^7} - \frac{i\left(14700\log\left(\frac{1}{\kappa}\right)+33967\right)}{12\pi^2\kappa^8} \\
&\quad + \frac{5\left(18\log\left(\frac{1}{\kappa}\right) - 3i\pi + 3569\right)}{6\pi^2\kappa^9} \ ,
\end{aligned}
$$

$$\tag{F.1}$$

up to $O(\kappa^{-10})$. Integrating this over κ, the Wilson loop is given by

$$\begin{aligned}
&\lambda(\kappa)\left\langle W_{1/6}\right\rangle_{g=0} \\
&= c_0 + \frac{1}{24\pi^2}\Bigg[3(-2i+\pi)\kappa + \frac{92i}{\kappa^3} - \frac{48}{\kappa^4} - \frac{4304i}{5\kappa^5} + \frac{672}{\kappa^6} + \frac{63734i}{7\kappa^7} + \frac{5i(14267i+12\pi)}{8\kappa^8} \\
&\quad - \frac{3i\left(2\kappa^9+8\kappa^7-24\kappa^5+160\kappa^3-1400\kappa-15i\right)\log\left(\frac{1}{\kappa}\right)}{\kappa^8}\Bigg],
\end{aligned} \tag{F.2}$$

up to $O(\kappa^{-9})$. Here the integration constant c_0 is generically required to satisfy the boundary condition $\lambda(\kappa)\left\langle W_{1/6}\right\rangle_{g=0}\Big|_{\kappa=0} = 0$. Here we assume $c_0 = 0$ as it is suggested by numerical integration of eq. (F.1).

The asymptotic behavior of κ for $\lambda \gg 1$ can be written as [34]

$$\kappa = e^{\pi\sqrt{2\hat{\lambda}}}\left(1 + \sum_{l=1}^{4} c_l\left(\frac{1}{\pi\sqrt{2\hat{\lambda}}}\right)\cdot e^{-2l\pi\sqrt{2\hat{\lambda}}} + O(e^{-10\pi\sqrt{2\hat{\lambda}}})\right), \tag{F.3}$$

where

$$\begin{aligned}
c_1(x) &= -2 + x, \\
c_2(x) &= 3 - \frac{x}{4} - \frac{3x^2}{2} - \frac{x^3}{2}, \\
c_3(x) &= \frac{1}{36}\left(18x^5 + 90x^4 + 195x^3 + 225x^2 - 158x - 360\right), \\
c_4(x) &= -\frac{1}{288}(x+2)\left(180x^6 + 900x^5 + 2412x^4 + 4080x^3 + 3773x^2 - 2219x - 7056\right).
\end{aligned} \tag{F.4}$$

Thus we obtain

$$\left\langle W_{1/6}\right\rangle_{g=0} = e^{\pi\sqrt{2\hat{\lambda}}}\sum_{l=0}^{9} w_l^{(0)}(\lambda)e^{-l\pi\sqrt{2\hat{\lambda}}} \tag{F.5}$$

up to $O(e^{-9\pi\sqrt{2\hat{\lambda}}})$. Here $w_l^{(0)}(\lambda)$'s are given by

$$\begin{aligned}
w_0^{(0)}(\lambda) &= \frac{1}{2\pi i\lambda}\left(-\frac{1}{2}\sqrt{2\hat{\lambda}} + \frac{1}{2\pi} + \frac{i}{4}\right), \\
w_1^{(0)}(\lambda) &= 0, \\
w_2^{(0)}(\lambda) &= \frac{1}{8\pi i\lambda}\left[-2\sqrt{2}(c_1+4)\sqrt{\hat{\lambda}} + ic_1\right], \\
w_3^{(0)}(\lambda) &= 0, \\
w_4^{(0)}(\lambda) &= -\frac{1}{8\pi i\lambda}\left[2\sqrt{2}\pi\sqrt{\hat{\lambda}}(c_2 - 4(c_1+3)) + c_1(c_1+8) - i\pi c_2 + 20\right],
\end{aligned}$$

$$
\begin{aligned}
w_5^{(0)}(\lambda) &= 0,\\
w_6^{(0)}(\lambda) &= \frac{1}{24\pi^2 i\lambda}\Big[-6\sqrt{2}\pi\sqrt{\hat\lambda}(4c_1(c_1+9)-4c_2+c_3+80)\\
&\quad +(c_1+4)(c_1(c_1+32)-6c_2+124)+3i\pi c_3\Big],\\
w_7^{(0)}(\lambda) &= 0,\\
w_8^{(0)}(\lambda) &= -\frac{1}{48\pi^2 i\lambda}\Big[-12\sqrt{2}\pi\sqrt{\hat\lambda}\left\{4\left(c_1\left(c_1^2+18c_1-2c_2+100\right)-9c_2+c_3+175\right)-c_4\right\}\\
&\qquad + c_1^4+88c_1^3-6c_1^2(c_2-204)+4c_1(-36c_2+3c_3+1480)\\
&\qquad + 6(c_2-84)c_2+48c_3-6i\pi c_4+9460\Big],\\
w_9^{(0)}(\lambda) &= 0,
\end{aligned}
\tag{F.6}
$$

where we define $c_{1,2,3,4} := c_{1,2,3,4}\left(\frac{1}{\pi\sqrt{2\hat\lambda}}\right)$.

F.2 Genus 1 contribution

In ref. [34], the expectation value of the 1/6-BPS Wilson loop at genus 1 is analytically calculated. By using the asymptotic behavior (F.3) of κ, the analytical result is expanded as

$$
\left\langle W_{1/6}\right\rangle_{g=1} = e^{\pi\sqrt{2\hat\lambda}}\sum_{l=0}^{8} w_l^{(1)}(\lambda)e^{-l\pi\sqrt{2\hat\lambda}} \tag{F.7}
$$

up to $\mathrm{O}(e^{-8\pi\sqrt{2\hat\lambda}})$. Here $w_l^{(1)}$'s are given by

$$
\begin{aligned}
w_0^{(1)} &= -\tfrac{1}{192\pi^3\lambda\hat\lambda}\Big[3+4\pi\sqrt{\hat\lambda}\Big(2i\sqrt{2}\pi\hat\lambda+(\pi-2i)\sqrt{h\lambda}-\sqrt{2}\Big)\Big],\\
w_1^{(1)} &= 0,\\
w_2^{(1)} &= \tfrac{1}{192\sqrt{2}\pi^4 i\lambda\hat\lambda^{3/2}}\Big[4\pi^3\hat\lambda^{3/2}\Big(4c_1\sqrt{\hat\lambda}-i\sqrt{2}c_1+16\sqrt{\hat\lambda}\Big)+8i\pi^2c_1\hat\lambda\\
&\quad -i\sqrt{2}\pi(7c_1+16)\sqrt{\hat\lambda}+6i(c_1+4)\Big],\\
w_3^{(1)} &= 0,\\
w_4^{(1)} &= \tfrac{1}{384\pi^5 i\lambda\hat\lambda^2}\Bigg[8\pi^4\Big(2\sqrt{2}\hat\lambda^{5/2}(c_2-4(c_1+3))-ic_2\hat\lambda^2\Big)\\
&\quad +8\pi^3\Big((c_1(c_1+8)+20)\hat\lambda^2+i\sqrt{2}(c_2+16)\hat\lambda^{3/2}\Big)-2i\pi^2\hat\lambda(2(c_1-8)c_1+7(c_2-8))\\
&\quad +i\sqrt{2}\pi\sqrt{\hat\lambda}(c_1(7c_1+8)+6c_2-92)-9i(c_1+4)^2\Bigg],\\
w_5^{(1)} &= 0,\\
w_6^{(1)} &= -\tfrac{1}{1152\pi^6 i\lambda\hat\lambda^{5/2}}\Big[-ic_1^3\Big(-8i\pi^4\hat\lambda^{5/2}-4\pi^3\hat\lambda^{3/2}+3\sqrt{2}\pi^2\hat\lambda+12\pi\sqrt{\hat\lambda}-18\sqrt{2}\Big)
\end{aligned}
$$

$$
\begin{aligned}
&+12c_1^2\left(-24\pi^4\hat{\lambda}^{5/2}-8i\pi^3\hat{\lambda}^{3/2}+16\sqrt{2}\pi^5\hat{\lambda}^3-6i\sqrt{2}\pi^2\hat{\lambda}+15i\pi\sqrt{\hat{\lambda}}+18i\sqrt{2}\right)\\
&+6c_1\Big(-4i\pi^3(c_2+58)\hat{\lambda}^{3/2}+8\pi^4\left((c_2-42)\hat{\lambda}^{5/2}-24i\sqrt{2}\hat{\lambda}^2\right)\\
&+i\sqrt{2}\pi^2(7c_2+82)\hat{\lambda}-3i\pi(3c_2-118)\sqrt{\hat{\lambda}}+288\sqrt{2}\pi^5\hat{\lambda}^3+144i\sqrt{2}\Big)\\
&+2\Big\{i\pi^3\hat{\lambda}^{3/2}(48c_2-21c_3-1408)+4\pi^4\hat{\lambda}^2\left(8\left((3c_2-62)\sqrt{\hat{\lambda}}-96i\sqrt{2}\right)+3i\sqrt{2}c_3\right)\\
&+12\pi^5\left(-8\sqrt{2}(c_2-20)\hat{\lambda}^3+c_3\left(2\sqrt{2}\hat{\lambda}^3-i\lambda^{5/2}\right)\right)+3i\sqrt{2}\pi^2\hat{\lambda}(4c_2+3c_3+512)\\
&-12i\pi(9c_2-202)\sqrt{\hat{\lambda}}+576i\sqrt{2}\Big\}\Big],\\
w_7^{(1)} &= 0,\\
w_8^{(1)} &= \frac{1}{4608\pi^7 i\lambda\hat{\lambda}^3}\Big[-ic_1^4\left(2\sqrt{2}\pi^3\lambda^{3/2}-16i\pi^5\lambda^3-8\pi^4\lambda^2+33\pi^2\lambda-12\sqrt{2}\pi\sqrt{\lambda}-90\right)\\
&+16c_1^3\left(48\sqrt{2}\pi^6\lambda^{7/2}-26i\sqrt{2}\pi^3\lambda^{3/2}-88\pi^5\lambda^3-24i\pi^4\lambda^2+27i\pi^2\lambda+84i\sqrt{2}\pi\sqrt{\lambda}+90i\right)\\
&+12c_1^2\Big\{3i\sqrt{2}\pi^3(\mathrm{c}2+32)\lambda^{3/2}-4i\pi^4(c_2+280)\lambda^2+8\pi^5\left((c_2-204)\lambda^3-96i\sqrt{2}\lambda^{5/2}\right)\\
&+6i\pi^2(2c_2+277)\lambda-6i\sqrt{2}\pi(3c_2-214)\sqrt{\lambda}+1152\sqrt{2}\pi^6\lambda^{7/2}+720i\Big\}\\
&-8c_1\Big\{-i\sqrt{2}\pi^3\lambda^{3/2}(72c_2-21c_3+6272)-4i\pi^4\lambda^2(24c_2+3c_3-2528)\\
&+8\pi^5\left(\lambda^3(-36c_2+3c_3+1480)+1920i\sqrt{2}\lambda^{5/2}\right)+3i\pi^2\lambda(60c_2-9c_3-5576)\\
&+192\sqrt{2}\pi^6(c_2-50)\lambda^{7/2}+24i\sqrt{2}\pi(9c_2-322)\sqrt{\lambda}-2880i\Big\}\\
&-4\Big\{8\pi^5\lambda^{5/2}\left(3c_2^2\sqrt{\lambda}-252c_2\sqrt{\lambda}-144i\sqrt{2}c_2+24c_3\sqrt{\lambda}+3i\sqrt{2}c_4+4730\sqrt{\lambda}+11496i\sqrt{2}\right)\\
&+i\sqrt{2}\pi^3\lambda^{3/2}\left(21c_2^2+492c_2+24c_3+18c_4-39802\right)\\
&-6i\pi^4\lambda^2\left(2c_2^2+232c_2-16c_3+7c_4-4996\right)-9i\pi^2\lambda\left(3c_2^2-236c_2+24c_3+7020\right)\\
&+24\pi^6\lambda^3\left(8\left(\sqrt{2}\sqrt{\lambda}(9c_2-c_3-175)+24i\right)+c_4\left(2\sqrt{2}\sqrt{\lambda}-i\right)\right)\\
&+96i\sqrt{2}\pi(9c_2-218)\sqrt{\lambda}-5760i\Big\}\Big],
\end{aligned}
\tag{F.8}
$$

where $c_{1,2,3,4}=c_{1,2,3,4}\left(\frac{1}{\pi\sqrt{2\hat{\lambda}}}\right)$.

G Another argument for derivation of positive-definite form

In this section, we show another argument for the derivation of 1/6-BPS Wilson loop in the positive-definite form (4.20).

We consider the unnormalized Wilson loop $\overline{W}(N;k_1,k_2)$ given by

$$\overline{W}(N;k_1,k_2) = \frac{1}{N!^2}\int \frac{d^N\mu}{(2\pi)^N}\frac{d^N\nu}{(2\pi)^N}\, e^{\mu_1}\frac{\prod_{i<j}\left[2\sinh\left(\frac{\mu_i-\mu_j}{2}\right)\right]^2\left[2\sinh\left(\frac{\nu_i-\nu_j}{2}\right)\right]^2}{\prod_{i,j}\left[2\cosh\left(\frac{\mu_i-\nu_j}{2}\right)\right]^2} \times \exp\left[\frac{i}{4\pi}\sum_{i=1}^{N}(k_1\mu_i^2+k_2\nu_i^2)\right], \tag{G.1}$$

where we don't impose $k_1+k_2=0$. Let us now use the Cauchy identity

$$\frac{\prod_{i<j}(u_i-u_j)(v_i-v_j)}{\prod_{i,j}(u_i+v_j)} = \sum_\sigma(-1)^\sigma\prod_i\frac{1}{u_i+v_{\sigma(i)}}\,, \tag{G.2}$$

where σ runs through all permutations. By setting $u_i=e^{\mu_i}, v_i=e^{\nu_i}$, it becomes

$$\frac{\prod_{i<j}\left[2\sinh\left(\frac{\mu_i-\mu_j}{2}\right)\right]\left[2\sinh\left(\frac{\nu_i-\nu_j}{2}\right)\right]}{\prod_{i,j}\left[2\cosh\left(\frac{\mu_i-\nu_j}{2}\right)\right]} = \sum_\sigma(-1)^\sigma\prod_i\frac{1}{2\cosh\left(\frac{\mu_i-\nu_{\sigma(i)}}{2}\right)}\,. \tag{G.3}$$

Then we obtain

$$\begin{aligned}\overline{W}_n(N;k_1,k_2) = {} & \frac{1}{N!}\sum_\sigma(-1)^\sigma\frac{1}{\pi^{2N}}\int d^Nxd^Ny\,\frac{1}{\prod_i 2\cosh x_i\cdot 2\cosh y_i}\int\frac{d^N\mu}{(2\pi)^N}\frac{d^N\nu}{(2\pi)^N}\\ & \times\exp\Bigg[\frac{ik_1}{4\pi}\left(\mu_1+\frac{2}{k_1}(x_1+y_1-i\pi)\right)^2+\frac{ik_1}{4\pi}\sum_{i=2}^{N}\left(\mu_i+\frac{2}{k_1}(x_i+y_i)\right)^2\\ & +\frac{ik_2}{4\pi}\sum_{i=1}^{N}\left(\nu_i+\frac{2}{k_2}(x_i+y_{\sigma(i)})\right)^2\Bigg]\\ & \times\exp\Bigg[-\frac{i}{\pi}\left(\frac{1}{k_1}(x_1+y_1-i\pi)^2+\frac{1}{k_2}(x_1+y_{\sigma(1)})^2\right)\\ & -\frac{i}{\pi}\sum_{i=2}^{N}\left(\frac{1}{k_1}(x_i+y_i)^2+\frac{1}{k_2}(x_i+y_{\sigma(i)})^2\right)\Bigg].\end{aligned} \tag{G.4}$$

Here we can easily perform the integrations over $\mu_2,\cdots,\mu_N$ and ν_i by the usual formula of the Fresnel integration. However, the integration over μ_1 is divergent for real k_1 since the offset is the complex number. Although each term is divergent, cancellation with each other may occur except for $N=1$.

Then, we assume

$$\overline{W}(N;k,-k) = \lim_{\epsilon\to+0}\overline{W}(N,k+i\epsilon,-k), \tag{G.5}$$

which corresponds to assume that $\overline{W}(N;k_1,k_2)$ on real k_1 axis is smoothly connected with $\overline{W}(N;k_1,k_2)$ on upper half plane of complex k_1 plane. Under this assumption, we obtain

$$\overline{W}(N,k,-k)$$

$$
\begin{aligned}
&= \frac{e^{\frac{\pi}{k}i}}{N!}\sum_\sigma (-1)^\sigma \frac{1}{\pi^{2N}}\int d^N x d^N y \, \frac{1}{\prod_i 2\cosh x_i \cdot 2\cosh y_i}\int \frac{d^N\mu}{(2\pi)^N}\frac{d^N\nu}{(2\pi)^N} \\
&\quad \exp\left[\frac{ik}{4\pi}\sum_{i=1}^N \mu_i^2 - \frac{ik}{4\pi}\sum_{i=1}^N \nu_i^2 - \frac{2i}{k\pi}\sum_{i=1}^N x_i(y_i - y_{\sigma(i)}) - \frac{2}{k}(x_1+y_1)\right] \\
&= \frac{e^{\frac{\pi}{k}i}}{N!}\sum_\sigma (-1)^\sigma \int \frac{d^N x}{(2\pi k)^N}\frac{e^{-\frac{x_1}{k}}}{2\cosh\left(\frac{x_1 - x_{\sigma(1)} - 2\pi i}{2k}\right)\prod_{i=2}^N 2\cosh\left(\frac{x_i - x_{\sigma(i)}}{2k}\right)\cdot \prod_{i=1}^N 2\cosh\frac{x_i}{2}}.
\end{aligned}
$$

We use the Cauchy identity ($\mu_1 = \frac{x_i - 2\pi i}{k}, \mu_{i\geq 2} = \frac{x_i}{k}, \nu_i = \frac{x_i}{k}$) again

$$
\begin{aligned}
& \sum_\sigma (-1)^\sigma \frac{1}{2\cosh\left(\frac{\mu_1 - \nu_{\sigma(1)}}{2}\right)}\prod_{i=2}^N \frac{1}{2\cosh\left(\frac{\mu_i - \nu_{\sigma(i)}}{2}\right)} \\
&= \frac{\prod_{j=2}^N \left[2\sinh\left(\frac{\mu_1-\mu_j}{2}\right)\right]\prod_{i<j, i\geq 2}\left[2\sinh\left(\frac{\mu_i-\mu_j}{2}\right)\right]\prod_{i<j}\left[2\sinh\left(\frac{\nu_i-\nu_j}{2}\right)\right]}{\prod_{j=1}^N\left[2\cosh\left(\frac{\mu_1-\nu_j}{2}\right)\right]\prod_{i,j,i\geq 2}\left[2\cosh\left(\frac{\mu_i-\nu_j}{2}\right)\right]} \qquad \text{(G.6)} \\
\leftrightarrow & \sum_\sigma (-1)^\sigma \frac{1}{2\cosh\left(\frac{x_1 - x_{\sigma(1)} - 2\pi i}{2k}\right)}\prod_{i=2}^N \frac{1}{2\cosh\left(\frac{x_i - x_{\sigma(i)}}{2k}\right)} \\
&= \frac{\prod_{j=2}^N \left[2\sinh\left(\frac{x_1-x_j-2\pi i}{2k}\right)\right]\prod_{i<j, i\geq 2}\left[2\sinh\left(\frac{x_i-x_j}{2k}\right)\right]\prod_{i<j}\left[2\sinh\left(\frac{x_i-x_j}{2k}\right)\right]}{\prod_{j=1}^N\left[2\cosh\left(\frac{x_1-x_j-2\pi i}{2k}\right)\right]\prod_{i,j,i\geq 2}\left[2\cosh\left(\frac{x_i-x_j}{2k}\right)\right]} \\
&= \frac{1}{2^N}\frac{1}{\cos\frac{\pi}{k}}\prod_{j=2}^N\left[\frac{\tanh\left(\frac{x_1-x_j-2\pi i}{2k}\right)}{\tanh\left(\frac{x_1-x_j}{2k}\right)}\right]\prod_{i<j}\left[\tanh\left(\frac{x_i-x_j}{2k}\right)\right]^2 \qquad \text{(G.7)}
\end{aligned}
$$

Therefore, By $\cosh(x - i\pi) = -\cosh x$,

$$
\begin{aligned}
Z_{ABJM}\langle\, W_{1/6}\,\rangle &= \frac{e^{\frac{\pi}{k}i}}{2^N N!}\frac{1}{\cos\frac{\pi}{k}}\int \frac{d^N x}{(2\pi k)^N}\, e^{-\frac{x_1}{k}}\prod_{j=2}^N\left[\frac{\tanh\left(\frac{x_1-x_j-2\pi i}{2k}\right)}{\tanh\left(\frac{x_1-x_j}{2k}\right)}\right] \\
&\quad \times \prod_{i<j}\left[2\tanh\left(\frac{x_i-x_j}{2k}\right)\right]^2\frac{1}{\prod_i 2\cosh\frac{x_i}{2}}.
\end{aligned}
$$

Since for large $|x_1|$,

$$
(\text{integrand}) \sim e^{(1/k-1/2)|x_1|},
$$

this should be divergent for $k \leq 2$.

References

[1] B. de Wit, M. Luscher, and H. Nicolai, *The Supermembrane Is Unstable*, *Nucl.Phys.* **B320** (1989) 135.

[2] T. Banks, W. Fischler, S. Shenker, and L. Susskind, *M theory as a matrix model: A Conjecture*, *Phys.Rev.* **D55** (1997) 5112–5128, [hep-th/9610043].

[3] H.-C. Kao, K.-M. Lee, and T. Lee, *The Chern-Simons coefficient in supersymmetric Yang-Mills Chern-Simons theories*, *Phys.Lett.* **B373** (1996) 94–99, [hep-th/9506170].

[4] A. Kapustin and M. J. Strassler, *On mirror symmetry in three-dimensional Abelian gauge theories*, *JHEP* **9904** (1999) 021, [hep-th/9902033].

[5] D. Gaiotto and X. Yin, *Notes on superconformal Chern-Simons-Matter theories*, *JHEP* **0708** (2007) 056, [arXiv:0704.3740].

[6] J. Bagger and N. Lambert, *Gauge symmetry and supersymmetry of multiple M2-branes*, *Phys.Rev.* **D77** (2008) 065008, [arXiv:0711.0955].

[7] A. Gustavsson, *Algebraic structures on parallel M2-branes*, *Nucl.Phys.* **B811** (2009) 66–76, [arXiv:0709.1260].

[8] G. Papadopoulos, *M2-branes, 3-Lie Algebras and Plucker relations*, *JHEP* **0805** (2008) 054, [arXiv:0804.2662].

[9] J. P. Gauntlett and J. B. Gutowski, *Constraining Maximally Supersymmetric Membrane Actions*, *JHEP* **0806** (2008) 053, [arXiv:0804.3078].

[10] M. Van Raamsdonk, *Comments on the Bagger-Lambert theory and multiple M2-branes*, *JHEP* **0805** (2008) 105, [arXiv:0803.3803].

[11] N. Lambert and D. Tong, *Membranes on an Orbifold*, *Phys.Rev.Lett.* **101** (2008) 041602, [arXiv:0804.1114].

[12] J. Distler, S. Mukhi, C. Papageorgakis, and M. Van Raamsdonk, *M2-branes on M-folds*, *JHEP* **0805** (2008) 038, [arXiv:0804.1256].

[13] D. Gaiotto and E. Witten, *Janus Configurations, Chern-Simons Couplings, And The theta-Angle in N=4 Super Yang-Mills Theory*, *JHEP* **1006** (2010) 097, [arXiv:0804.2907].

[14] K. Hosomichi, K.-M. Lee, S. Lee, S. Lee, and J. Park, *N=4 Superconformal Chern-Simons Theories with Hyper and Twisted Hyper Multiplets*, *JHEP* **0807** (2008) 091, [arXiv:0805.3662].

[15] O. Aharony, O. Bergman, D. L. Jafferis, and J. Maldacena, *N=6 superconformal Chern-Simons-matter theories, M2-branes and their gravity duals*, *JHEP* **0810** (2008) 091, [arXiv:0806.1218].

[16] J. M. Maldacena, *The Large N limit of superconformal field theories and supergravity*, *Adv.Theor.Math.Phys.* **2** (1998) 231–252, [hep-th/9711200].

[17] S. Gubser, I. R. Klebanov, and A. M. Polyakov, *Gauge theory correlators from noncritical string theory*, *Phys.Lett.* **B428** (1998) 105–114, [hep-th/9802109].

[18] E. Witten, *Anti-de Sitter space and holography*, *Adv.Theor.Math.Phys.* **2** (1998) 253–291, [hep-th/9802150].

[19] N. Itzhaki, J. M. Maldacena, J. Sonnenschein, and S. Yankielowicz, *Supergravity and the large N limit of theories with sixteen supercharges*, *Phys.Rev.* **D58** (1998) 046004, [hep-th/9802042].

[20] W. Bietenholz and J. Nishimura, *Ginsparg-Wilson fermions in odd dimensions*, *JHEP* **0107** (2001) 015, [hep-lat/0012020].

[21] W. Bietenholz and P. Sodano, *A Ginsparg-Wilson approach to lattice Chern-Simons theory*, hep-lat/0305006.

[22] J. Giedt, *Progress in four-dimensional lattice supersymmetry*, *Int.J.Mod.Phys.* **A24** (2009) 4045–4095, [arXiv:0903.2443].

[23] M. Hanada, L. Mannelli, and Y. Matsuo, *Large-N reduced models of supersymmetric quiver, Chern-Simons gauge theories and ABJM*, *JHEP* **0911** (2009) 087, [arXiv:0907.4937].

[24] T. Ishii, G. Ishiki, S. Shimasaki, and A. Tsuchiya, *N=4 Super Yang-Mills from the Plane Wave Matrix Model*, *Phys.Rev.* **D78** (2008) 106001, [arXiv:0807.2352].

[25] H. Kawai, S. Shimasaki, and A. Tsuchiya, *Large N reduction on group manifolds*, *Int.J.Mod.Phys.* **A25** (2010) 3389–3406, [arXiv:0912.1456].

[26] M. Honda, G. Ishiki, J. Nishimura, and A. Tsuchiya, *Testing the AdS/CFT correspondence by Monte Carlo calculation of BPS and non-BPS Wilson loops in 4d N=4 super-Yang-Mills theory*, *PoS* **LAT2011** (2011) 244, [arXiv:1112.4274].

[27] J. Nishimura, *Non-lattice simulation of supersymmetric gauge theories as a probe to quantum black holes and strings*, *PoS* **LAT2009** (2009) 016, [arXiv:0912.0327].

[28] M. Honda, G. Ishiki, S.-W. Kim, J. Nishimura, and A. Tsuchiya, *Supersymmetry non-renormalization theorem from a computer and the AdS/CFT correspondence*, *PoS* **LATTICE2010** (2010) 253, [arXiv:1011.3904].

[29] V. Pestun, *Localization of gauge theory on a four-sphere and supersymmetric Wilson loops*, arXiv:0712.2824.

[30] J. K. Erickson, G. W. Semenoff, and K. Zarembo, *Wilson loops in $N = 4$ supersymmetric Yang-Mills theory*, *Nucl. Phys.* **B582** (2000) 155–175, [hep-th/0003055].

[31] N. Drukker and D. J. Gross, *An Exact prediction of N=4 SUSYM theory for string theory*, *J.Math.Phys.* **42** (2001) 2896–2914, [hep-th/0010274].

[32] A. Kapustin, B. Willett, and I. Yaakov, *Exact Results for Wilson Loops in Superconformal Chern-Simons Theories with Matter*, *JHEP* **1003** (2010) 089, [arXiv:0909.4559].

[33] M. Marino and P. Putrov, *Exact Results in ABJM Theory from Topological Strings*, *JHEP* **1006** (2010) 011, [arXiv:0912.3074].

[34] N. Drukker, M. Marino, and P. Putrov, *From weak to strong coupling in ABJM theory*, *Commun.Math.Phys.* **306** (2011) 511–563, [arXiv:1007.3837].

[35] C. P. Herzog, I. R. Klebanov, S. S. Pufu, and T. Tesileanu, *Multi-Matrix Models and Tri-Sasaki Einstein Spaces*, *Phys.Rev.* **D83** (2011) 046001, [arXiv:1011.5487].

[36] N. Drukker, M. Marino, and P. Putrov, *Nonperturbative aspects of ABJM theory*, arXiv:1103.4844.

[37] M. Marino, *Lectures on localization and matrix models in supersymmetric Chern-Simons-matter theories*, *J.Phys.* **A44** (2011) 463001, [arXiv:1104.0783].

[38] H. Fuji, S. Hirano, and S. Moriyama, *Summing Up All Genus Free Energy of ABJM Matrix Model*, *JHEP* **1108** (2011) 001, [arXiv:1106.4631].

[39] K. Okuyama, *A Note on the Partition Function of ABJM theory on S^3*, *Prog.Theor.Phys.* **127** (2012) 229–242, [arXiv:1110.3555].

[40] M. Marino and P. Putrov, *ABJM theory as a Fermi gas*, arXiv:1110.4066.

[41] M. Bershadsky, S. Cecotti, H. Ooguri, and C. Vafa, *Kodaira-Spencer theory of gravity and exact results for quantum string amplitudes*, *Commun.Math.Phys.* **165** (1994) 311–428, [hep-th/9309140].

[42] M. Hanada, M. Honda, Y. Honma, J. Nishimura, S. Shiba, *et. al.*, *Numerical studies of the ABJM theory for arbitrary N at arbitrary coupling constant*, arXiv:1202.5300.

[43] M. Honda, M. Hanada, Y. Honma, J. Nishimura, S. Shiba, *et. al.*, *Monte Carlo studies of 3d N=6 SCFT via localization method*, arXiv:1211.6844.

[44] C. Faber and R. Pandharipande, *Hodge integrals and Gromov-Witten theory*, math/9810173.

[45] M. Marino, S. Pasquetti, and P. Putrov, *Large N duality beyond the genus expansion*, *JHEP* **1007** (2010) 074, [arXiv:0911.4692].

[46] A. Klemm, M. Marino, M. Schiereck, and M. Soroush, *ABJM Wilson loops in the Fermi gas approach*, arXiv:1207.0611.

[47] D. L. Jafferis, *The Exact Superconformal R-Symmetry Extremizes Z*, *JHEP* **1205** (2012) 159, [arXiv:1012.3210].

[48] N. Hama, K. Hosomichi, and S. Lee, *Notes on SUSY Gauge Theories on Three-Sphere*, *JHEP* **1103** (2011) 127, [arXiv:1012.3512].

[49] J. Polchinski, *Dirichlet Branes and Ramond-Ramond charges*, *Phys.Rev.Lett.* **75** (1995) 4724–4727, [hep-th/9510017].

[50] E. Witten, *String theory dynamics in various dimensions*, *Nucl.Phys.* **B443** (1995) 85–126, [hep-th/9503124].

[51] E. Cremmer, B. Julia, and J. Scherk, *Supergravity Theory in Eleven-Dimensions*, *Phys.Lett.* **B76** (1978) 409–412.

[52] M. Huq and M. Namazie, *KALUZA-KLEIN SUPERGRAVITY IN TEN-DIMENSIONS*, *Class.Quant.Grav.* **2** (1985) 293.

[53] I. Campbell and P. C. West, *N=2 D=10 Nonchiral Supergravity and Its Spontaneous Compactification*, *Nucl.Phys.* **B243** (1984) 112.

[54] W. Nahm, *Supersymmetries and their Representations*, *Nucl.Phys.* **B135** (1978) 149.

[55] J. Bagger, N. Lambert, S. Mukhi, and C. Papageorgakis, *Multiple Membranes in M-theory*, arXiv:1203.3546.

[56] M. Duff and K. Stelle, *Multimembrane solutions of $D = 11$ supergravity*, *Phys.Lett.* **B253** (1991) 113–118.

[57] R. Gueven, *Black p-brane solutions of $D = 11$ supergravity theory*, *Phys.Lett.* **B276** (1992) 49–55.

[58] G. Gibbons and K.-i. Maeda, *Black Holes and Membranes in Higher Dimensional Theories with Dilaton Fields*, *Nucl.Phys.* **B298** (1988) 741.

[59] G. T. Horowitz and A. Strominger, *Black strings and P-branes*, *Nucl.Phys.* **B360** (1991) 197–209.

[60] E. Witten and D. I. Olive, *Supersymmetry Algebras That Include Topological Charges*, *Phys.Lett.* **B78** (1978) 97.

[61] E. Bogomolny, *Stability of Classical Solutions*, *Sov.J.Nucl.Phys.* **24** (1976) 449.

[62] M. Prasad and C. M. Sommerfield, *An Exact Classical Solution for the 't Hooft Monopole and the Julia-Zee Dyon*, *Phys.Rev.Lett.* **35** (1975) 760–762.

[63] M. Duff, J. T. Liu, and R. Minasian, *Eleven-dimensional origin of string-string duality: A One loop test*, *Nucl.Phys.* **B452** (1995) 261–282, [hep-th/9506126].

[64] E. Bergshoeff, E. Sezgin, and P. Townsend, *Supermembranes and Eleven-Dimensional Supergravity*, *Phys.Lett.* **B189** (1987) 75–78.

[65] M. Duff, P. S. Howe, T. Inami, and K. Stelle, *Superstrings in D=10 from Supermembranes in D=11*, *Phys.Lett.* **B191** (1987) 70.

[66] R. Sorkin, *Kaluza-Klein Monopole*, *Phys.Rev.Lett.* **51** (1983) 87–90.

[67] D. J. Gross and M. J. Perry, *Magnetic Monopoles in Kaluza-Klein Theories*, *Nucl.Phys.* **B226** (1983) 29.

[68] P. Townsend, *D-branes from M-branes*, *Phys.Lett.* **B373** (1996) 68–75, [hep-th/9512062].

[69] C. Schmidhuber, *D-brane actions*, *Nucl.Phys.* **B467** (1996) 146–158, [hep-th/9601003].

[70] O. Aharony, S. S. Gubser, J. M. Maldacena, H. Ooguri, and Y. Oz, *Large N field theories, string theory and gravity*, *Phys.Rept.* **323** (2000) 183–386, [hep-th/9905111].

[71] I. R. Klebanov, *World volume approach to absorption by nondilatonic branes*, *Nucl.Phys.* **B496** (1997) 231–242, [hep-th/9702076].

[72] G. Gibbons and P. Townsend, *Vacuum interpolation in supergravity via super p-branes*, *Phys.Rev.Lett.* **71** (1993) 3754–3757, [hep-th/9307049].

[73] L. Avdeev, O. Tarasov, and A. Vladimirov, *VANISHING OF THE THREE LOOP CHARGE RENORMALIZATION FUNCTION IN A SUPERSYMMETRIC GAUGE THEORY*, *Phys.Lett.* **B96** (1980) 94–96.

[74] M. T. Grisaru, M. Rocek, and W. Siegel, *Zero Three Loop beta Function in N=4 Superyang-Mills Theory*, *Phys.Rev.Lett.* **45** (1980) 1063–1066.

[75] W. E. Caswell and D. Zanon, *ZERO THREE LOOP BETA FUNCTION IN THE N=4 SUPERSYMMETRIC YANG-MILLS THEORY*, *Nucl.Phys.* **B182** (1981) 125.

[76] M. F. Sohnius and P. C. West, *Conformal Invariance in N=4 Supersymmetric Yang-Mills Theory*, *Phys.Lett.* **B100** (1981) 245.

[77] P. S. Howe, K. Stelle, and P. Townsend, *Miraculous Ultraviolet Cancellations in Supersymmetry Made Manifest*, *Nucl.Phys.* **B236** (1984) 125.

[78] G. 't Hooft, *A Planar Diagram Theory for Strong Interactions*, *Nucl.Phys.* **B72** (1974) 461.

[79] J. Kinney, J. M. Maldacena, S. Minwalla, and S. Raju, *An Index for 4 dimensional super conformal theories*, *Commun.Math.Phys.* **275** (2007) 209–254, [hep-th/0510251].

[80] N. Lambert and C. Papageorgakis, *Relating U(N)xU(N) to SU(N)xSU(N) Chern-Simons Membrane theories*, *JHEP* **1004** (2010) 104, [arXiv:1001.4779].

[81] D. Bashkirov and A. Kapustin, *Dualities between $N = 8$ superconformal field theories in three dimensions*, *JHEP* **1105** (2011) 074, [arXiv:1103.3548].

[82] M. Honda and Y. Honma, *3d superconformal indices and isomorphisms of M2-brane theories*, arXiv:1210.1371.

[83] O. Aharony, O. Bergman, and D. L. Jafferis, *Fractional M2-branes*, *JHEP* **0811** (2008) 043, [arXiv:0807.4924].

[84] D. Bashkirov and A. Kapustin, *Supersymmetry enhancement by monopole operators*, *JHEP* **1105** (2011) 015, [arXiv:1007.4861].

[85] S. Kim, *The Complete superconformal index for N=6 Chern-Simons theory*, *Nucl.Phys.* **B821** (2009) 241–284, [arXiv:0903.4172].

[86] Y. Imamura and S. Yokoyama, *Index for three dimensional superconformal field theories with general R-charge assignments*, *JHEP* **1104** (2011) 007, [arXiv:1101.0557].

[87] N. Hama, K. Hosomichi, and S. Lee, *SUSY Gauge Theories on Squashed Three-Spheres*, *JHEP* **1105** (2011) 014, [arXiv:1102.4716].

[88] Y. Imamura and D. Yokoyama, *N=2 supersymmetric theories on squashed three-sphere*, *Phys.Rev.* **D85** (2012) 025015, [arXiv:1109.4734].

[89] D. Gang, *Chern-Simons theory on L(p,q) lens spaces and Localization*, arXiv:0912.4664.

[90] F. Benini, T. Nishioka, and M. Yamazaki, *4d Index to 3d Index and 2d TQFT*, *Phys.Rev.* **D86** (2012) 065015, [arXiv:1109.0283].

[91] Y. Imamura and D. Yokoyama, S^3/Z_n *partition function and dualities*, arXiv:1208.1404.

[92] K. Ohta and Y. Yoshida, *Non-Abelian Localization for Supersymmetric Yang-Mills-Chern-Simons Theories on Seifert Manifold*, arXiv:1205.0046.

[93] H. Lu, C. Pope, and J. Rahmfeld, *A Construction of Killing spinors on S**n*, *J.Math.Phys.* **40** (1999) 4518–4526, [hep-th/9805151].

[94] G. Festuccia and N. Seiberg, *Rigid Supersymmetric Theories in Curved Superspace*, *JHEP* **1106** (2011) 114, [arXiv:1105.0689].

[95] A. Kapustin, B. Willett, and I. Yaakov, *Exact results for supersymmetric abelian vortex loops in 2+1 dimensions*, arXiv:1211.2861.

[96] N. Drukker, T. Okuda, and F. Passerini, *Exact results for vortex loop operators in 3d supersymmetric theories*, arXiv:1211.3409.

[97] O. Aharony, J. Marsano, S. Minwalla, K. Papadodimas, and M. Van Raamsdonk, *The Hagedorn - deconfinement phase transition in weakly coupled large N gauge theories*, *Adv.Theor.Math.Phys.* **8** (2004) 603–696, [hep-th/0310285].

[98] N. Drukker, J. Plefka, and D. Young, *Wilson loops in 3-dimensional N=6 supersymmetric Chern-Simons Theory and their string theory duals*, *JHEP* **0811** (2008) 019, [arXiv:0809.2787].

[99] B. Chen and J.-B. Wu, *Supersymmetric Wilson Loops in N=6 Super Chern-Simons-matter theory*, *Nucl.Phys.* **B825** (2010) 38–51, [arXiv:0809.2863].

[100] S.-J. Rey, T. Suyama, and S. Yamaguchi, *Wilson Loops in Superconformal Chern-Simons Theory and Fundamental Strings in Anti-de Sitter Supergravity Dual*, *JHEP* **0903** (2009) 127, [arXiv:0809.3786].

[101] M. Benna, I. Klebanov, T. Klose, and M. Smedback, *Superconformal Chern-Simons Theories and AdS(4)/CFT(3) Correspondence*, *JHEP* **0809** (2008) 072, [arXiv:0806.1519].

[102] N. Drukker and D. Trancanelli, *A Supermatrix model for N=6 super Chern-Simons-matter theory*, *JHEP* **1002** (2010) 058, [arXiv:0912.3006].

[103] M. Marino, *Chern-Simons theory, matrix integrals, and perturbative three manifold invariants*, *Commun.Math.Phys.* **253** (2004) 25–49, [hep-th/0207096].

[104] M. Aganagic, A. Klemm, M. Marino, and C. Vafa, *Matrix model as a mirror of Chern-Simons theory*, *JHEP* **02** (2004) 010, [hep-th/0211098].

[105] R. Dijkgraaf and C. Vafa, *N=1 supersymmetry, deconstruction, and bosonic gauge theories*, hep-th/0302011.

[106] R. Dijkgraaf, S. Gukov, V. A. Kazakov, and C. Vafa, *Perturbative analysis of gauged matrix models*, *Phys.Rev.* **D68** (2003) 045007, [hep-th/0210238].

[107] R. Emparan, C. V. Johnson, and R. C. Myers, *Surface terms as counterterms in the AdS / CFT correspondence*, *Phys.Rev.* **D60** (1999) 104001, [hep-th/9903238].

[108] A. Cagnazzo, D. Sorokin, and L. Wulff, *String instanton in AdS(4) x CP**3*, *JHEP* **1005** (2010) 009, [arXiv:0911.5228].

[109] I. R. Klebanov and A. A. Tseytlin, *Entropy of near extremal black p-branes*, *Nucl.Phys.* **B475** (1996) 164–178, [hep-th/9604089].

[110] H. Ooguri, C. Vafa, and E. P. Verlinde, *Hartle-Hawking wave-function for flux compactifications*, *Lett.Math.Phys.* **74** (2005) 311–342, [hep-th/0502211].

[111] J. Ambjorn, L. Chekhov, C. Kristjansen, and Y. Makeenko, *Matrix model calculations beyond the spherical limit*, *Nucl.Phys.* **B404** (1993) 127–172, [hep-th/9302014].

[112] G. Akemann, *Higher genus correlators for the Hermitian matrix model with multiple cuts*, *Nucl.Phys.* **B482** (1996) 403–430, [hep-th/9606004].

[113] O. Bergman and S. Hirano, *Anomalous radius shift in AdS(4)/CFT(3)*, *JHEP* **0907** (2009) 016, [arXiv:0902.1743].

[114] N. Kawahara, J. Nishimura, and A. Yamaguchi, *Monte Carlo approach to nonperturbative strings - Demonstration in noncritical string theory*, *JHEP* **0706** (2007) 076, [hep-th/0703209].

[115] A. Kapustin, B. Willett, and I. Yaakov, *Nonperturbative Tests of Three-Dimensional Dualities*, *JHEP* **1010** (2010) 013, [arXiv:1003.5694].

[116] W. Krauth, H. Nicolai, and M. Staudacher, *Monte Carlo approach to M theory*, *Phys.Lett.* **B431** (1998) 31–41, [hep-th/9803117].

[117] I. Kanamori, *A Method for Measuring the Witten Index Using Lattice Simulation*, *Nucl.Phys.* **B841** (2010) 426–447, [arXiv:1006.2468].

[118] N. Halmagyi and V. Yasnov, *The Spectral curve of the lens space matrix model*, *JHEP* **0911** (2009) 104, [hep-th/0311117].

[119] M.-x. Huang and A. Klemm, *Holomorphic Anomaly in Gauge Theories and Matrix Models*, *JHEP* **0709** (2007) 054, [hep-th/0605195].

[120] K. Becker, M. Becker, and A. Strominger, *Five-branes, membranes and nonperturbative string theory*, *Nucl.Phys.* **B456** (1995) 130–152, [hep-th/9507158].

[121] T. Suyama, *On Large N Solution of ABJM Theory*, *Nucl.Phys.* **B834** (2010) 50–76, [arXiv:0912.1084].

[122] M. Hanada, Y. Hyakutake, J. Nishimura, and S. Takeuchi, *Higher derivative corrections to black hole thermodynamics from supersymmetric matrix quantum mechanics*, *Phys.Rev.Lett.* **102** (2009) 191602, [arXiv:0811.3102].

[123] M. Hanada, J. Nishimura, Y. Sekino, and T. Yoneya, *Monte Carlo studies of Matrix theory correlation functions*, *Phys.Rev.Lett.* **104** (2010) 151601, [arXiv:0911.1623].

[124] M. Hanada, J. Nishimura, Y. Sekino, and T. Yoneya, *Direct test of the gauge-gravity correspondence for Matrix theory correlation functions*, *JHEP* **1112** (2011) 020, [arXiv:1108.5153].

[125] D. R. Gulotta, C. P. Herzog, and S. S. Pufu, *From Necklace Quivers to the F-theorem, Operator Counting, and T(U(N))*, *JHEP* **1112** (2011) 077, [arXiv:1105.2817].

[126] D. R. Gulotta, J. Ang, and C. P. Herzog, *Matrix Models for Supersymmetric Chern-Simons Theories with an ADE Classification*, *JHEP* **1201** (2012) 132, [arXiv:1111.1744].

[127] D. R. Gulotta, C. P. Herzog, and T. Nishioka, *The ABCDEF's of Matrix Models for Supersymmetric Chern-Simons Theories*, *JHEP* **1204** (2012) 138, [arXiv:1201.6360].

[128] M. Hanada, C. Hoyos, and H. Shimada, *On a new type of orbifold equivalence and M-theoretic AdS_4/CFT_3 duality*, *Phys.Lett.* **B707** (2012) 394–397, [arXiv:1109.6127]. 8 pages, updated references, published version.

[129] M. Hanada, C. Hoyos, and A. Karch, *Generating new dualities through the orbifold equivalence: a demonstration in ABJM and four-dimensional quivers*, *JHEP* **1201** (2012) 068, [arXiv:1110.3803].

[130] S. Hawking and G. Ellis, *The Large scale structure of space-time*, .

[131] K. Becker, M. Becker, and J. Schwarz, *String theory and M-theory: A modern introduction*, .

[132] M. Clark and A. Kennedy, *The RHMC algorithm for two flavors of dynamical staggered fermions*, *Nucl.Phys.Proc.Suppl.* **129** (2004) 850–852, [hep-lat/0309084].